NASA/CR-2001-210650

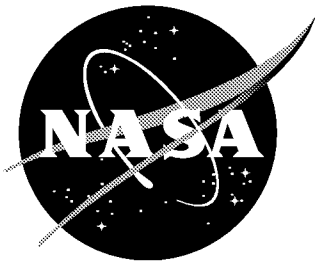

AST Composite Wing Program – Executive Summary

Michael Karal
The Boeing Company, Long Beach, California

March 2001

The NASA STI Program Office ... in Profile

Since its founding, NASA has been dedicated to the advancement of aeronautics and space science. The NASA Scientific and Technical Information (STI) Program Office plays a key part in helping NASA maintain this important role.

The NASA STI Program Office is operated by Langley Research Center, the lead center for NASA's scientific and technical information. The NASA STI Program Office provides access to the NASA STI Database, the largest collection of aeronautical and space science STI in the world. The Program Office is also NASA's institutional mechanism for disseminating the results of its research and development activities. These results are published by NASA in the NASA STI Report Series, which includes the following report types:

- TECHNICAL PUBLICATION. Reports of completed research or a major significant phase of research that present the results of NASA programs and include extensive data or theoretical analysis. Includes compilations of significant scientific and technical data and information deemed to be of continuing reference value. NASA counterpart of peer-reviewed formal professional papers, but having less stringent limitations on manuscript length and extent of graphic presentations.

- TECHNICAL MEMORANDUM. Scientific and technical findings that are preliminary or of specialized interest, e.g., quick release reports, working papers, and bibliographies that contain minimal annotation. Does not contain extensive analysis.

- CONTRACTOR REPORT. Scientific and technical findings by NASA-sponsored contractors and grantees.

- CONFERENCE PUBLICATION. Collected papers from scientific and technical conferences, symposia, seminars, or other meetings sponsored or co-sponsored by NASA.

- SPECIAL PUBLICATION. Scientific, technical, or historical information from NASA programs, projects, and missions, often concerned with subjects having substantial public interest.

- TECHNICAL TRANSLATION. English-language translations of foreign scientific and technical material pertinent to NASA's mission.

Specialized services that complement the STI Program Office's diverse offerings include creating custom thesauri, building customized databases, organizing and publishing research results ... even providing videos.

For more information about the NASA STI Program Office, see the following:

- Access the NASA STI Program Home Page at ***http://www.sti.nasa.gov***

- E-mail your question via the Internet to help@sti.nasa.gov

- Fax your question to the NASA STI Help Desk at (301) 621-0134

- Phone the NASA STI Help Desk at (301) 621-0390

- Write to:
  NASA STI Help Desk
  NASA Center for AeroSpace Information
  7121 Standard Drive
  Hanover, MD 21076-1320

NASA/CR-2001-210650

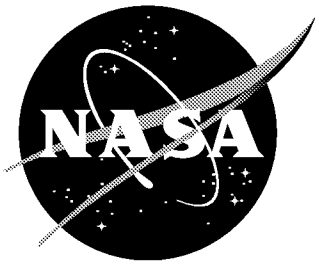

AST Composite Wing Program – Executive Summary

Michael Karal
The Boeing Company, Long Beach, California

National Aeronautics and
Space Administration

Langley Research Center
Hampton, Virginia 23681-2199

Prepared for Langley Research Center
under Contract NAS1-20546

March 2001

Available from:

NASA Center for AeroSpace Information (CASI)
7121 Standard Drive
Hanover, MD 21076-1320
(301) 621-0390

National Technical Information Service (NTIS)
5285 Port Royal Road
Springfield, VA 22161-2171
(703) 605-6000

Foreword

This report was prepared by The Boeing Company – Phantom Works, under NASA Contract NAS1-20546, "Technology Verification of Composite Primary Wing Structures for Commercial Transport Aircraft". The objectives of this contract are to perform design, analysis, fabrication, assembly and testing verification of an all composite wing structure for commercial transport aircraft. The major goal is to meet a target of reduced weight and manufacturing cost as it compares to conventional aluminum transport aircraft structure. The contract was managed by the NASA Langley Research Center, Hampton Virginia with Mr. Benson Dexter as the COTR.

Table of Contents

Section		Page
	Foreword	**iii**
1.	**Introduction**	**1**
2.	**Full-Scale Stitched/Resin Film Infused Wing**	**3**
	2.1 Baseline Concept Description	3
	2.2 Definition of Aircraft System Influences	6
	2.3 Outboard Wing Box Detail Design	10
	2.4 Assembly Tooling Design and Build	14
	2.5 Full-Scale Composite Wing Structural Verification	16
	2.6 Weight Trade Study Results and Summary	17
3.	**Semi-Span Wing Design, Analysis, and Supporting Technology**	**24**
4.	**Design Development Test Articles (DDTA's)**	**33**
	4.1 Durability and Damage Tolerance (D&DT) Studies	41
5.	**Manufacturing Studies—Process Development**	**51**
	5.1 S/RFI	51
	5.2 RFI Temperature Cycle Development	51
	5.3 Effects of Processing Pressure	53
	5.4 Resin Allocation	55
	5.5 VARTM Process Studies	56
	5.6 VARTM Unitized Structure Development	58
6.	**Semi-Span Fabrication**	**61**
	6.1 Cover Panels Tooling and Component Fabrication	61
7.	**Semi-Span Test Description**	**78**
	7.1 Overview	78
	7.2 Structural Loading Hardware	78
	7.3 Cover Panel Repair Design	79
	7.4 Strain Gages	80
8.	**Concluding Remarks**	**85**
9.	**References**	**87**

List of Illustrations

Figure		Page
1	MD-90-40X baseline aircraft	3
2	Full scale MD-90-40X wing structural arrangement	4
3	Baseline system design for full-scale wing	7
4	Cover panel structural concept	11
5	Fourteen-tube stringer	13
6	Outboard wing box assembly sequence	15
7	Full-scale wing test arrangement	17
8	Composite wing box weight summary	18
9	Comparison of composite wing upper and lower cover panel weights	19
10	Composite wing upper cover panel weight breakdown	19
11	Composite wing lower cover panel weight breakdown	20
12	Composite wing substructure weight summary	20
13	Baseline aircraft configuration and 41 foot Semi-Span composite wing	24
14	Integrated cover panels	25
15	Semi-Span wing box	26
16	The Semi-Span composite wing test article mounted to the Langley strongback	27
17	Semi-Span structural arrangement	28
18	The global finite element model of the Semi-Span composite wing	32
19	Master panel skin stitching configuration	34
20	Master panel stitching frame tool	34
21	A typical inner mold line tooling block used to RFI process DDTA panels	35
22	General master panel configuration	36
23	Component specifications for the master panel configurations	36
24	DDTA Test Specimens (number in parenthesis refers to the number of replicates for each different specimen)	38
25	Comparison of the spar cap shear strength of different test configurations	40
26	Cross-section of typical three-stringer DSD test article	42
27	Compression and tension slot geometries used to simulate DSD	43
28	A compression test article and antibuckling guides	44

List of Illustrations (Continued)

Figure		Page
29	A tension test article positioned in the loading frame	45
30	Close-up view of compression test article failure zone	46
31	Tension test article trans-laminar shear damage zones	47
32	Plot of tension strains indicating development of a shear failure zone	47
33	Far-field strain results for a tension test article	49
34	Photoelastic fringe pattern from a compression test article under load	49
35	Schematic of RFI process showing OML and IML tooling, preform, resin, and direction of resin flow through preform	55
36	Schematic of a typical VARTM process	58
37	Wing cover panel part processed using the VARTM –PB process	59
38	Cost savings from reduced fastener count and automation	60
39	Advanced stitching machine gantry with 4 stitching heads and bobbins assemblies	63
40	Semi-Span wing cover panel with complex contoured loft structure on advanced stitching machine	63
41	Semi-Span wing cover panel design	65
42	Base skin lay-up with spar caps	66
43	Stitched skin with integral spar caps	66
44	Stitching of stringer to skin	67
45	Stitching of rib clip to skin	68
46	Stitched wing cover panel preform	68
47	Stitched resin film infused Semi-Span wing cover panel	69
48	Semi-Span structural arrangement	70
49	Cover panel locating features	71
50	Lower cover panel fastener hole processing	72
51	Rib web to spar web clip installation	72
52	Upper cover Transition Splice Fitting (TSF) installation	73
53	Lower cover Transition Splice Fitting (TSF) installation	73
54	Rear spar installation	74
55	Main landing gear fitting installation	74
56	Side-of-body bulkhead	75

List of Illustrations (Continued)

Figure		Page
57	Rib 13 saddle installation	75
58	Test hardware setup	78
59	Trimetric view of Semi-Span repair	81
60	Plan view of lower cover gage locations and labels	81
61	Plan view of upper cover gage locations and labels	82
62	Trimetric view of global model	82
63	Trimetric view of detail stringer runout FEM	83
64	Semi-Span lower cover panel failure	84
65	NASA Pre-test analysis on Wing Tip condition displacement	84

List of Tables

Table		Page
1	Weight Savings of Composite Wing in Room Temperature/Dry and Extreme Environmental Conditions	21
2	Semi-Span Composite Wing Cover Panel and Spar Laminates	29
3	Summary of DDTA Test Specimens	37
4	DDTA #3 Tension Runout Test Results	39
5	DDTA #3 and D4 Compression Runout Test Results	39
6	Test Matrix for DSD Evaluations	42
7	Summary of GENOA Predictions with Experimental Results	48
8	S/RFI QFD Matrix	52
9	RFI Processing Results of Lower Cover Panel	69
10	Wing Box Cost Analysis Summary including Cover Panel "Actuals"	77

1. Introduction

Since the introduction of carbon fiber composites in the 1960's, they have proven their merit in high performance applications that are generally associated with military aircraft. These high performance applications have demonstrated that primary aircraft structures made from carbon fiber composites can achieve weight savings of 20% to 30% over similarly designed metal structures. However, this level of weight saving and improved performance was only realized by accepting a significant cost penalty for the enhanced composite structure. Future advanced commercial aircraft applications will place a high priority on developing cost effective designs, and improved performance will rarely be accepted as justification for a higher cost composite structural component. The realization of this situation has put pressure on governmental research agencies and aircraft manufacturers to fund various efforts that strive to lower constituent material costs and developing cost effective manufacturing processes for composite structures.

Part of this research effort to develop cost effective composite manufacturing processes includes the NASA Airframe Materials and Structures element of the Advanced Subsonic Technology (AST) program, which grew out of the Advanced Composite Technology (ACT) program. The latter ACT program was initiated in 1989, and its composite research results identified both manufacturing cost and damage tolerance barriers to the application of these materials in commercial transport primary structures. This long-term government and industry development effort is continuing to show positive results, and the Boeing Company is participating in the AST program through the development of stitched/resin film infusion (S/RFI) technology under NASA Langley contract NAS1-20546.

Various types of textile composites have been evaluated for their ability to provide low cost composite structures. Through-the-thickness stitching of dry preforms, combined with resin infusion, showed a good potential for overcoming cost and damage tolerance issues related to using carbon fiber composites in primary structures of commercial aircraft. Stitching through dry fabric made it possible to incorporate various elements of a wing torque box (i.e., wing skin, stiffeners, intercostal clips, and spar caps) into an integral structure that eliminates the requirement for thousands of mechanical fasteners. Replacing mechanical fasteners with a highly automated stitching process has the potential of significantly reducing manufacturing costs of composite structures. This advance in composite structure fabrication is a positive indication that progress is continuing to be made toward reaching the long desired affordability goals for these materials, while retaining their weight advantage over metallic designs.

In the 1980's, toughened resin systems began to show promise for improving the damage tolerance of carbon fiber composites, but the high cost of these new resin systems detracted from their damage tolerance benefits. Development of through-the-thickness stitching of dry preforms was viewed as a low cost alternative to toughened resin systems in the previous ACT program efforts. Combining less expensive brittle resins with through-the-thickness stitching offered improved damage tolerant composite structures at an affordable cost.

AST program element goals included making composite wing structures 25 percent lighter, reducing fabrication costs by 20 percent, and reducing airline operating costs by 4 percent as compared to current aluminum wing designs. These goals were shown to be achievable by the NASA/Boeing AST Composite Wing Program (NAS1-20546). These achievements are documented and discussed in this executive summary of the AST Composite Wing Program. This report describes a weight trade study utilizing a wing torque box design applicable to a 220-passenger commercial aircraft and was used to verify the weight savings a S/RFI structure would offer compared to an identical aluminum wing box design. This trade study was performed in the AST Composite Wing program, and the overall weight savings for the

composite box are reported relative to the aluminum baseline. Previous program work involved the design of a S/RFI baseline wing box structural test component and its associated testing hardware. This detail structural design effort which is known as the "semi-span" in this report, was completed under a previous NASA contract. (ref. NAS1-18862)

The full-scale wing design was based on a configuration for a MD-90-40X airplane, and the objective of this structural test component was to demonstrate the maturity of the S/RFI technology through the evaluation of a full-scale wing box/fuselage section structural test. However, scope reductions in the AST Composite Wing Program prevented the fabrication and evaluation of this wing box structure. Results obtained from the weight trade study and the full-scale test component design effort will be discussed herein.

2. Full-Scale Stitched/Resin Film Infused Wing

2.1 Baseline Concept Description

This section of the summary addresses the airplane configuration assumptions and wing design requirements used to define the baseline wing test component. The configuration used for the study was the MD-90-40X airplane, which would be representative of a tail-mounted engine design. Loads data and systems analyses were performed by the Twin-Jet commercial design division of the Douglas Products Group (DPG) in Long Beach. All of the structural analysis studies were performed by the Phantom Works Divisions located in Long Beach and St. Louis.

Airplane Description

Baseline Configuration. The MD-90-40X configuration was selected for the AST Composite Wing Program (see Figure 1). The X2 wing was developed from the DPG MD9040W2 wing and then re-optimized to include additional Advanced Composites Technology (ACT) program constraints. In addition to changes in performance requirements, several manufacturing-specific constraints were added to minimize fabrication costs: straight rear spar, a 112-inch maximum spar-to-spar spacing (stitching machine limit), minimum radius of curvature between spars of 200 inches, and constraint of the chord and incidence at the side of body to facilitate integration into the MD-80/90 fuselage. These requirements led to a larger chord at the planform break and also influenced the wing sweep.

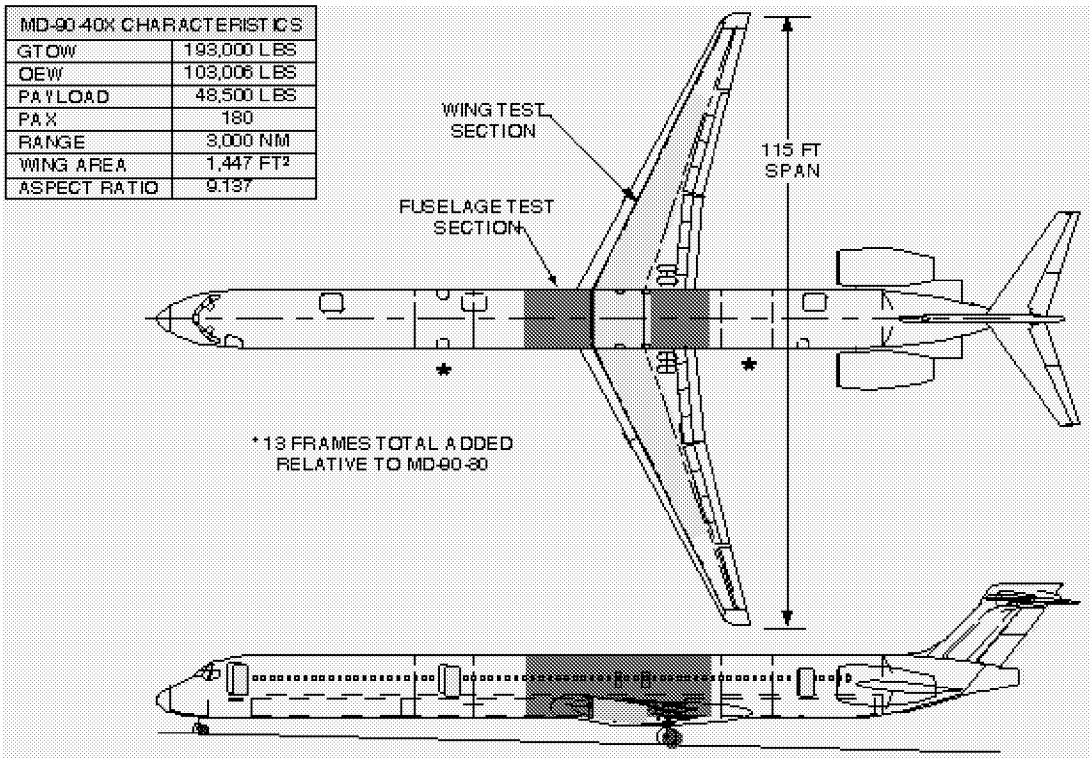

Figure 1. MD-90-40X baseline aircraft.

The primary difference between the wing geometry selected for this study and those used on previous composite wing studies is that it has a higher aspect ratio planform and a supercritical airfoil. The use of supercritical airfoils is driven by improvements in aerodynamics and not related to the material/structural concept selection for the wing. The aspect ratio of the wing, on the other hand, is directly a function of the materials and structures available. As the aspect ratio is increased, aerodynamic performance improves. Through the use of composite materials, with higher directional stiffness capabilities, higher wing aspect ratios can be achieved with smaller weight penalties than for comparable aluminum geometries.

The general arrangement drawing for the MD-90-40X came from a 1995 multidisciplinary optimization (MDO) study. This study defined the wing planform, surface geometry, and main landing gear locations. The structural requirements to keep the front and rear spars straight and limit the box width (stitching limit on panel) had a significant influence on the final planform shape. Ribs are nominally spaced at 35-inch intervals, and bulkheads are located to react discrete point loads at the side-of-body, landing gear, flap, and aileron bracket locations. The wing structural layout used for the preliminary design studies is shown in Figure 2.

Wing Splice. Several different wing join locations were studied before selecting the side-of-body concept. The two most promising candidates were the centerline splice (concept used on C-17) and the side-of-body splice (concept used on MD-11).

Center Line Splice Concept. The obvious advantage of a center splice is that there is only one major joint instead of two. Indeed, in considering the wing assembly in isolation, it was estimated that the join time was approximately 44% less than for double-splice arrangements. This seemingly overwhelming advantage, however, was negated by the increased assembly time required to integrate the wing into the

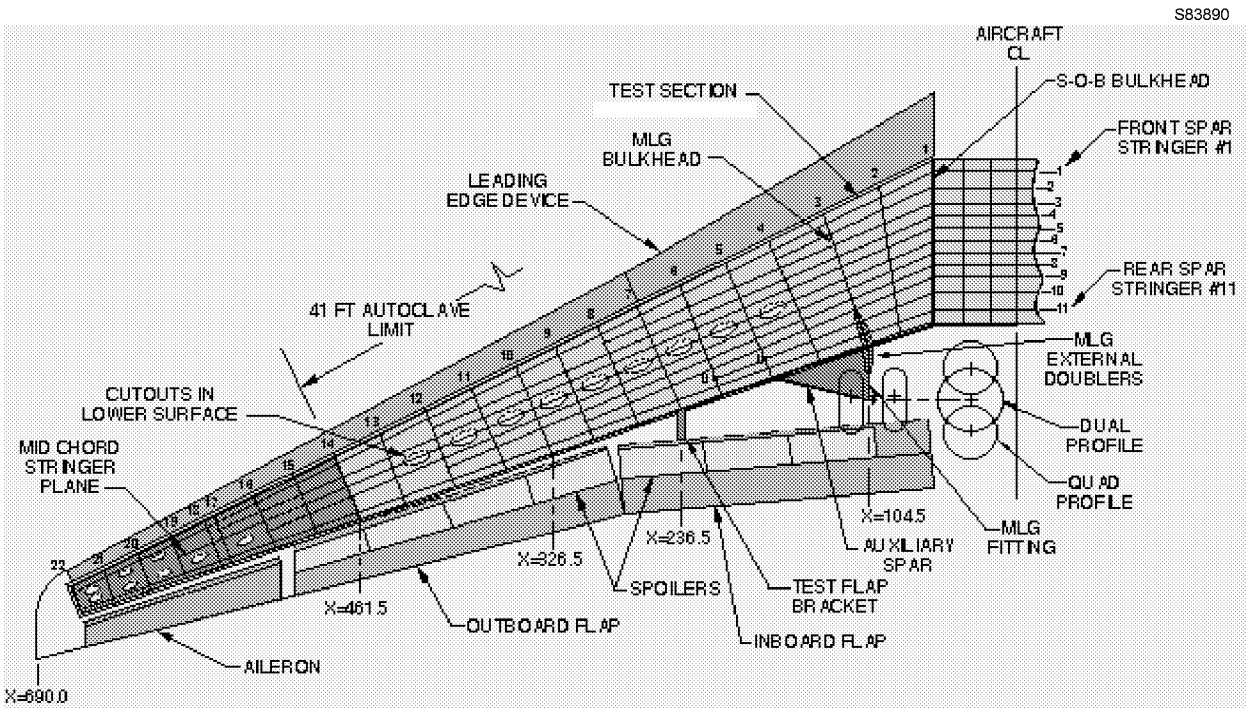

Figure 2. Full scale MD-90-40X wing structural arrangement.

fuselage. This increase was due primarily to extensive modifications to the existing fuselage that would be necessary to accept the chevron-shaped center wing box. Some of the problems associated with the chevron center box are listed below.

- The V-shaped front spar encroaches on the under-floor cargo volume. It also requires a complete reconfiguration of the existing pressure bulkhead at the forward end of the cutout in the fuselage pressure shell.
- The box cross section at the centerline is deeper than for a constant-section center box. It extends below the fuselage shell and requires a larger wing/fuselage fillet fairing and more complex keel structure.
- The sudden changes of load paths at the centerline require a heavy bulkhead to react the kick loads. These kick loads act in opposing directions in the upper and lower cover panels, which creates a twisting moment on the box. The resulting nonuniform loading in the center box adds a significant weight penalty.

Side-of-Body Splice Concept. This type of splice is used on MD-11 aircraft. It has the advantage of having a constant-section center box, with identically shaped interior ribs. The constant section is compatible with the constant bending moment that results from symmetric loading conditions. Regardless of where the splice is located, there will be a heavy side-of-body bulkhead to transfer wing shear and torque loads into the fuselage. These bulkheads also react the kick loads that occur at a side-of body splice. At this location, external splice plates with protruding-head bolts can be used in the cover panel joints, because these are within the wing/fuselage fairing and aerodynamic flushness is not required.

On the basis of manufacturing and engineering evaluations, the side-of-body bulkhead concept was found to be the most favorable location for splicing the wing on the MD-90-40X configuration. Manufacturing personnel contributed their views to the study and it was agreed that the center wing box should not be delivered as a complete assembly but as separate pieces. This allows the wing (tip-to-tip) to be assembled as a single unit before installation on the fuselage.

Spar Reference Planes. Spars are in vertical planes in the full-scale box. This simplifies the intercept at the side-of-body bulkhead between the outer and center spar segments. Sloping spar planes were considered in 1996 as a means of reducing the angle with the direction of stitching motion, but this was not adopted.

Rib Planes. Ribs are in a vertical plane relative to the airplane coordinate system. It would be structurally advantageous to make them perpendicular to dihedral planes, but this advantage is offset by the increase in manufacturing costs. Following conventional practice, planes were originally perpendicular to the rear spar [References 1, 2]. They were later redesigned perpendicular to the mid-box axis for the full-scale box to simplify the manufacture of intercostal rib clips.

Human factor studies led to an increase in the width of the root bay for the semi-span design, and these considerations were incorporated into the full-scale wing design.

FAA Compliance

The full-scale wing box was designed to meet all applicable FAR requirements for composite structures. The methodology used as the certification basis was taken directly from the FAA Advisory Circular 20-107A (Composite Aircraft Structure). Compliance for the full-scale wing will be shown either analytically or by test and will take full advantage of the building-block approach established earlier in the program.

2.2 Definition of Aircraft System Influences

A Unigraphics solid model layout was created for each of the systems components shown in Figure 3 to verify the volumetric requirements for the wing.

Slats. The hybrid systems are based upon MD-12X hydraulic drive/torque tube designs coupled with the existing MD-90-30 cable/track design. These systems utilize gear boxes in lieu of rotary actuators to drive the cable system and slat segments. Carry-over of a slat track design minimizes cuts/breaks in the wing-under-slat (WUS) structure, which allows the skin structure to contribute to wing bending and torsional load carrying capability. This feature was particularly attractive for the composite wing because of its lower torsional stiffness.

During the preliminary design phase of the project, no definition of WUS structure, slat X-section, or slat segments was available. Slat mechanical systems were conceived around best-guess approximations of existing MD-90-30 features. Baseline assumptions included a six-slat segment on each side of the wing (0 through 5), each of which was scaled to meet the MD-90-40X wing loads. Each set of slats was scaled using two different factors, one for the inboard slats (fuselage to inboard/outboard aero split line) and another for the outboard slats. Slat segment splits were altered slightly to clear existing wing box ribs.

The drive gear box envelope was sized to fit the outboard location in the wing; all seven of the gear boxes are identical for the sake of commonality. Drive points for the slats were chosen at each segment split, and an idler track was located at the midpoint. For slats 0 and 5, the second drive track was located at each edge of the segment. This arrangement gives two independent drive tracks per slat segment and satisfies design requirements for redundancy.

Dual system hydraulic power drive units (PDU) were sized at 66% of the MD-12X Sundstrand design. This resulted in a very conservative envelope estimate (the wing span of the MD-90-40X is one-half the wing span of the MD-12X). Location of the PDU in the wing was as far outboard as the wing leading edge (L/E) cross section would allow. In the drawing file previously mentioned, the PDU and gear boxes are simplified depictions representing only the part envelope. The mounting interfaces for these components are also simplified.

The locations of the drive gear boxes can be altered inboard/outboard as required for detailed cable system design (e.g., turnbuckle locations) or to alleviate space conflicts with other systems. Cable diameters and displacements were estimated directly from the MD-90-30 without any scaling factors. Torque tube supports and specific cable pulleys/brackets were not modeled.

Flaps. An MD-12X flap system was baselined. It consists of a dual system hydraulic PDU with interconnecting torque tubes and rotary actuators at each flap hinge to drive the segments.

Components were sized using a 66% factor relative to the MD-12X Sundstrand design. For the preliminary design, the goal was to size one actuator for the inboard flaps and the other actuator for the outboard flaps. This was achieved with only one exception—the outboard actuator on the outboard flap. Because of insufficient spar depth, the actuator was sized slightly below 66% to fit. This deviation was considered acceptable because the systems design effort is only supporting the structures design at this point in the program. In reality, the rear spar plane, L/E flap, and actuators would all undergo iterative compromises/changes to reach an integrated solution that resulted in identical PDUs for the flaps and slats.

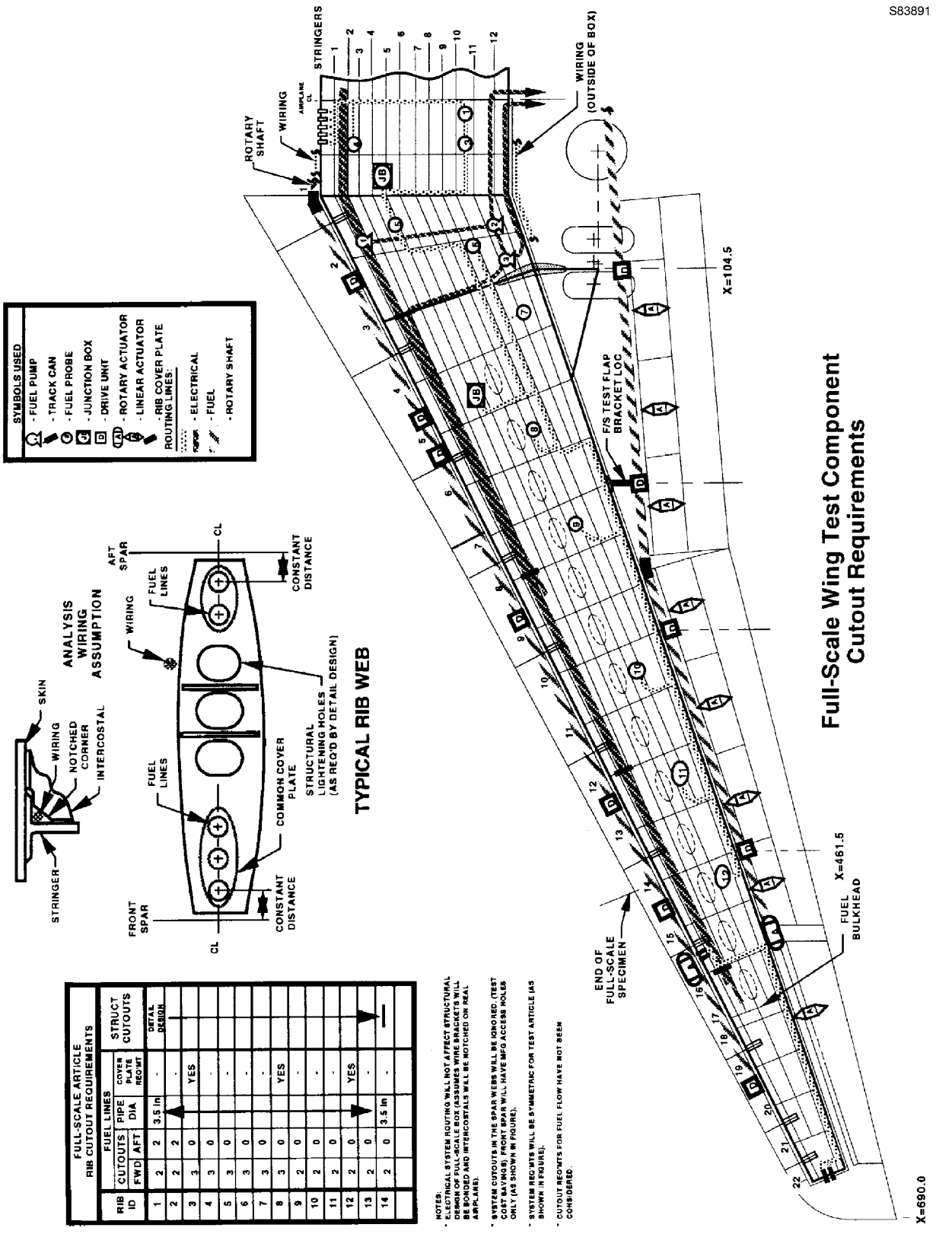

FULL-SCALE ARTICLE RIB CUTOUT REQUIREMENTS

RIB ID	FUEL LINES: CUTOUTS FWD	CUTOUTS AFT	PIPE DIA	COVER PLATE REQ'MT	STRUCT CUTOUTS
1	2	2	3.5 in	-	DETAIL DESIGN
2	2	2	◀	-	◀
3	3	0	◀	YES	◀
4	3	0	◀	-	◀
5	3	0	◀	-	◀
6	3	0	◀	-	◀
7	3	0	◀	-	◀
8	3	0	◀	YES	◀
9	2	0	◀	-	◀
10	2	0	◀	-	◀
11	2	0	◀	-	◀
12	2	0	◀	YES	◀
13	2	0	◀	-	◀
14	2	0	3.5 in	-	—

NOTES:
- ELECTRICAL SYSTEM ROUTING WILL NOT AFFECT STRUCTURAL DESIGN OF FULL-SCALE WING. ELECTRICAL CUTOUTS WILL BE BONDED AND INTERCOSTALS WILL BE NOTCHED ON REAL AIRPLANE).
- SYSTEM CUTOUTS IN THE SPAR WEBS WILL BE IGNORED. (TEST COST SAVINGS); FRONT SPAR WILL HAVE MFG ACCESS HOLES ONLY (AS SHOWN IN FIGURE).
- SYSTEM REQ'MTS WILL BE SYMMETRIC FOR TEST ARTICLE (AS SHOWN IN FIGURE).
- CUTOUT REQ'MTS FOR FUEL FLOW HAVE NOT BEEN CONSIDERED.

Figure 3. Baseline system design for full-scale wing.

Because no definition of flap cross section or flap extend positions was available (though a single segmented Fowler flap was specified in the configuration memo), a number of assumptions were made for the baseline flap design. A Fowler mechanism was not defined for the model. This was beyond the scope of the project and could not be accomplished without specific definition of flap cross section and extended positions. Instead, the number of hinges per segment and hinge station locations were taken from the initial structural arrangement drawing. Then, structural attach points were estimated to facilitate a conceptual design. Again, without an exact Fowler mechanism definition, exact attach/hinge points could not be modeled. Although the envelope and mounting interfaces of rotary actuators were simplified, they still have the general look of the MD-12X Sundstrand actuators and provide an adequate representation for the structural design of the composite wing.

Spoilers. The fly-by-wire system is modeled after the MD-95 spoiler controls. This system utilizes "banana links" between the spoiler surface and the actuator. These are identical to those used on all twin-jets. No torsion bars are used to maintain a closing force on the surface, as this is done by the actuator. The actuator was modeled after the MD-95 spoiler actuator, which was not finalized at the time of the model creation. Thus, the actuator shown in the composite wing model is only representative of the approximate envelope required.

Electrical. The electrical systems on a composite wing are slightly different from those of a conventional wing. Because the structure no longer serves as a conductive path, separate provisions must be made to accommodate electrical system grounding. Wing systems that were previously grounded to the structure must now carry their grounds back to the fuselage via a common ground wire. While this consideration is important for the electrical system design, its impact on the structural design and wing volume requirements is negligible. In the electrical system preliminary design layout, the wire routing is shown along with cross-sectional area requirements for the wire bundles at each rib station.

In addition to the grounding issue, there are other unique requirements of a composite wing that should be considered. Standoff brackets will be aluminum with a layer of fiberglass at the interface to avoid dissimilar-metals corrosion with the composite structure. Metal conduits (fuel pipes) within the composite wing may need to be grounded. For lightning strikes, the external surface must have a conductive material applied. Electrical system brackets and supports should be bonded rather than mechanically attached to the structure.

Fuel Systems. The fuel systems in this wing are based on the MD-90-30 twin-jet design but are sized for the MD-90-40X requirements. There were no unique requirements for fuel systems on a composite wing.

The fill receptacle, manifold, and a fill shutoff valve for each tank are located in the right wing leading edge. A fuel pipe from each valve takes the fuel to its assigned tank. A flat switch system signals the fill valve to close when the tank is full. There is one float switch in the center tank and two flat switches in the left and right tanks. Both float switches in the left and right tanks must be floated to close the valve. This is to accommodate the angle of the ramp on which the airplane may be parked.

The forward and aft auxiliary tank fill systems are piped from their fill valves to the point where they enter the center tank.

The tank vent system allows air to escape as the tank is being filled. It also allows air to escape during a climb and air to enter during a descent.

The open ends of the vent pipes in the left and right tanks are located as high as possible in the tanks. A "cobra head" is located at the inboard end of each tank. This is a high point in the piping that trapped fuel

may enter during maneuvers to minimize fuel migration. A float-controlled vent valve, located at the cobra head, opens during climb to vent air that would otherwise blow fuel out of the submerged open end into the center tank. The left and right tank vents empty into the center tank.

The center tank vent open outlet is as high in that tank as possible at the mid-chord of the wing box. From this high point, a pipe runs forward to the high point in a climb orientation. A climb vent float valve is located at this point for the same purpose as it is in the main tanks. This pipe joins a pipe that runs from the vent box near the left wing tip to the vent box near the right wing tip. This allows all of the tanks to be vented either to the right vent box or to both vent boxes.

The forward and center box tank vents feed into the overboard vent piping.

Two pumps in each tank feed the two main engines and the auxiliary power unit (APU). An additional pump using battery power is used to start the APU or an engine when other electric power is not available. This pump is located in the right wing.

The two pumps in the center tank are arranged in series in order to double the output pressure and override the main tank pumps as long as there is fuel in the center tank. These pumps operate through a relief valve and supply fuel to both engines at the same time.

One pump in each of the main tanks is located at the aft end of the tank for nose-up or level flight. The other pump is located farther forward to accommodate nose-down conditions. Either pump is capable of supplying both engines at the same time, although this is not normal operation. In case of an abnormal engine-inoperative condition, there is a cross-feed valve in the front spar of the right tank that allows an engine to be fed from the opposite tank.

There are four float switches in the center tank. Two of the switches start the transfer when there is space in the center tank to accommodate the fuel, and the other two switches turn the transfer off if there is less fuel usage than normal.

A manually operated valve connected to the fill manifold permits defueling the aircraft on the ground through the refueling provisions. Normally, the regular fuel pumps in the tank are used to pump the fuel out through the defuel valve and fill receptacle. The cross-feed valve must also be opened to defuel the left main tank.

Environmental Control Systems. The Environmental Control Systems group at DPG established the ice protection system design requirements for the MD-90-40X composite wing. A thermal analysis was conducted to predict temperatures to which the structure could be exposed during normal ice protection system operation as well as those temperatures and pressures associated with a ruptured ice protection supply duct.

The ice protection system design requirements established for the MD-90-40X configuration are based on the MD-90 airplane. The system has the following characteristics:

- Ice protection shall be accomplished using pneumatic air. The slat skins and slat internal structure shall be metallic to withstand ice protection supply air temperatures during normal operation.

- Overboard exhaust shall be provided as part of the wing ice protection system to ensure proper performance.

- A means shall be provided to prevent the buildup of clear ice on the wing upper surface due to cold-soaked fuel.

A thermal model of the composite wing was created to predict temperatures to which the structure would be exposed during normal ice protection system operation. The case investigated was a 15,000-foot-altitude hold for 45 minutes with a 20°F ambient air temperature. Assumptions used in the analysis were (1) the ice protection system is a double-skin passage-piccolo tube configuration as used on the MD-90; (2) ice protection system temperatures, pressures, and air flow rates used in the analysis were equivalent to those of the MD-90; and (3) the ice protection supply duct and piccolo tube routing is based on the MD-90 design.

Temperatures and fixed leading edge air pressure differential resulting from a ruptured supply duct were determined. The case investigated was sea level takeoff on a 32°F day. For the analysis, it was assumed that the supply duct completely separated, which maximizes the effects of temperature and pressure. It was also assumed that the supply duct would have pneumatic overheat detection sensors adjacent to it similar to the MD-90 installation. Once the surrounding air temperature reaches 180°+10°F, the sensors will transmit a signal to relays, which in turn will close the wing ice protection shutoff valve. The time from duct rupture until overheat detection and ice protection system shutdown could be as long as 20 seconds.

2.3 Outboard Wing Box Detail Design

The cover panels for the full-scale test article are designed using stitched/RFI technology. Six different cover panels are necessary to complete the structural box, three upper (left, right, and center) and three lower. Each panel has integral stringers, spar caps, rib intercostals, and skin buildups co-cured together into a final skin panel assembly. The general structural concepts for the cover panels are shown in Figure 4.

For the full-scale design, the 0-degree direction is parallel to the mid-box axis for the outer wing and the rear spar plane for the center wing box. This was done to keep the fuel access cutouts as far from the spars as possible.

The use of a repeatable balanced stack of layers was used for the full-scale component. Fiber percentages are restricted to fall within a given design envelope for bolted repairs.

The Saertex warp/knit approach uses a 44/44/12 pattern. The fiber areal weight for the 44/44/12 layup is 1425 gm/m^2 with a cured laminate thickness of 0.055 inch per stack. To reduce the warp/knit stack, 0-degree layers are combined in pairs. Because the 0-degree layers would not be held in place by 0-degree stitching, 45-degree fibers are placed on the outer layers of the stack. AS4 fibers were selected as a standard. IM7 fibers were substituted for AS4 fibers in 0-degree layers of tension panels. This fiber selection was baselined for the full-scale component, and for the semi-span wing (this will be discussed in a later section). Stiffening members (stringers, spar caps, and rib clips) are stitched to the skin to form an integral dry perform. The skin between the stringers is also stitched.

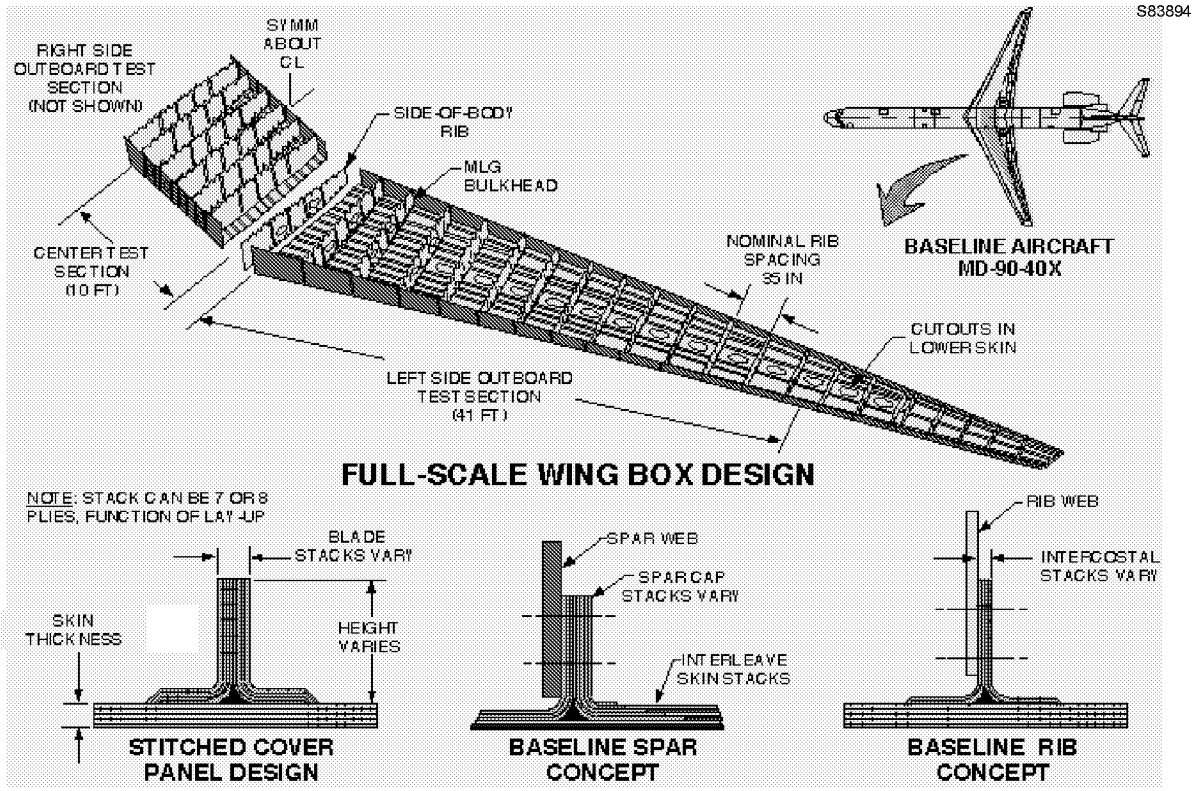

Figure 4. Cover panel structural concept.

In the baseline design, spar caps are similar to stringers but, in addition to carrying spanwise loads, they are also loaded in shear and transverse tension or compression. Three design concepts for an improved cap flange to skin interface were evaluated for the full-scale component:

1. For High Shear Loads: This design concept is used in the semi-span box design and is conservative but costly to fabricate. Skin and spar cap flange stacks are terminated in steps such that when joined together they form a series of staggered butt splices. The whole assembly is then stitched through the thickness to form an integral part of the cover panel dry perform.

2. For Moderate Shear Loads: This design concept would be similar to a stringer section but with a higher stitching density for attaching the flanges to the skin. The strength of this arrangement was established by analysis, and where this strength is exceeded, Concept 1 would be used.

3. For Low Shear Loads: A single stitched resin interface is capable of transferring loads in the lightly loaded regions of the front spar. This concept would be less labor-intensive than the other two, yet it would still provide adequate strength.

The final determination of spar cap configurations depends on the detail design integration requirements and on the established spar cap design values. The approach is to use different concepts at different locations depending on the magnitude of the shear stresses. The front spar, for example, is not highly loaded in shear, and a simple design such as Concept 3 may suffice, whereas the inboard end of the rear spar will require a much stronger design such as Concept 1.

Skin Buildups. In the root splice region, where the outer wings attach to the center wing section, there is a buildup of skin thickness to accommodate the splice bolt loads. In this region, skin thickness is increased to the same level as the stringer flanges, where possible, to present a flush face that will permit the installation of inner splice plates without the need for shimming.

The lower loft surface of the full-span box has significant compound curvature. It was not possible to lay down large Saertex stack pieces on this surface without developing wrinkles and fiber crimping. The selected solution was to cut the stack pieces lengthwise and join them, in the fuel access door region, in a staggered butt-joint fashion. The full-scale wing, having no under-wing engines, has a reduced amount of compound curvature. This, combined with the possible availability of a more loosely knit stack, may make it possible to eliminate the spanwise butt-splice.

Stringers. Both the upper and lower stringers use braided material. The slight drop in modulus for the braided stringers compared to warp knitted stringers can be accommodated and does not affect the final panel strengths or significantly impact final panel weights.

These include the maximum overall height permitted by the stitching machine, blade instability, and the provision of adequate widths to allow bolted repairs. Common stringer configurations and height transitions are used, and where the stringers joggle over a stack drop-off in the skin, a single-taper cut is made in the IML tooling to accommodate the step in stringer height.

For the full-scale wing box design, one stringer is located parallel and next to the front spar and another is located parallel and next to the rear spar. This is done to ensure no interference with internal fittings at discrete load locations (such as flap mounting locations). The remainder of the stringers are oriented parallel to the mid-box plane and run out at rib locations before intercepting the stringers that are parallel to the spars. Stringer planes on both upper and lower surfaces of the full-scale box will be essentially identical in planform to permit rib vertical stiffeners to be parallel.

The basic cross section of stringers is shown in Figure 5. Material for all stringers, upper and lower cover panels, is Fiber Innovations (0±60)-degree triaxially braided tubes. Tubes are folded flat, forming a "stack" that cures out to a thickness of 0.048 inch. Stringers are made in an "onion skin" style with a 14-tube stringer as the largest. By removing the outer stacks on either side of a 14-tube stringer, a 12-tube stringer is formed with the same internal cross-section. This applies to each successively smaller stringer—10 tubes, 8 tubes, etc. Stringers vary in height in 0.25-inch increments, measured from the intersection of the stringer centerline and the IML. This incremental stringer height constraint was imposed to minimize the number of stringer height transitions, which also reduced the manufacturing costs of the full-scale cover panels.

Each tube of the stringer is the same width. Termination of the tubes at the skin IML is shown in Figure 5. An angle of 45 degrees was selected for the flange bevel. When the width of each tube is calculated around the blade-to-flange radius, the outer tubes fall short of reaching the skin.

Fill material in the triangular-like void under the blade will be made of woven carbon fiber that is nearly triangular in shape. Because the void has a constant cross section, with the exception of very minor geometric changes due to the blade-to-flange angle, the fill material is the same for the full length of each stringer. Stringers are made by stacking tubes of correct length, and stitching the blade portion together. Flanges can then be bent out and the stringer stitched to the IML of the skin. The first stitch row defines the tangent point of the radius between the blade and the flanges and is a constant distance from the flange end of the tubes. Blade height can then be trimmed. Note that this trim operation is delayed to the last possible point, after the blade is stitched together.

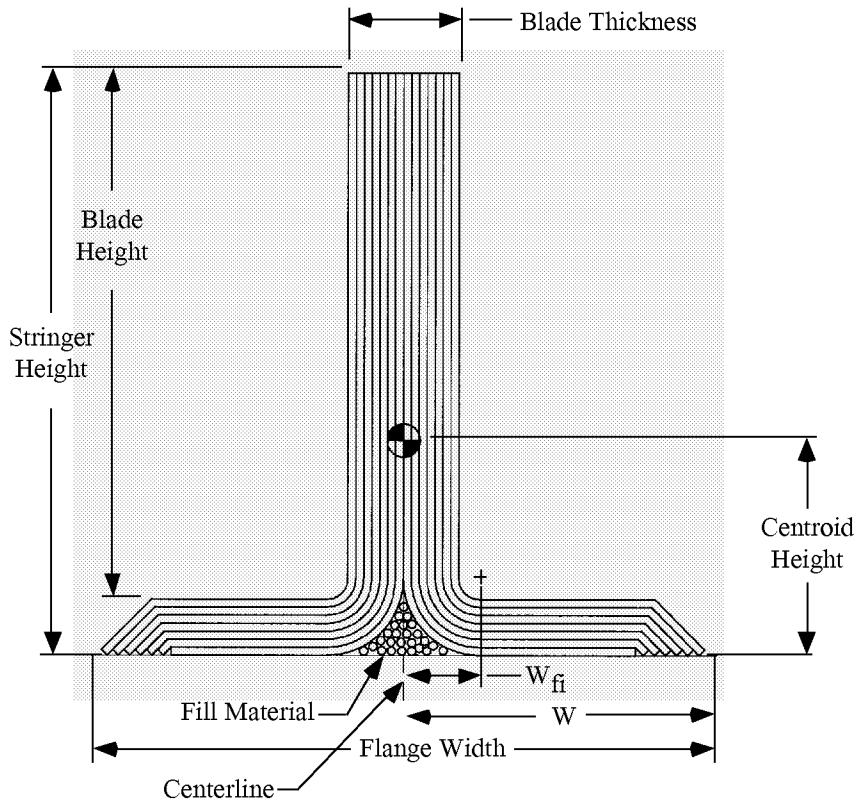

Figure 5. Fourteen-tube stringer.

Substructure Design. Substructure developments on the full-span configuration initially focused primarily on hand lay-up fabrication approaches. The S/RFI approach was subsequently selected for spar webs to meet damage tolerance and bolted joint requirements. Substructure design work for the ribs and bulkheads was limited to structure that provides the necessary strength and stiffness to meet design requirements with limited attempts to optimize the substructure for low-cost fabrication approaches. For the full-scale wing component, preliminary efforts concentrated on establishing design/manufacturing concepts for the ribs and bulkheads that take advantage of low-cost manufacturing processes in a large-scale fabrication environment. The full-scale MD-90-40X wing configuration was still being defined, so the semi-span configuration (Figure 2) was used as a baseline for these studies because it was mature enough to allow realistic cost estimates to be created.

Preliminary design/manufacturing concepts for the full-scale test component substructure were arranged into three categories and evaluated by an Integrated Product Development (IPD) team. The categories were:

- Webs – design/manufacturing concepts pertaining to web fabrication only.
- Stiffeners – design/manufacturing concepts pertaining to stiffener fabrication only.
- Stiffener/Web – design/manufacturing concepts pertaining to combined stiffener/web fabrication.

Main Landing Gear Bulkhead. The main landing gear (MLG) bulkhead was designed from the beginning to be an integrally stiffened aluminum machining. This is in part due to the high concentrated loads introduced to the wing at this location from the braked-roll, takeoff roll, and one-wheel landing load conditions. In addition, previous analyses performed for the semi-span wing indicated that significant stress concentrations existed around the mouseholes for the skin stringers. An optimized composite bulkhead design would require large ply buildups in the area of the mouseholes, resulting in a part that would be very labor intensive and expensive to fabricate by hand layup. As previously noted, all other composite ribs for the full-scale wing were designed with a laminate family tailored for use with an automated tape laying fabrication process to provide for ply drop-offs. The thickest laminate in this family is approximately 0.25 inch. The required thickness near the aft MLG bulkhead mouseholes would need to be significantly thicker and would not necessarily belong to the same laminate family. Thus, a separate setup and run would be required for tape laying the MLG bulkheads, plus the associated costs to store a number of bulkheads if more than one were made at a time. A machined part would allow the use of integral stiffeners in the design, reducing part count. A machined part also allows for the use of local thickness increases near areas of stress concentrations to be inexpensively incorporated.

Center Wing Box

Front Spar Splice. Front and rear spars also splice at the side-of-body bulkhead. The front spar splice is a double-shear joint. Aluminum interior and exterior splice plates sandwich the composite center and outboard front spar webs and caps. Splice plates are dog bone shaped to splice both webs and caps. Two staggered rows of 5/16-inch-diameter bolts are used through each spar web to meet sealing requirements. Six 5/16-inch-diameter bolts through each spar cap transfer the cap loads across the joint. Larger fasteners were preferred. However, the 4.0-inch spar cap height limitation (due to the stitching machine capacity) restricted the size.

Rear Spar Splice

Trapezoidal Panel

The trapezoidal panel is a cantilevered beam attached to the rear spar at the side-of-body joint. It extends aft as a moment arm to react torque in the wing box. The bending loads in the trap panel are transferred to the wing box through an external cap (ski fitting) on the lower surface, which extends forward of the rear spar and mates to the lower skin splice plate. On the upper surface, the base flange of the flex tee extends aft, mating to the top of the trapezoidal panel. Vertical shear loads are transferred through fasteners common to the rear spar splice plate bathtub. In addition, two large tension bolts carry vertical shear loads by fastening through the bathtub portion of the lower external skin splice and the ski fitting.

2.4 Assembly Tooling Design and Build

Assembly Fixture and Build Process. The integral cover panels used in the baseline design greatly simplify the wing box assembly process. Because the rib and spar caps are already stitched and cured to the skin, the substructure details are reduced to flat plates with vertical stiffeners. As the box is assembled, these members are mechanically attached to the integral caps that are part of the cover panel in a manner similar to the semi-span design (see reference 3.0 Semi-Span). The major structural components needed to complete the outboard section of the full-scale wing are shown in Figure 6.

An assembly jig was designed and built to allow assembly of the outer wing boxes (left and right sides). One side of the jig, attached to the upper cover panel, can be moved along tracks to provide access to the ribs and the inner moldline (IML) of the skin panels. Indexing parts on the two sides of the jig ensure repeatable and precise positioning of the upper and lower panels relative to each other when the jig is closed. Fastener holes for attaching the ribs to the intercostals are located and drilled when the jig is open.

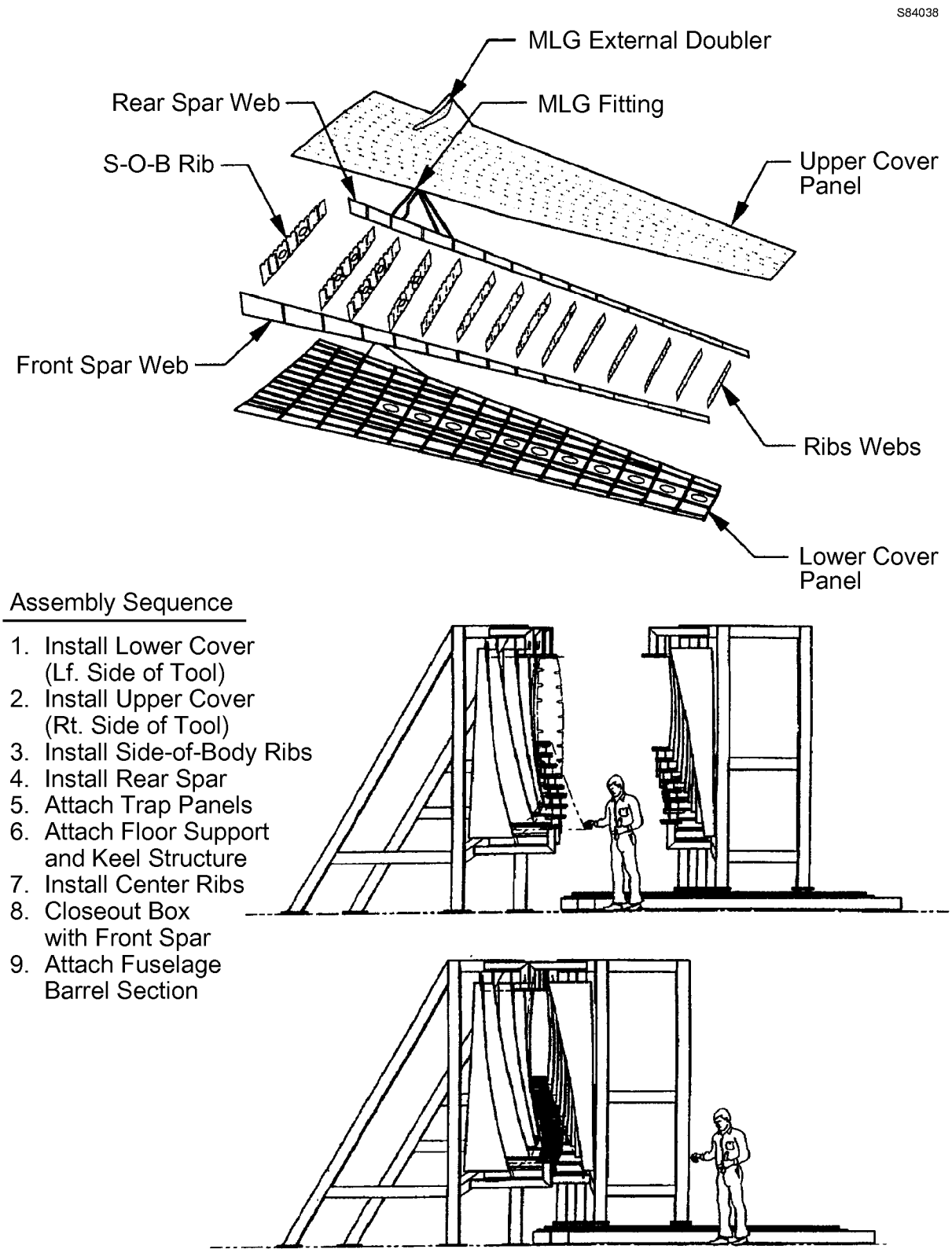

Figure 6. Outboard wing box assembly sequence.

The assembly sequence for the outboard wing boxes is as follows: Assembly would start with installation of cover panels. Rib webs are located on the intercostals using pilot holes. Temporary attachments are used to position the ribs to the upper and lower covers. The lower cover temporary attachments are then removed and the jig is opened with the ribs attached to the upper cover. The attachment holes are then processed in this opened condition. After the jig is closed, the ribs are again temporarily attached to the lower cover. The upper cover temporary attachments are then removed and the jig is opened. Fastener holes in the lower cover are then processed and the permanent fasteners installed. When the jig is again closed, permanent fasteners are used to attach the upper cover to the ribs. The outboard and inboard spar web sections are then located and installed. After the MLG fitting has been craned into position on the assembly fixture, the skin doublers are placed into position and used to attach the MLG fitting to the upper and lower covers of the wing box. The MLG-to-spar web attach angles are then installed. Final close-out of the outboard wing box occurs with installation of the outboard and then inboard front spar web sections.

The two completed outboard boxes are then joined to the center wing box at the side-of-body (SOB) bulkhead. The center wing box is then assembled around each outboard wing. Once the entire wing is completed, it would be mated with a section of fuselage barrel. The full-scale test article would then be complete, and installation of the load application/reaction hardware would be initiated.

2.5 Full-Scale Composite Wing Structural Verification

Testing Considerations and Development

The full-scale test component consists of a composite wing box attached to an aluminum fuselage barrel. The approximate overall dimensions of the component relative to the MD-90-40X airplane baseline are shown in Figure 7. The fuselage barrel is supported at each end and the wing is loaded by a series of load jacks. Apart from the features that affect load transfer across the wing/fuselage interface, the fuselage itself will not be evaluated during the test.

The objective of the test program was to validate the structural integrity of the design by subjecting the test component to a variety of load conditions that closely simulated the actual flight loads of the baseline aircraft. This close simulation is of critical importance, because the weight and cost of the aircraft must be accurately predicted based on the design and performance database developed for the full-scale test component.

The testing approach selected for the full-scale wing is a commonly used technique that approximates the flight loads environment for the ground testing of large-scale wing structures. To truly replicate the flight conditions, the applied loads must be proportionally distributed across both the upper and lower surfaces of the wing box as pressure forces. Because this is difficult to achieve, and would place a constraint on the out-of-plane deformations of skin elements, a more practical approach is to apply individual point loads at discrete locations on the wing. Then, as the number of point loads is increased, the discrete loading will more closely resemble the continuous pressure distribution of a true flight condition. Fabrication and testing of the full-scale wing was not conducted due to NASA funding constraints and subsequent reductions in program scope.

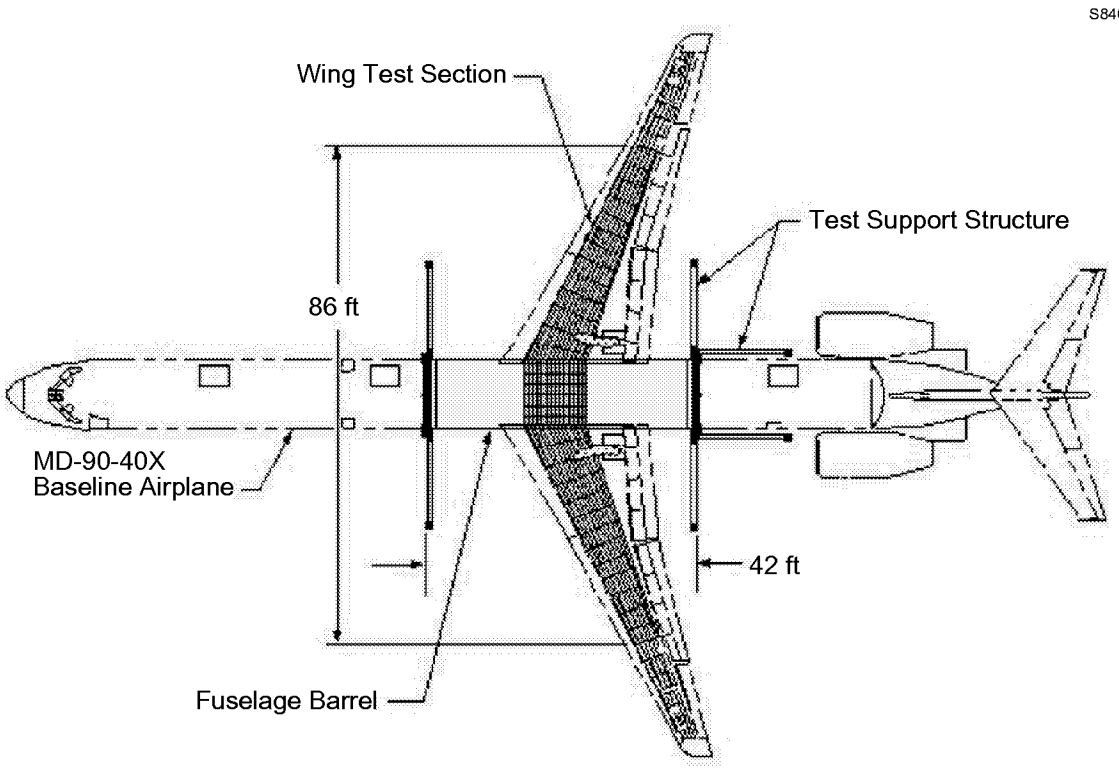

Figure 7. Full-scale wing test arrangement.

2.6 Weight Trade Study Results and Summary

Trade Study Results

The composite wing box weights are summarized in this section for one side of the outboard wing box. Each cover panel includes the skin, stringers, spar caps, and intercostals. In the following discussion, the skin with stringers, spar caps, and intercostals will be referred to as the cover panel. The substructure includes the spar webs, rib webs, stiffeners, and rib-to-spar attach brackets. The results are discussed below.

The composite wing box weight results, both in the room temperature/dry and in the extreme environmental conditions, are shown in Figure 8. Because of the reductions of design strength values in hot/wet and cold/dry conditions, the weights of upper and lower covers and skin pad-ups in the extreme environmental conditions are slightly higher than those in the room temperature/dry condition. The total weight of the fasteners remains the same because they are made of metal and influences from extreme environmental conditions are minor. The total weight of the substructure changes slightly only because they were designed mainly from the stiffness requirements. It is noticed that even though the weights of upper and lower cover panels increase slightly, the weight percentages of structural components are similar in the RT/dry and in the extreme environmental conditions. The cover panels, including the skin pad-ups, make up 75% (in the RT/dry condition) or 76% (in the extreme environmental conditions) of the total weight. The substructure makes up 20% (in the RT/dry condition) or 19% (in the extreme environmental conditions) of the total weight, and the fasteners make up 2% of the total weight of the composite wing.

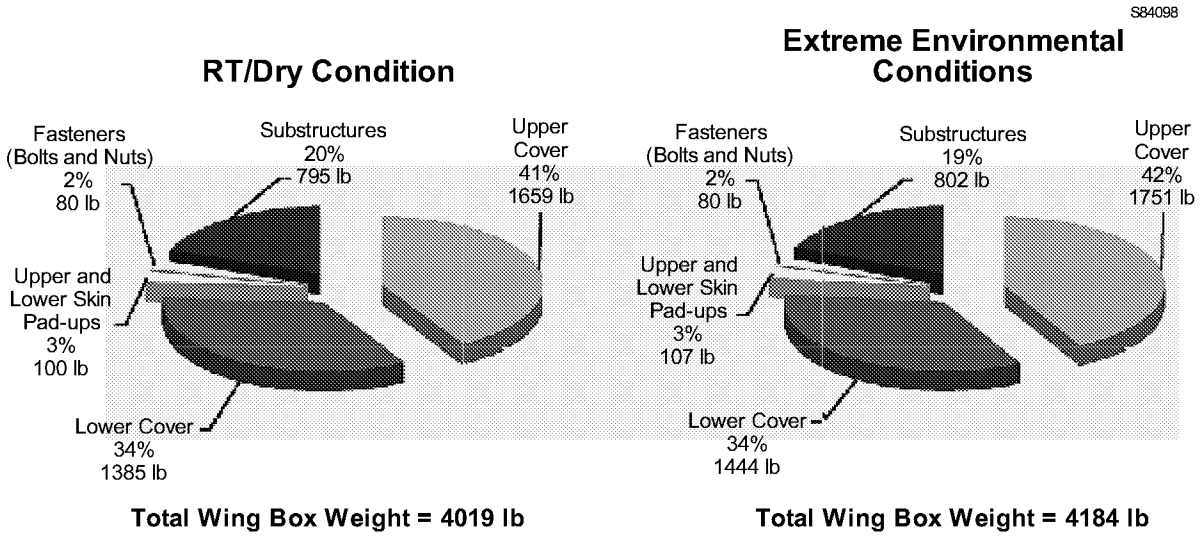

Figure 8. Composite wing box weight summary.

Figure 9 compares the weights of the upper and lower cover panels. The upper skin is heavier than the lower skin (895 pounds versus 761 pounds in the RT/dry condition and 974 pounds versus 803 pounds in the extreme environmental conditions). Also, the upper stringers/caps are heavier than the lower stringers/caps (694 pounds versus 544 pounds in the RT/dry condition and 707 pounds versus 561 pounds in the extreme environmental conditions). This is because the upper cover was mainly designed by compression loads, and the lower cover was mainly designed by tension loads in the 2.5-g upbending condition. The stringent CAI strength and structural stability criteria imposed on the upper cover (for compression) gave it some weight penalty over the lower cover. Another reason for the lighter lower cover is that the IM7/AS4 hybrid fibers were used in the lower skin and the AS4 fibers were used in the upper skin as the basic fabrics. The IM7/AS4 hybrid fibers outperformed the AS4 fibers in tension properties and gave the lower cover some weight saving advantages over the upper cover.

The weight breakdowns of each cover panel are shown in Figures 10 and 11. It is interesting to note that in both cover panels, the upper and lower skin weights make up similar percentages (54% and 56% for the upper and 55% for the lower) of the panel weights.

Substructure weights are summarized in Figure 12. Because substructures were designed mostly by stiffness requirements rather than by strength criteria, their weight differences are minimal in the RT/dry and in the extreme environmental conditions. The substructures include the spars, ribs, and bulkheads but not the side-of-body bulkhead or any external fittings. The weights in Figure 12 also exclude fasteners and spar access hole cover panels. The front spars make up 23% (in the RT/dry condition) or 24% (in the extreme environmental conditions), the rear spars make up 21%, and the ribs make up 38% of the substructure weight. Also, the MLG bulkhead makes up 10% (in the RT/dry condition) or 9% (in the extreme environmental conditions) and the rib/spar attachment brackets make up 8% of the substructure weight.

S84099

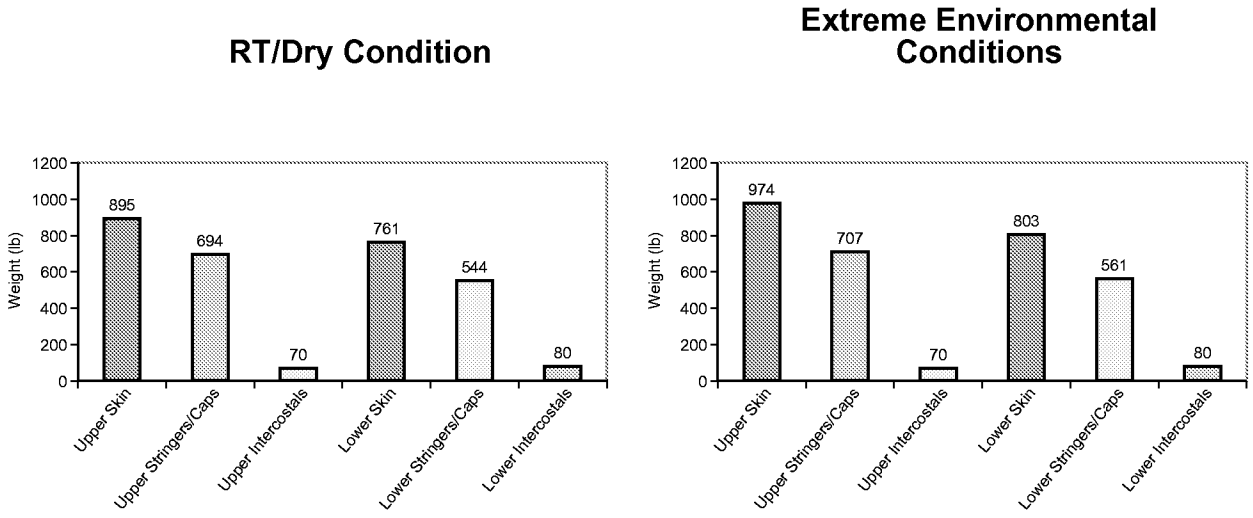

Figure 9. Comparison of composite wing upper and lower cover panel weights.

S84100

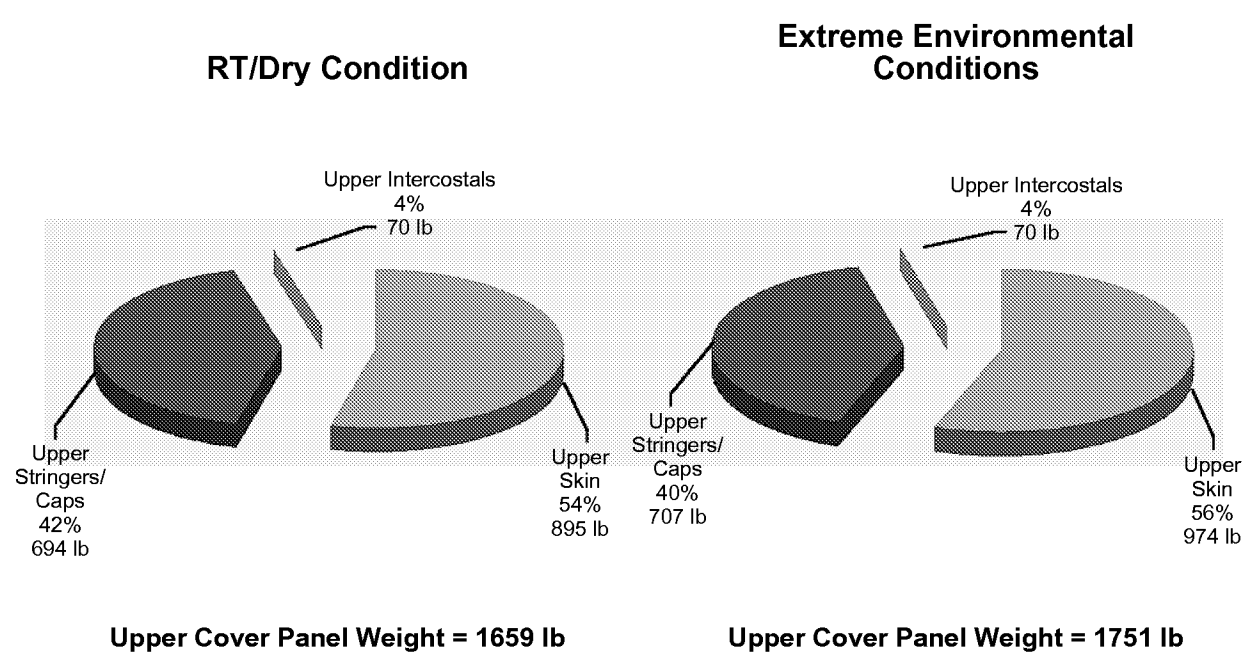

Figure 10. Composite wing upper cover panel weight breakdown.

The weight savings of the composite wing in the trade studies are listed in Table 1. This table includes results of the composite wing both in the room temperature/dry condition and in the extreme environmental conditions. Weights of the aluminum wing, with wing tip deflection imposed as a constraint, are used for the weight saving calculations. The results show that the total weight saving for the composite wing box over the aluminum wing box is 32.4% in the RT/dry condition and 29.6% in the extreme environmental conditions. Structural components in the extreme environmental conditions show

S84101

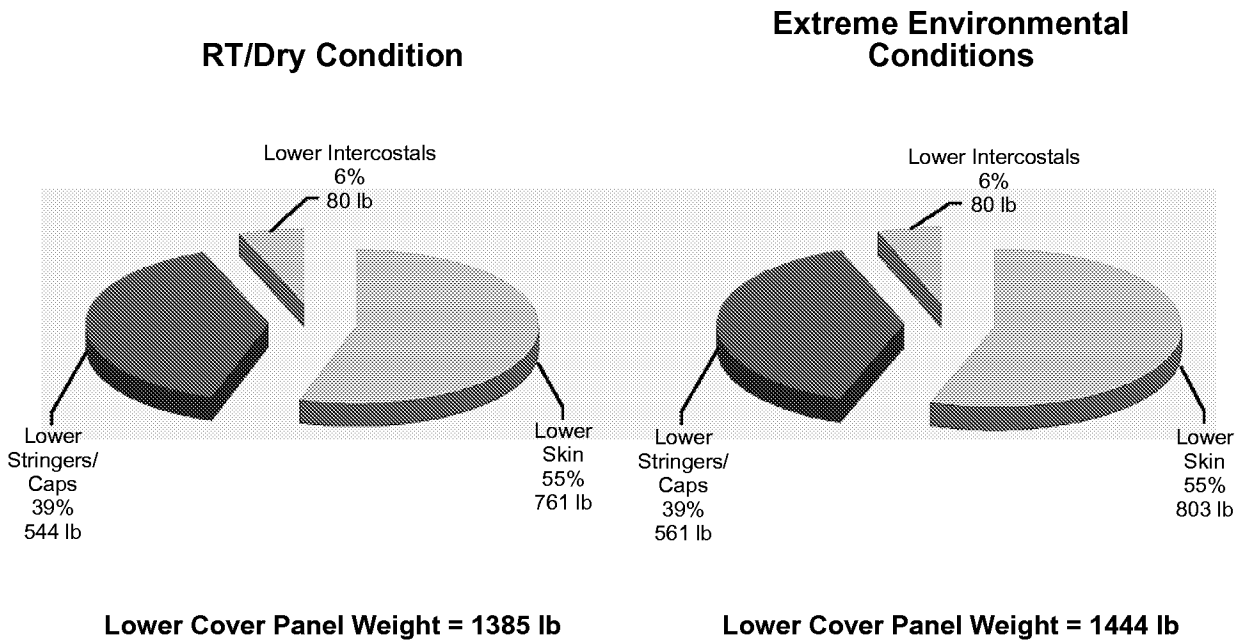

Figure 11. Composite wing lower cover panel weight breakdown.

S84103

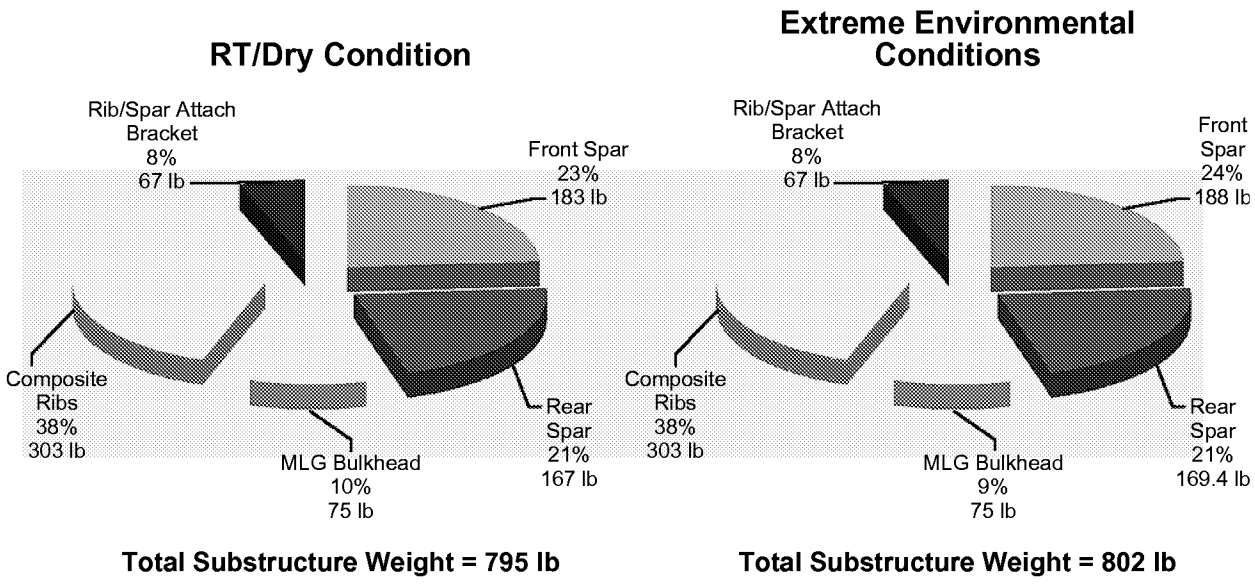

Figure 12. Composite wing substructure weight summary.

a weight saving of 24% for the upper cover, 39% for the lower cover, 24% for the spar webs, 26% for the ribs/bulkheads, -26% for the rib/spar shear clips and attachment brackets, 11% for the bolts and nuts, and 32% for the pad-ups.

Table 1. Weight Savings of Composite Wing in Room Temperature/Dry and Extreme Environmental Conditions

Components	Aluminum Wing Weight (lb.)	Trade Study (Baseline) Stitched/RFI Composite Wing (at Room Temperature/Dry) Weight (lb.)	Comp/AL Wt. Ratio	Part Wt. Saving (%)	(w/ Environmental Effects) Weight (lb.)	Comp/AL Wt. Ratio	Part Wt. Saving (%)
Upper Skin	1212	895	0.74		974	0.80	
Upper Stringer	664	542	0.82		552	0.83	
Upper Spar Cap	407	152	0.37		155	0.38	
Upper Intercostal (or Shear Clip)	30	70	2.36	28%	70	2.36	24%
Lower Skin	1588	761	0.48		803	0.51	
Lower Stringer	536	413	0.77		425	0.79	
Lower Spar Cap	210	131	0.62		136	0.65	
Lower Intercostal (or Shear Clip)	17	80	4.72	41%	80	4.72	39%
Front Spar Web	235	183	0.78		188	0.80	
Rear Spar Web	232	167	0.72	25%	169	0.73	24%
Ribs (excluding MLG Bulkhead)	422	303	0.72		303	0.72	
MLG Bulkhead	89	75	0.84	26%	75	0.84	26%
Rib/Spar Shear Clip & Attach. Bracket	53	67	1.26	-26%	67	1.26	-26%
Bolts & Nuts	90	80	0.89	11%	80	0.89	11%
Pad-up (at SOB)	5	25	4.91		26	5.27	
Pad-up (at MLG)	4	31	7.63		33	8.18	
Pad-up (at Access Holes on Lower Cover)	149	45	0.30	37%	47	0.32	32%
Total (lbs. or Saving):	**5942**	**4019**		**32.4%**	**4184**		**29.6%**
Weight Saving (%)		32.4%			29.6%		

Summary

In the trade studies, tension and compression repair design values (in the RT/dry condition) were obtained from single-repair tests with non-test-section (or premature) failures. The tension repair test, which failed in the grips with a total load of 822 kips, generated a design stress of 50 ksi for the upper cover panels (with all AS4 fibers in the fabric) and 55 ksi for the lower cover panels (with IM7/AS4 hybrid fibers in the fabric). The compression repair test, which failed at the bolt hole of the supporting structure with the test rib subjected to a load of 863 kips, generated a design stress of -45 ksi for both the upper and the lower panels. However, the above noted tension repair design values (50 ksi for upper cover panels and 55 ksi for lower cover panels) and compression repair design values (-45 ksi for both upper and lower cover panels) are considered to be too conservative. Since there is no other justifiable repair design values to use at the time the trade studies were performed, these low repair design values were still used in the analysis.

The optimal airfoil and planform configurations chosen for the generic 220-passenger aircraft composite wing resulted in an aspect ratio of 12.1, which is too high for the aluminum wing. Generally, the aspect ratio of production aluminum wings is around 8.5. The advantage of using the high aspect ratio for the composite wing is to be able to achieve a better aerodynamic performance. However, using the high aspect ratio for aluminum wings generates a high wing tip deflection that makes designers worry about the wing's aileron effectiveness and aeroelasticity effects (such as flutter). Therefore, deflection constraint, which is similar to applying the equivalent bending stiffness as the composite wing, was imposed on the wing tip of the aluminum wing. The aluminum wing weight was re-calculated by imposing a stiffness constraint that required the wing tip deflection of the aluminum wing to be the same

as that of the composite wing. The aluminum wing results from this study showed that a 1010-pound weight would be added to the aluminum wing if the bending stiffness (or wing tip deflection) constraint was imposed. This made the weight savings of the composite wing over the aluminum wing become 32.4% for the RT/dry condition and 29.6% for the extreme environmental conditions. The stiffness requirement imposed on the aluminum wing has been a common practice in other past composite programs. A more realistic comparison between aluminum and composite structures (wing, fuselage and tail) should be made at the full-scale airplane level rather than the component level. Re-sizing of the airplane could have significant weight implications.

The results from trade studies show that most of the weight saving came from the lower wing cover. The upper cover, which is subjected to the CAI strength limitation, had smaller weight saving compared to the aluminum upper cover. It is well understood that stitching improves the composite CAI strengths of the composite structures, particularly for thick laminates. However, the CAI strengths of the thin laminates with stitching are still low. Therefore, future studies should investigate how to improve the CAI strengths for the thin laminates with stitching.

The NASA Advanced Subsonic Technology (AST) Composite Wing Program was established to demonstrate the feasibility (cost and weight) of fabricating composite primary wing structures for future commercial transport aircraft. It is understandable that the future composite wing box for commercial aircraft will be somewhat different from the AST composite wing, but it is believed that many of the obstacles have been evaluated in the AST program. During the course of the trade studies, several critical design factors, which had impact on the final weight savings, were discovered. Most of the factors are related to composite wing design. Some of them were well understood before the trade studies were conducted, and others were discovered doing the trade studies. Observations from the trade studies on the design of a stitched composite wing box are as follows:

1. The current organic resin system (3501-6 epoxy) used in the RFI process must be replaced by a more advanced resin system because the strength reductions for the 3501-6 in extreme environmental conditions are too high.

2. The stitching fibers (Kevlar 29) currently used in the manufacturing process are very moisture-absorbent in wet conditions. It is suspected that the reductions of the CAI strengths in the hot/wet condition are the results of using this type of stitching fiber. It is preferable to use less moisture-absorbent stitching fibers for future designs. Resin/fiber combinations that are micro-crack resistant should be evaluated.

3. The CAI strengths for the upper cover are low for thin-laminate structures, even with stitching. The low strengths had a significant impact on the weight savings in the wing tip area. A more impact-resistant resin should be considered for the upper cover in order to achieve a higher weight saving.

4. The composite intercostals are much heavier than the butterfly clips used for the aluminum wing. It is suggested that the intercostal design concept be further investigated in future composite wing designs from a weight and manufacturing cost consideration.

5. The torsional stiffness of the composite wing is less than the stiffness of the aluminum wing. As a result, the composite wing tip twists more than the aluminum wing. This can be improved by using more 45-degree fibers in the fabric. The contents of the 0-, 45-, and 90-degree fibers should be optimized for future composite wing designs.

6. The non-buckling design requirement at DUL on the upper and lower covers may be too stringent. A different criterion, which allows the skins to buckle at DLL, should be investigated and analytically validated by large component tests.

3. Semi-Span Wing Design, Analysis, and Supporting Technology

A specific objective of the semi-span wing development was to demonstrate technology readiness through processing, scale-up, and structural testing. This semi-span wing box was initially aimed at developing and verifying design and manufacturing techniques to be used in the design, manufacture, and test of a follow-on full-scale aircraft wing.

To develop detail design features of a composite wing, along with the associated analytical and manufacturing techniques, a representative composite wing box structure was established. The wing box was derived from an aircraft representative of the next generation of commercial aircraft. This next-generation twin-engined aircraft carries up to 220 passengers. It has a supercritical airfoil wing with an aspect ratio of 12:1 that was optimized using composite material properties. The semi-span test box represents the first 42 feet of the wing starting from the aircraft side-of-body splice out towards the wing tip (Figure 13).

The semi-span wing box consists of an upper and lower S/RFI cover, two spars, and 18 ribs. The rib spacing is a nominal 30 inches. To take advantage of the S/RFI process, many components were integrated into the cover panels to reduce the assembled part count, thousands of fasteners, and their associated costs. Each cover panel consists of multiple stacks of uniaxial warp knit carbon fiber material that is stitched together to form the wing skin. Additional structural details are also stitched into the skin panel to form an assembly: blade stiffeners to give added stability, and interleaved spar caps and intercostal clips for substructure attachment. The completed dry preform assembly (Figure 14) is then placed inside rigid tooling and infused with resin in an autoclave. The spacing between the stringers was set at 7.6 inches. As a comparison, typical aluminum wing panels normally have a 6.5-inch stringer spacing.

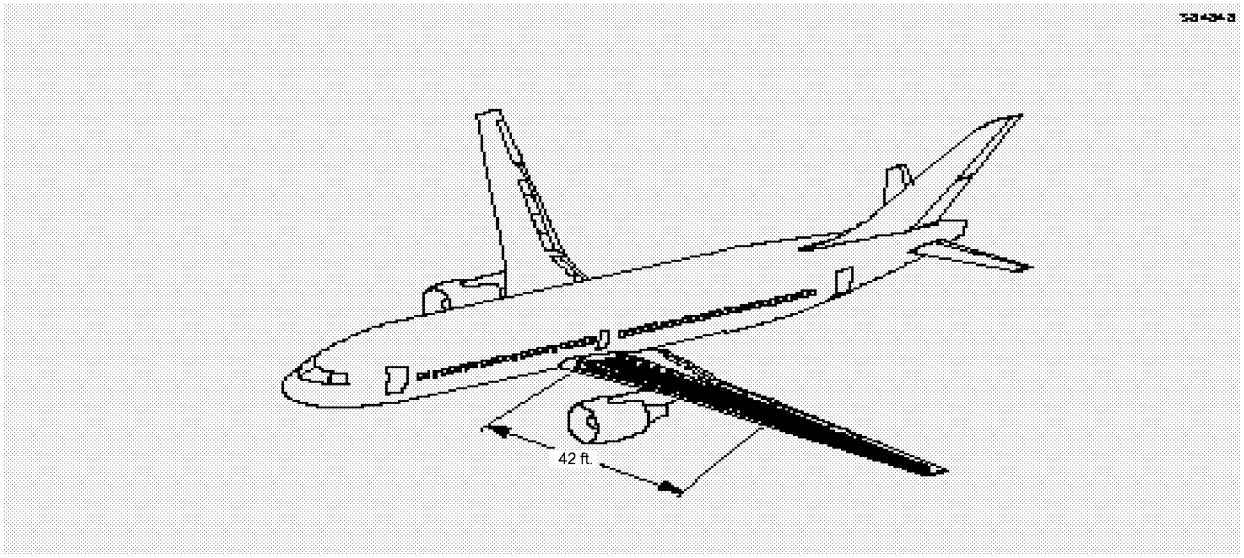

Figure 13. Baseline aircraft configuration and 42 foot Semi-Span composite wing.

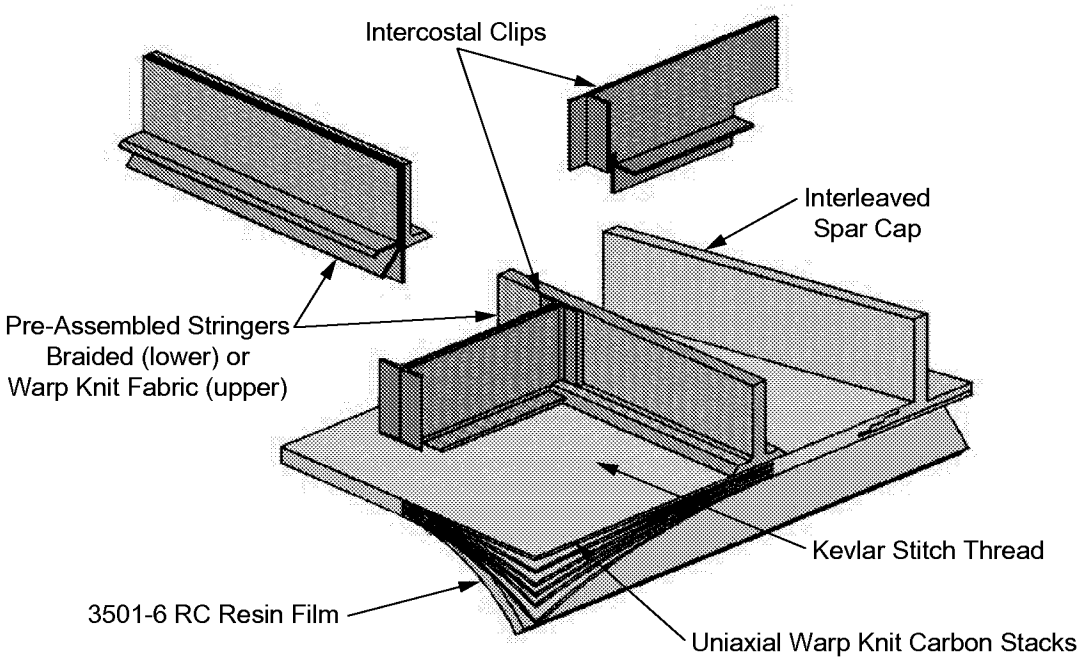

Figure 14. Integrated cover panels.

The semi-span substructure consists of ribs, bulkheads, and spar webs. The ribs and bulkheads are made of conventional tape layup carbon composite prepreg. The spar webs are S/RFI multiaxial warp knit material dominated by 45-degree fibers. The substructure stiffening elements are fabricated by secondarily bonding precured stiffeners to precured flat webs. The ribs and bulkheads have predetermined pilot holes. The spar webs are drilled full size in place with the covers using drill templates prior to bonding of the stiffeners. The substructure is assembled to the cover panels using mechanical fasteners to complete the box assembly (Figure 15).

The semi-span wing box is not an optimized wing box design. It does, however, contain many important design features which have emerged as potential solutions to issues that need to be addressed in the design of an S/RFI composite wing box for commercial aircraft applications. They include:

Stringer and spar cap blade height and thickness transitions.
Interleaving of the spar caps.
Metallic fittings at load-introduction points.
Tight tolerance planer mating surfaces (no shims).
Stringer transitions over skin stacks.
Buildups for root splice and off-axis material buildup at MLG attachment.
Spanwise stack splice.
Strengthened intercostal tab attachments with mechanical fasteners.
Access and systems cutouts in the lower cover, spar webs, ribs and bulkheads.
Internal and external skin stack terminations both chordwise and spanwise.
Inboard (joint) and outboard stringer runouts.
Spar cap darting.
The use of filler material in the intercostal-to-stringer flanges.

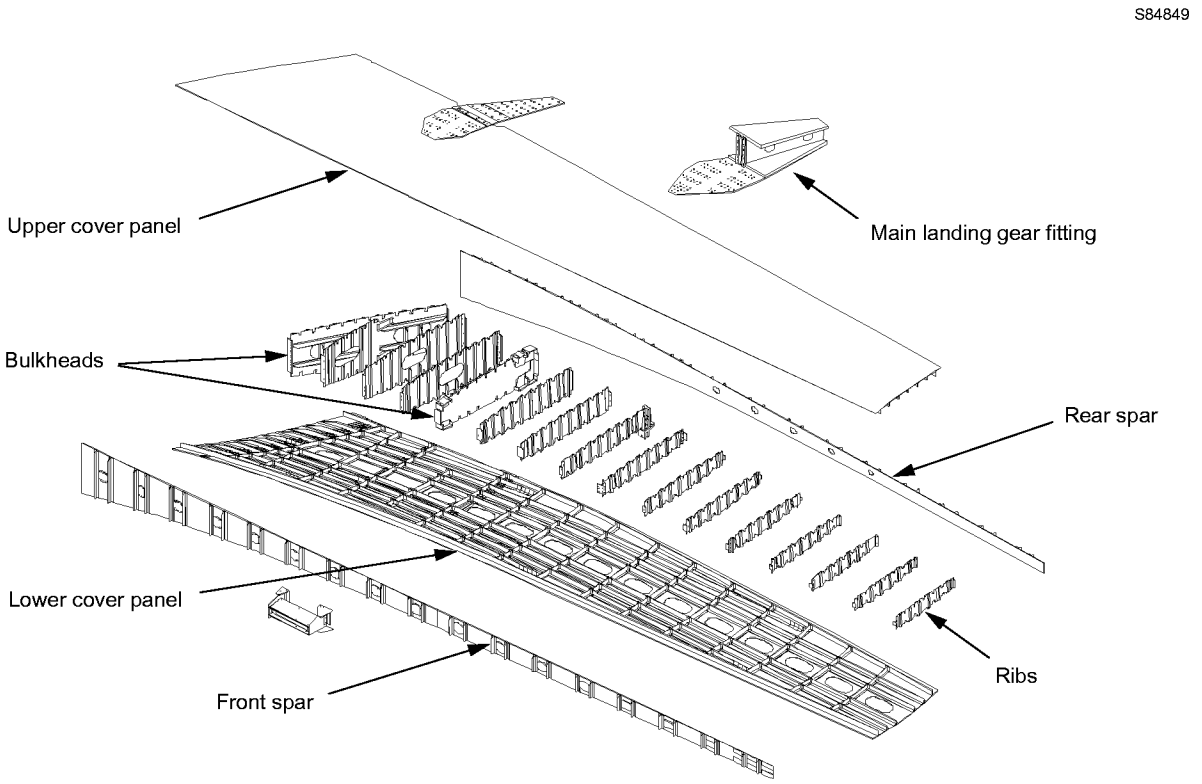

Figure 15. Semi-Span wing box.

Limited access at the wing tip.
Box assembly (drilling and the installation of fasteners).
Damage tolerance and discrete source damage repair.

The completed wing box was shipped to the NASA Langley Research Center, where it was mounted to a test wall and tested to demonstrate that the above wing box features and the techniques needed to fabricate and assemble it can be used to build next-generation aircraft. Loads were introduced with hydraulic jacks to simulate representative aircraft design requirements. A series of tests concluded with the box being damaged by impact, repaired, and tested to design limit load and then to the ultimate failure load.

Analysis Introduction

This section presents the stress analysis for the advanced subsonic technology (AST) semi-span composite wing box fabricated under NASA contract NAS1-20546. The baseline aircraft selected for this study is the D-3308-4 configuration of the proposed Boeing 220-passenger, single-class, transport aircraft shown in Figure 15. The design weights for this aircraft are maximum take off gross weight (MTOGW) = 180 kips and maximum landing weight (MLW) = 167.5 kips. The semi-span wing component is a proof-of-concept test article that will reduce the manufacturing risk for fabrication of a full-scale composite wing. The semi-span wing box does not include optimized stringer and rib spacing. The semi-span composite wing box is based on a nonbuckled design.

The semi-span composite wing box is 42 feet long, measured along the front spar span, extending from the side-of-body to station Xrs = 545. The wing box test article was mounted to the Langley strong-back and has been static tested (Figure 16). The semi-span composite wing considers five basic design conditions for analysis: (a) 2.5-g upbending, (b) -1.0-g downbending, (c) braked roll, (d) 9.0-g forward emergency landing, and (e) 15-psi fuel overpressure. In addition the wing is tested for discrete-source-damage at 70% of 2.5-g DLL and with repairs including undetectable damage at 2.5-g upbending DUL. The test loads are applied to the wing box structure by eight discrete actuator load points. The main landing gear loads and engine dead weight are introduced into the wing box by a dummy gear fitting and a dummy pylon structure.

Structural Arrangement

The composite wing box is a conventional two-spar wing design. The semi-span wing structural test article is a truncated representation of the baseline left-hand side structural box and extends from the side-of-body for a length of 42 feet, measured along the front spar (Figure 13).

The semi-span wing test article consists of upper and lower cover panels, front and rear spars, ribs, and bulkheads (Figure 17). The major components are the integrally stiffened cover panels. Each contains skin, stringers, spar caps, and intercostal clips. These subcomponents are stitched together to form a single dry-fiber preform, which is then infiltrated with resin and cured by the resin film infusion (RFI) process. The spar webs are also stitched RFI components. The ribs and bulkheads are carbon-fiber tape layed with no stitching.

S84846

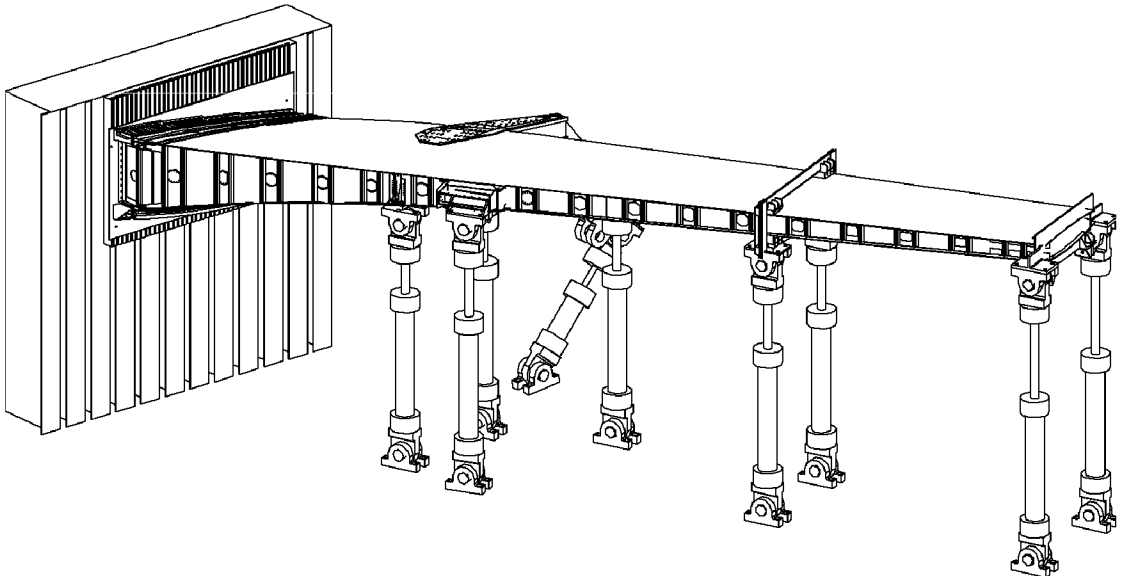

Figure 16. The Semi-Span composite wing test article mounted to the Langley strongback.

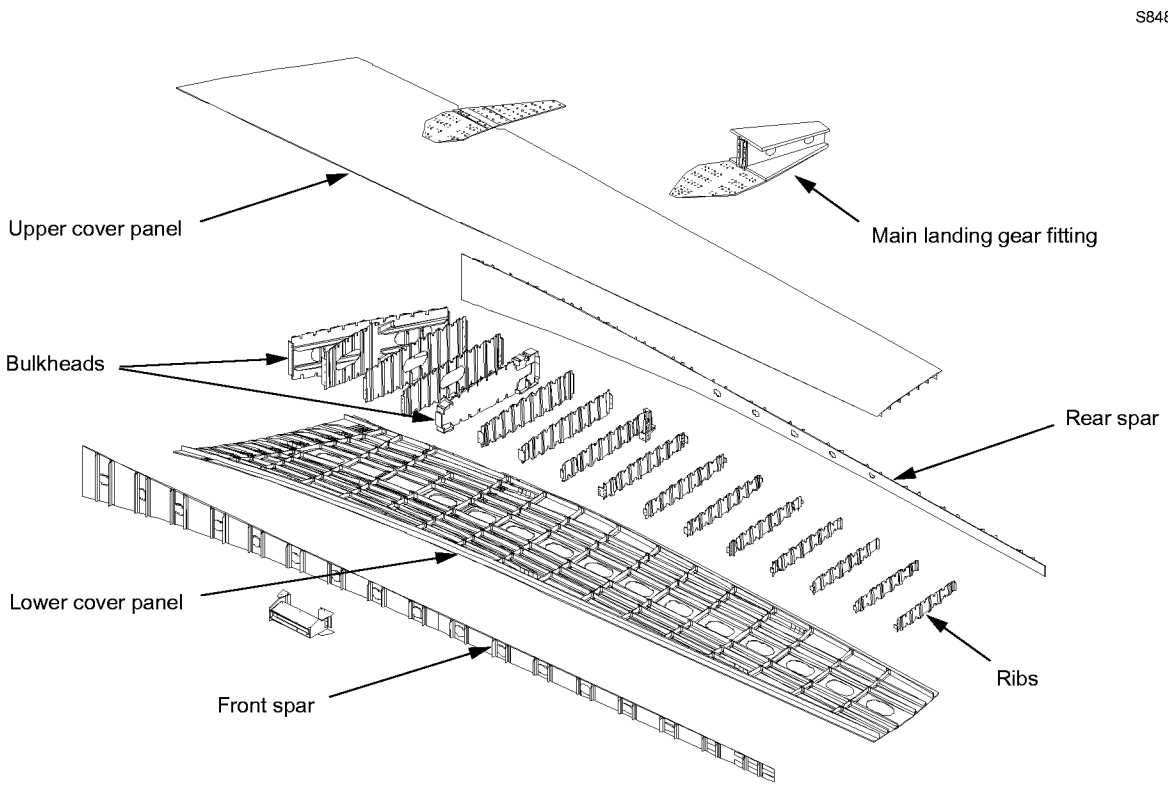

Figure 17. Semi-Span structural arrangement.

There are a series of access holes in the lower cover panel at mid chord. The spar webs contain access holes that represent location for the installation of control system features such as slat cans and fuel in the front spar. The wing box also contains simulated mounting points for the engine pylon attachment. Rib 6, the main landing gear bulkhead serves as a fuel barrier between the inboard and outboard fuel tanks. The skin buildup at the wing root simulates a feature of a side-of-body splice, where the wing meets the carry through structure.

Material Definition. The semi-span wing program uses carbon/epoxy composite laminates, which consist of either dry-fiber multilayer stitched preforms or 2-D triaxial braided stitched preforms for the lower cover stringers. A reduced catalyst 3501-6 resin is used in the resin-film-infusion (RFI) process to impregnate the dry fiber preforms.

The composite fabric materials used in the semi-span composite wing laminates are listed in Table 2.

The Saertex warp/knit fabric is designated as DMS2436D Type 1 and Type 2. This material is a multiaxial carbon fiber fabric. Type 1 laminates consist of AS4 fibers only. Type 2 laminates consist of IM7 fibers in the 0-degree direction and AS4 fibers in the 45- and 90-degree directions. The laminate classes also specify the fiber pattern (0°/45°/90°). Class 72 and Class 74 have fiber pattern percentages of (44.9/42.9/12.2) and (30.0/59.9/10.1) respectively.

Table 2. Semi-Span Composite Wing Cover Panel and Spar Laminates

Upper Cover Skin	DMS-2436D, Type 1, Class 72
Lower Cover Skin	DMS-2436D, Type 2, Class 72
Spar Web	DMS-2436D, Type 2, Class 74
Upper Spar Cap and Stringers	DMS-2436D, Type 1, Class 72
Lower Spar Cap	DMS-2436D, Type 2, Class 72
Intercostals	DMS-2436D, Type 2, Class 72
Lower Stringers	Triaxial Braided composite

The Fiber Innovation braided fabric has no Boeing material specification currently. This material is a 2-D triaxial braided fabric that consists of (0±60)-degree braid, AS4 6k bias fibers, and IM7 36k axial fibers. The bias fibers and axial fibers make up, respectively, 56% and 44% of the total fibers.

The lower cover skin and spar caps use Type 2 laminates because they have higher tensile strength. Other structural members using Type 2 laminates include the spar webs and intercostals. The upper cover skin, stringers, and spar caps use Type 1 laminates because they have higher compression strength. The lower stringers use the triaxial braided composite material because of the lower surface curvature of the lower cover panel. The bulkheads and ribs are stiffened panels that use a carbon/epoxy (AS4 fibers/3501-6 resin) prepreg tape DMS 2224 material. For example bulkhead 6 is 0.55 inch thick with a quasi-isotropic lay-up, ribs 7-17 are 0.143 inch thick with a [0, 0, 45, -45, 90, 0, 45, -45, 0, 90, 45, -45, 0]s lay-up [Reference 3].

Design Criteria

This section defines the criteria used to design the semi-span composite wing box. The design criteria address strength, stability, reparability, and damage tolerance requirements.

Cover Panels

The semi-span wing cover panels consists of two cover panels, upper and lower. Both upper and lower cover panels contain skins, stringers, spar caps, and intercostal clips, which are stitched together in a dry carbon-fiber preform and then infiltrated with resin and cured by the resin film infusion (RFI) process. The detailed design of the semi-span was completed in NASA contract NAS1-18862 [References 1, 2].

The cover panel critical design condition is the 2.5-g upbending case. The other loading conditions (-1.0-g downbending, braked roll, 9.0-g forward emergency landing, and 15-psi fuel overpressure) are generally not critical for the cover panel structural integrity with the exception of the main landing gear region. Braked roll is also a critical case in this region. The following design criteria applies to the semi-span wing.

The maximum number of skin stacks and stringer flange tubes together shall not exceed 17 (the stitching machine's current limitation).

The minimum stringer blade height-to-thickness ratio is 5 to 1 (to ensure an adequate edge distance for repair for fittings and attachments).

The maximum stringer height-to-thickness ratio is not constrained, but the blade height-to-thickness is limited by buckling and crippling checks.

The stringer blade height shall be greater than five times the repair bolt diameter.

The maximum total height of the stringer blade plus the skin thickness shall not exceed 4.00 inches (the stitching machine's current limitation).

The minimum stiffening ratio ($AE_{stringer}/AE_{skin+stringer}$) is 0.35 (for crack propagation) for both upper and lower cover panels. This is required to prevent discrete source damage from growing beyond the adjacent stringers and causing a catastrophic failure.

The stringer flange thickness-to-skin thickness ratio shall be greater than 0.5 (this is also for crack propagation prevention).

Structural stability: The semi-span composite wing box is based on a nonbuckled design. This includes general (global) buckling of cover panels, local (lateral and torsional) buckling of the stringer blade, and local buckling of the skin panel. The minimum margin of safety for general (global) buckling (Euler mode) of the cover panels at DUL is 0.15. The minimum margin of safety for local lateral and torsional buckling of a stringer blade at DUL is 0.10. The minimum margin of safety for skin panel local buckling at DUL is 0.00.

Discrete source damage: Maximum damage size consists of severing one stringer and the adjacent skin bays up to, but not including, the adjacent stringer flanges. The maximum running load carrying capability for this type of damage is 70% of DLL due to maneuver loads.

Impact damage limits: The impact energy is less than or equal to 100 ft-lb on the external surface of the upper and lower skins. The impact energy is less than 20 ft-lb on the internal surface of skins, stringers, and intercostal clips.

Detectable damage: The indentation caused by impact on the composite surface exceeds 0.10 inch.

Undetectable damage: The indentation caused by a static indentation load on external surface of the skin is 0.10 inch or less. The composite wing box is required to carry 100% of DUL with undetectable damage.

Reparability: All detectable and discrete source damage will be repaired, and all structure repaired shall carry 100% of DUL.

Spars. The semi-span composite wing spar caps and webs are designed as nonbuckled structure and are subjected to the same load conditions described for the cover panels.

Structural stability: The semi-span wing spars are a nonbuckled design with a minimum buckling margin of safety of 0.15.

Impact damage limits: The spars are considered internal structure and are required to meet the 20 ft-lb impact energy criteria and still carry 100% DUL.

9.0-g crash: The front spar is subjected to significant pressure loads in a crash and must contain the fuel within the wing box in this event.

A double row or staggered double row of fasteners is required to attach the spar web to the upper and lower spar caps to prevent fuel leakage.

Ribs and Bulkheads. Structural stability: The semi-span wing ribs and bulkheads are a nonbuckled design with a minimum buckling margin of safety of 0.15.

Impact damage limits: The ribs are considered internal structure and are required to meet the 20 ft-lb impact energy criteria and still carry 100% DUL.

9.0-g crash: Bulkhead 2 and the main landing gear Bulkhead 6 are subjected to large lateral pressure loads. All other ribs are not subjected to large lateral pressure loads.

To minimize costs, the composite ribs are designed with as much commonality as is practical to allow batch processing of multiple ribs. The ribs have a carbon-fiber tape laid construction and are not optimized for weight. Composite rib stiffeners are a common type that can be cured in long lengths and then cut to size.

A positive margin of safety is required for stiffeners in both crippling and strength checks.

A positive margin of safety for minimum rib stiffness (enforcing a node) is required to ensure the skin cover will buckle between ribs and not over multiple rib bays.

Load Introduction Hardware. All test hardware shall be designed to have an additional factor of safety of 1.5 applied to ensure that failure occurs within the test specimen region.

Global FEM. A NASTRAN global finite element model of the semi-span composite wing box was created to develop internal loads for the wing box structure. The global model is also intended to provide a basis from global/local analyses which, detailed models of such components as the main landing gear bulkhead, stringer runouts, access hole cutouts on the lower cover panel, and side-of-body splices are created.

The global FEM is a symmetric half-shell model (Figure 18) consisting of a left wing. The wing box section extends from the side-of-body to the Rib 18. The global FEM is restrained at the side-of-body in six degrees of freedom. The wing box is modeled to include enough details to yield accurate internal loads for all the structural components. The cover panels are modeled by plate elements, with three to four elements between each rib bay and one element between each stringer-to-stringer bay. Both the cover panels are modeled geometrically at the outer moldline. The wing cover panels are modeled at the outer moldline with plate elements and the stringers are modeled by cbeam elements, offset to their geometric centroid and then tied to the skin panels by multiple-point-constraints. All the lower cover access holes are also modeled in detail to get the correct load distributions for the cutout regions. For the spars, the webs are modeled as plate elements, and the stiffeners as cbeam elements, lying in the spar reference plane. Two to four elements are used to span the depth for mesh density, and two to four elements are used between the rib stations to match the mesh of the cover panels. Details of the cutouts in the webs are not included in the global model; however, their details are modeled in the global/local analysis. All the rib webs are modeled by plate elements and their stiffeners are modeled by cbeam elements. Rib web access holes are modeled in Ribs 2 through 5.

The global FEM also has the main landing gear attachment, which includes the main landing gear fitting and the external doublers. The main landing gear fitting is attached to the wing box via the external doublers and the rear spar at Rib 6.

S84856

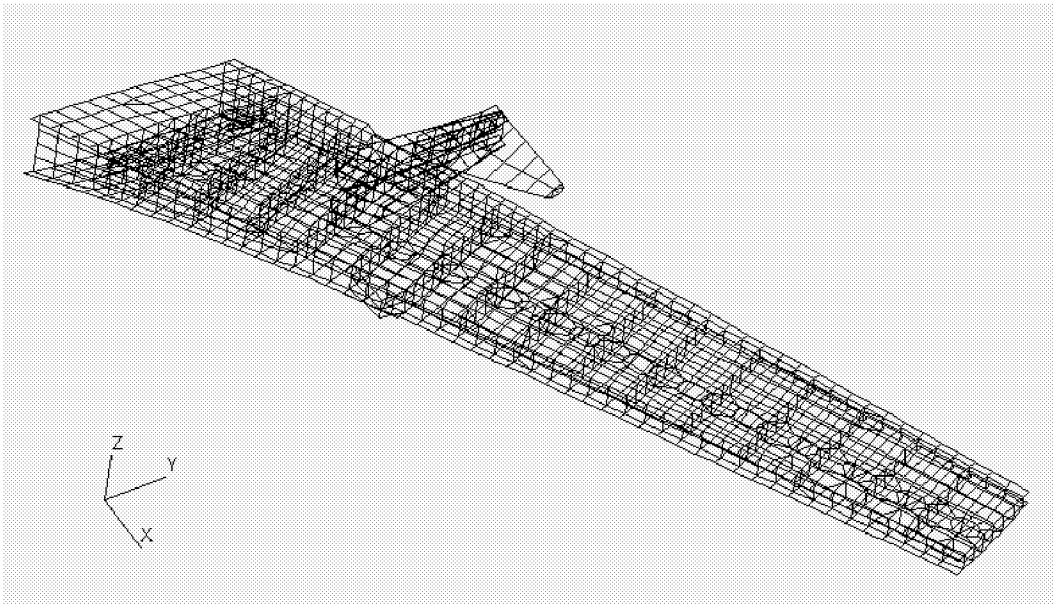

Figure 18. The global Finite element model of the Semi-Span composite wing.

The global FEM uses compression stiffness properties for the upper cover and tension stiffness properties for the lower cover. The spar webs use compression stiffness properties. This approach provides accurate deflection calculations of the wing box for the critical 2.5-g upbending case.

The model has approximately 3800 nodes and 3770 elements, with approximately 22,800 degrees of freedom.

4. Design Development Test Articles (DDTA's)

Introduction

The fabrication and evaluation of the Design Development Test Articles (DDTAs) were conducted in parallel to the development of the semi-span wing test article. Fabricating and testing the DDTAs provided building block manufacturing experiences with larger S/RFI structures, provided design values for key structural features, enabled different design approaches to be evaluated, and demonstrated the structural performance on the subcomponent level for S/RFI structures. Each of these goals benefited the development of S/RFI technology and aided in the development of the semi-span test article. In this section, the Advanced Subsonic Technology (AST) Wing DDTA program is summarized

Master Panel General Fabrication and Respective Approach

Tooling Description

A stitching frame for both the thick and thin master panel configurations was designed to support two full preforms in a side by side stitching configuration. The primary purpose of a stitching frame is to secure the Saertex material edges down with a series of clamps and allow the stitching head to stitch the preform. A typical skin stitching pattern for a full-sized two preform master panel is shown in Figure 19. However, fabric handling problems such as sagging at the center section of the side-by-side preforms was experienced during initial DDTA stitching tasks. The solution to this issue was to stitch only one preform at a time.

Figure 20 is an illustration of the master panel stitching frame tool used to stitch the large DDTA preforms. To reduce fabricating cost and weight issues associated with fabricating the stitching frames, 6061-T6 aluminum alloy material was selected and used to fabricate all the required stitching frame components. The stitching frame details were precision machined with computer controlled equipment and then jig-bored to control tolerances between mating detail assemblies. Assembly of the stitching frame was accomplished using a series of steel brackets, clamps, and fasteners. The stitching frame was also equipped with a number of precision pins along the edges of the aluminum frame. These pins were required for the precise location of stringers and intercostal clip preform details on the skin during the stitching process. A complete master panel consists of as many as five stiffeners and two rib planes of intercostal clips.

Use of the stringer and intercostal jig tooling requires that the preform details are properly trimmed to the correct dimensions. Next, these stringer and intercostal details are loaded into their appropriate jig such that the blades are located solidly into the tool. A series of bolts is then tightened to secure the stringer or intercostal preforms in these locating tooling jigs. Once the blades are secured in the tooling, the preform flanges are folded out and fillets are inserted into the void zone left by the flanges. Fillets are required in stringer or intercostal preforms that have more than four stacks of Saertex material, and both unidirectional twisted tow and woven fillet materials were used over the course of the DDTA fabrication effort.

Once a jig is located in its proper position, the flanges of the specific preform component are stitched to the panel skin. In order to prevent the jig from interfering with the stitching head motion, the first flange stitch row begins 0.40 inches from the stringer blade. This stitching constraint still allowed five stitch rows to be sewn on either flange of a stringer or intercostal preform.

S84522

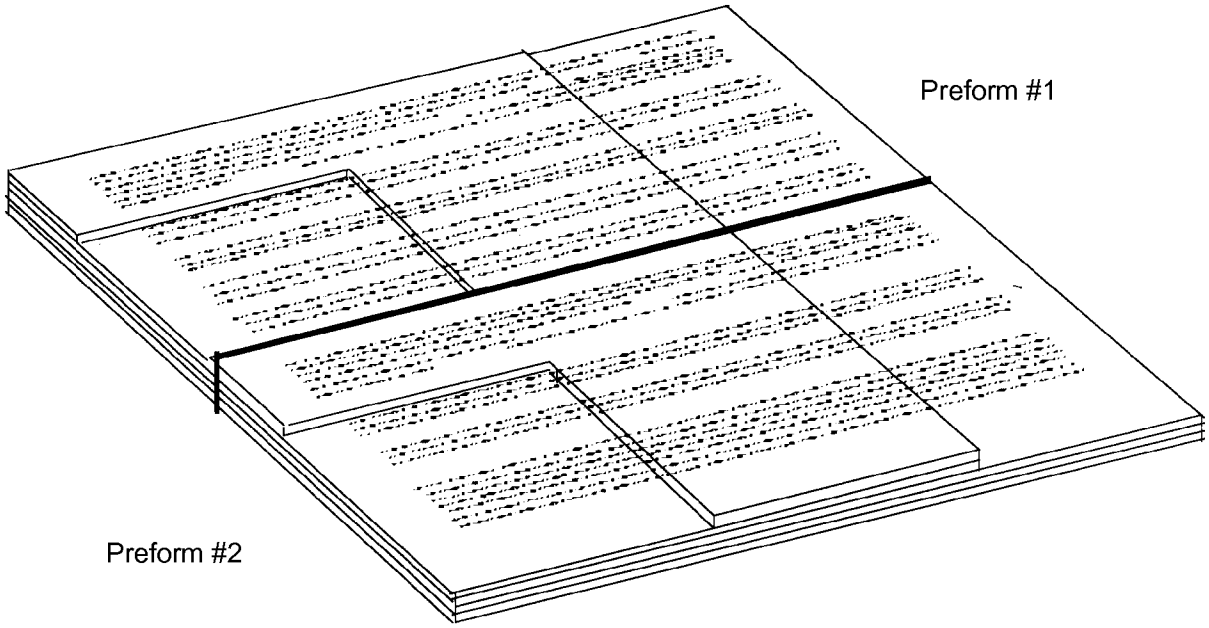

Figure 19. Master panel skin stitching configuration.

S84523

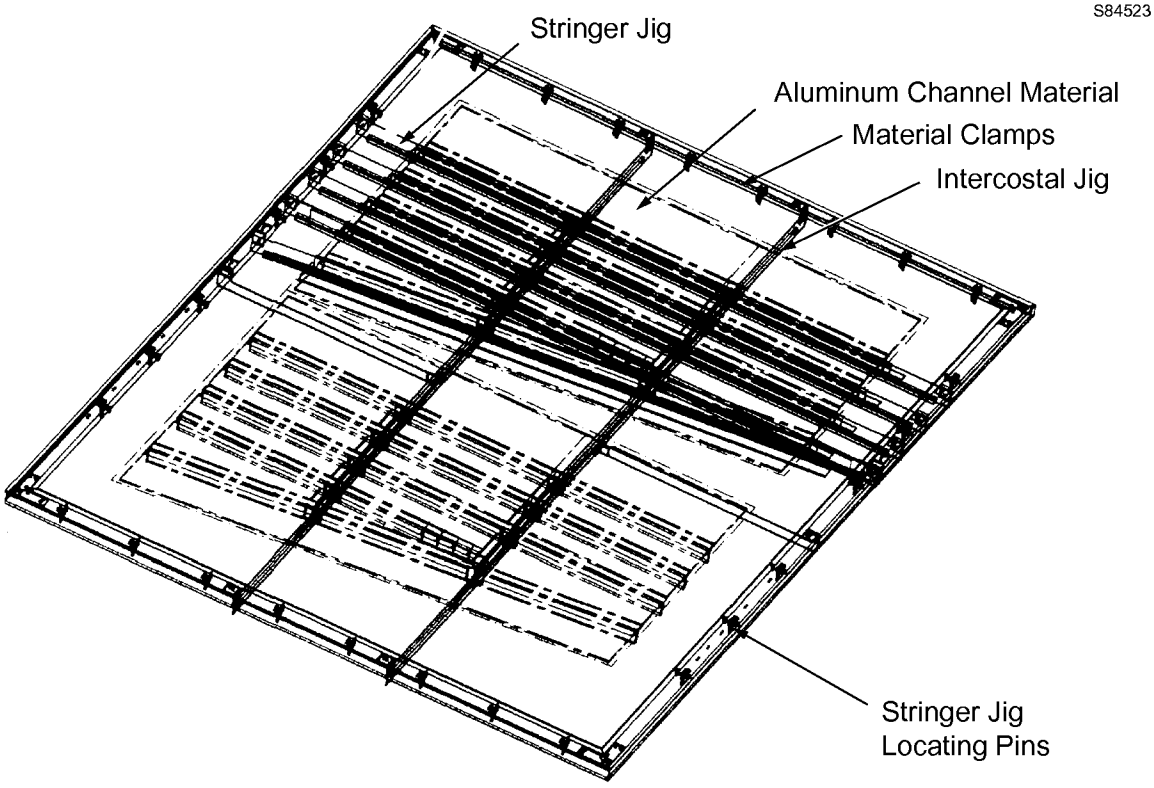

Figure 20. Master Panel Stitching Frame Tool.

During the early RFI process development stages on the AST Composite Wing program, autoclave procedures for cure cycles were established. It was determined the heat-up rate and cool down period for smaller structural panels could be achieved using a solid aluminum block design approach for the inner mold line (IML) tools. The RFI tooling blocks are designed to form the inner mold line of the panel by applying pressure to the stringer blades, intercostal clips, and IML interface during the RFI cure process. Additionally, the use of solid aluminum blocks was found to also save machining cost and processing time. The size and complexity of the DDTA panels were determined to be within the established processing boundaries where the use of aluminum blocks was an adequate RFI tooling approach.

All RFI tooling blocks for DDTA panels were solid and fabricated from 6061-T6 Aluminum alloy material as illustrated in Figure 21. After the machining process was complete, all tooling blocks were thoroughly inspected to cover unacceptable dimensions or defects.

Description of the DDTA Master Panel Configurations "A" and "B"

The master panel concept was developed by manufacturing engineering's desire to use common stitching and resin film infusion (RFI) tools to fabricate the design development test articles (DDTA). DDTA panels that utilized this master panel concept included the following panels: DDTA #3 and D4, Stringer Runout (tension and compression); DDTA #6, Upper Skin and Stringer (compression); DDTA #9, Bulkhead (shear), DDTA #19, Skin Ply Drop-Off (tension and compression); and DDTA #20, Rib Clip Pull-Off.

The "A" version of the master panel represented a thick configuration; whereas, master panel "B" was a thin configuration. A typical master panel preform, shown in Figure 22, consisted of a skin panel that had a 90-inch length and a 58-inch width. This preform was fabricated with three full-length stringers, a stringer runout, an angled spar-cap, and intercostal clips. The schematic diagram shown in Figure 23 highlights the differences between panel versions "A" and "B" in terms of number of Saertex skin stacks, stringer thickness, and stringer height.

S84524

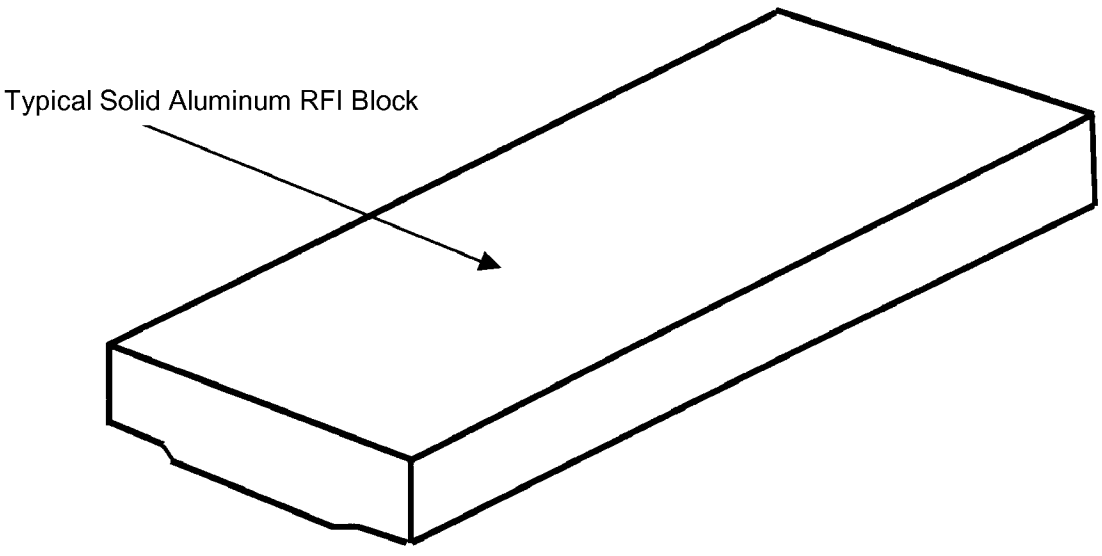

Figure 21. A typical inner mold line tooling block used to RFI process DDTA panels.

S84525.1

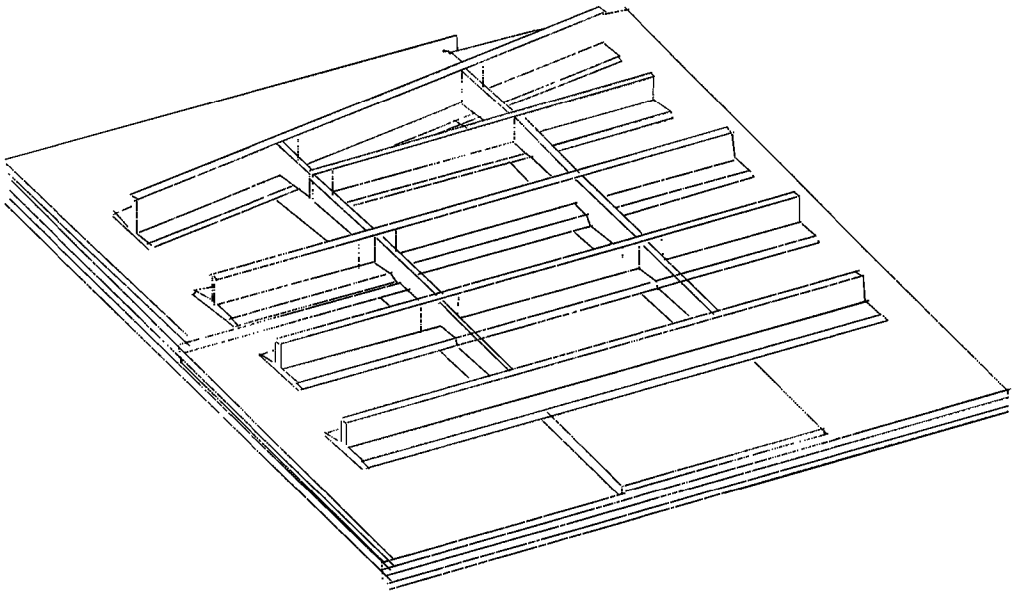

Figure 22. General master panel configuration.

S84526.1

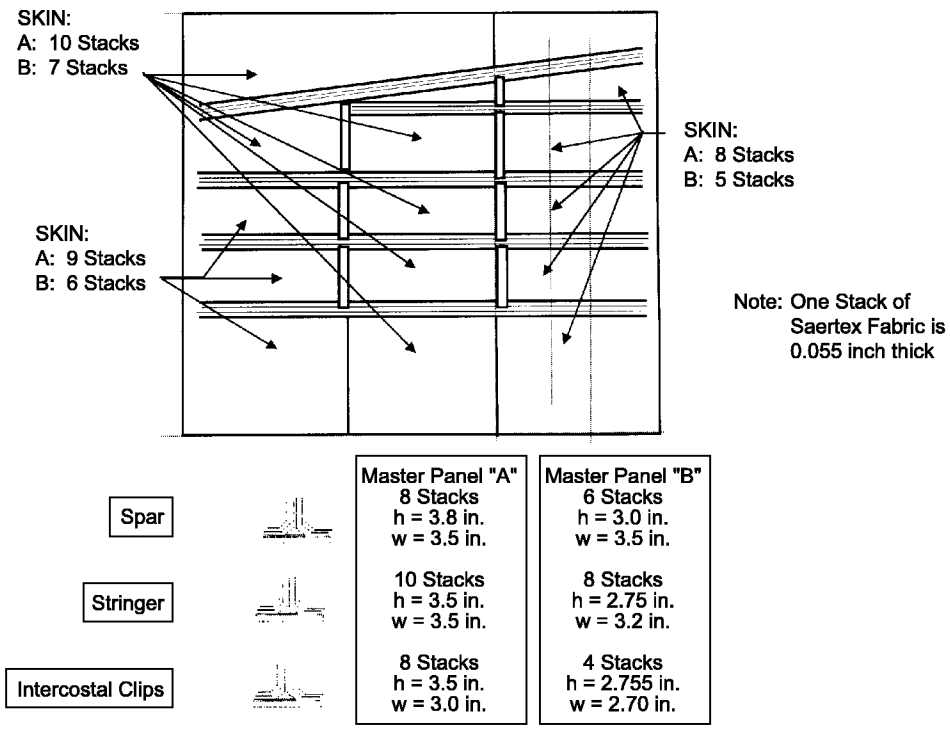

Figure 23. Component specifications for the master panel configurations.

Table 3 provides a summary of each of the DDTA test configurations. This summary includes a brief description, number of specimens, and the key results that were obtained or the planned objective. The geometry of each of these specimens is shown in Figure 24.

Table 3. Summary of DDTA Test Specimens

ID	Description	Number of Specimens	Key Results/Objectives
1	Upper cover root splice	1	Demonstrated joint design details to support semi-span wing analysis.
3	Stringer runout	5 - compres. 5 - tension	Established runout strengths, need to improve tension runout design to eliminate stringer separation at runout.
6	Upper cover compression panels	3 - one bay 4 - three bay	Stitching prevents stringer debonding and enables significant increase in postbuckling strength.
9	Intercostal shear	4	Shear running load allowable of 2.16 kips/in defined.
16	Spar cap shear	13	Thick interleaved design performed best. Established allowable running loads.
19	Stack drop-off compression	2	1- or 2-stack drop-offs do not reduce design strength based upon CAI.
20	Intercostal tension	12	Thick flange configuration enhances performance. Two 5/16" diameter bolts improves strength, one bolt does not.
A2	Repair panels	2	Objective is to establish repair design values. Assembly suspended for both specimens, partial assemblies in storage.
D1	Postbuckling crippling specimens	12	Investigate stringer blade buckling and crippling of S/RFI materials. Specimens are scheduled to be tested by NASA.
D2	4-stringer postbuckling compression panels	12	Examine post buckling behavior of S/RFI 4-stringer panels. Specimens are scheduled to be tested by NASA.
D4	Compression stringer runout	3	Constant height runout design performed best.
E2	High load joints	1 - compres. joint 1 - tension joint	Demonstrated compression joint details. Work on tension joint specimen suspended.
F1	Spar web shear	2	Designed to investigate failure of the spar web at a cutout location before overall panel buckling occurs.
G1	Darted spar cap shear	6	Darts did not significantly affect shear strength.

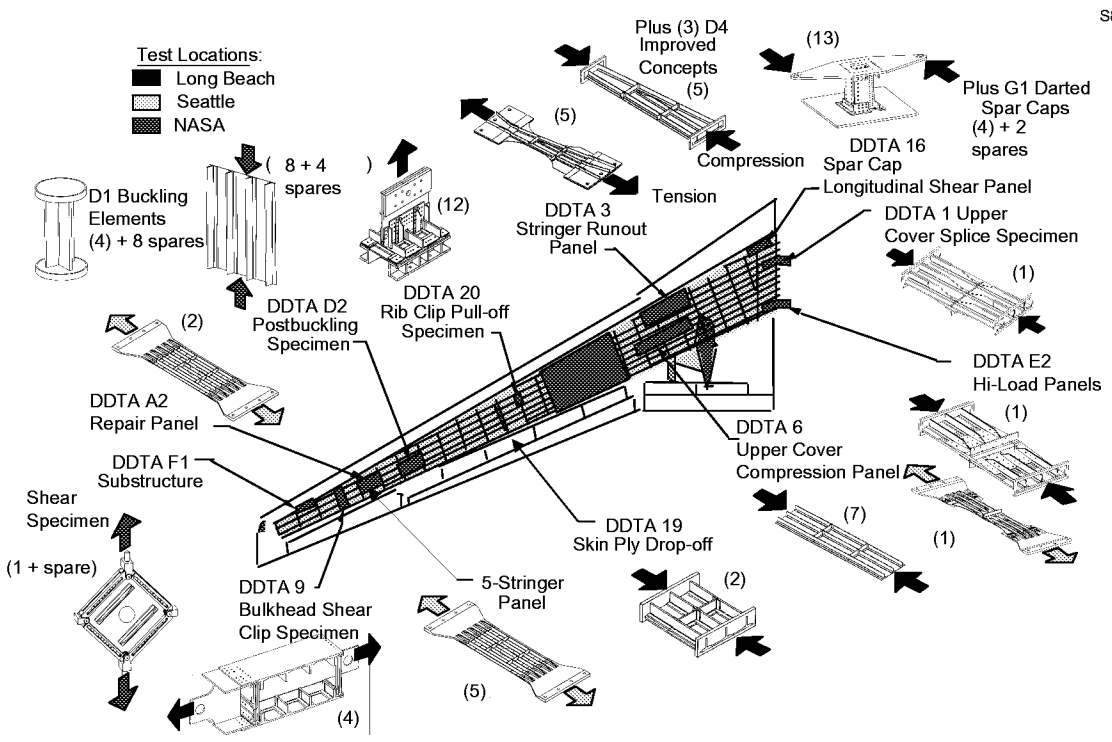

Figure 24. DDTA Test Specimens (number in parenthesis refers to the number of replicates for each different specimen).

Final Conclusions for DDTA Testing

In the Design Development Test Article test program, many large test elements were fabricated and tested. The test program provided valuable fabrication experience and structural verification of stitched resin film infusion component designs. It demonstrated the structural performance of many different design features including heavily loaded splice joints, stringer runouts, intercostals, and spar caps. It also provided verification of the analytical methods developed for S/RFI structure. For example, the test of the Upper Cover Root Splice Joint (DDTA #1) established that the analysis methods used for the semi-span test article were conservative. Additionally, design values were derived for intercostal shear and tensile strengths, spar cap shear strength, and stack drop-offs. For instance, the DDTA #9 tests defined an intercostal shear design value of 2.16 kips/in, and the DDTA #9 analysis indicated that this was conservative because in the test specimen the load was not evenly distributed to three intercostal tabs. The information generated from the DDTA tests was essential for the development and analysis of the semi-span wing test article. The DDTA testing also provided a means to compare different structural design configurations. Some of these comparisons are discussed in the following paragraphs.

In the DDTA #3 and D4 tests, a constant height and two tapered height stringer runout designs were evaluated for both a thin and a thick configuration. Table 4 provides a summary of the tension stringer runout tests and Table 5 summarizes the compression stringer runout tests. In each of the tension stringer runout tests, the terminated stringer delaminated from the skin. The initial delamination was arrested by the stitches, but at higher loads the delamination propagated along the entire length of the terminated stringer transferring the load to the remaining two stringers and skin prior to the overall failure. The initial and final delamination load levels are listed in Table 4 for each specimen. Although the thick

Table 4. DDTA #3 Tension Runout Test Results

ID No.	Configuration	Design Ultimate Load (kips)	Initial Delam. Load (kips)	Final Delam. Load (kips)	Actual Failure Load (kips)
6	Thick Constant	807	660	676	988
8	Thick Tapered	811	309	874	1129
9	Thin Tapered*	560	414	626	732
10	Thin Tapered	560	368	604	773

*fatigued loaded

Table 5. DDTA #3 and D4 Compression Runout Test Results

ID No.	Configuration	Design Ultimate Load (kips)	Initial Delam. Load (kips)	Final Delam. Load (kips)	Actual Failure Load (kips)
1	Thick Tapered (11°)*	595	610	700	706
2	Thick Tapered (11°)	595	610	none	644
D4-1	Thick Tapered (8°)*	595	none	none	714
D4-2	Thick Tapered (8°)	595	none	none	665
D4-3	Thick Constant with pad-up	595	unknown	none	767
4	Thin Tapered* (11°)	405	none	none	347
5	Thin Tapered (11°)	405	none	none	375
3	Thin Constant	415	none	none	470

*fatigued loaded

tapered design sustained higher ultimate loads, delamination initiated at 309 kips which is less than half the load needed to initiate delamination in the thick constant height design. In all of the tension runout specimens, final delamination occurred at loads 15 to 32% below the ultimate failure load. Although the final delaminations occurred above the design ultimate loads, additional design improvement should be investigated to prevent delamination and enable better structural performance. This might include reducing the taper angle, increasing the compliance of the stringer, or adding double density stitching or mechanical fasteners at the tip of the runout.

In the compression runout tests, stringer delamination was less of a problem. In the thin tapered specimens and the thick tapered specimens with an 8° runout taper, post test examinations showed no indication of delamination between the terminated stringer and skin. In the thick tapered specimens with an 11° runout taper, strain gage data indicated the occurrence of limited delamination in the two specimens at 610 kips and extended delamination in one specimen at 700 kips just prior to failure. The thick constant height specimen had limited delamination (5-6 inches) at the tip, but the delamination did not propagate further along the stringer as was observed in the tension specimens. Overall, the constant height runouts performed better than the tapered runout for both the thick and thin configurations in these compression evaluations.

In the DDTA #16 and G1 tests, the shear strength of spar caps was determined for several different configurations as shown in Figure 25. These results clearly show that the introduction of darts (cuts in the spar cap which prevent wrinkling) do not affect the shear strength of the spar cap. The results also show that the interleaved geometry provides a significant benefit for the thick configurations and that the use of double density stitching enhances the performance of the thick non-interleaved configuration.

In the tests of the intercostal tension specimens (DDTA #20), the thick configuration, e.g., the 8-stack intercostal blade, sustained loads almost twice as high as the thin configurations which had only 4 stack blades. The improved performance of the thick configuration is attributed in part to the increased stiffness of the thicker flange. In the thick configuration, it is currently hypothesized that the compliance of the tabs and flange were well matched so that failure occurred simultaneously in both enabling higher loads to be achieved. Whereas, in the thin configuration, the tabs loaded up and failed, then the flanges loaded up and failed which limited the maximum load capacity of the intercostal. It would be beneficial to conduct analysis to better understand how the thickness of the intercostal blade and flange affect the compliance and load sharing in these specimens. In both configurations, the inclusion of tab fillets was found to be beneficial and increased the specimen strength. Whereas, adding bolts only helped when two 5/16" diameter bolts were used in each tab.

In addition to these key results, the DDTA #6 compression tests on the 1-bay 2-stringer panels demonstrated that stitching delayed stringer delamination and enabled loads to be carried that were 140% and 80% above the buckling load for specimens having 2- and 3-stack skins respectively. Evaluation of the DDTA #19 stack drop-off specimens, that had impact damage, showed residual strengths 15% above CAI strength predictions. This indicated that neither a 1- or 2-stack drop-off effected the design strength

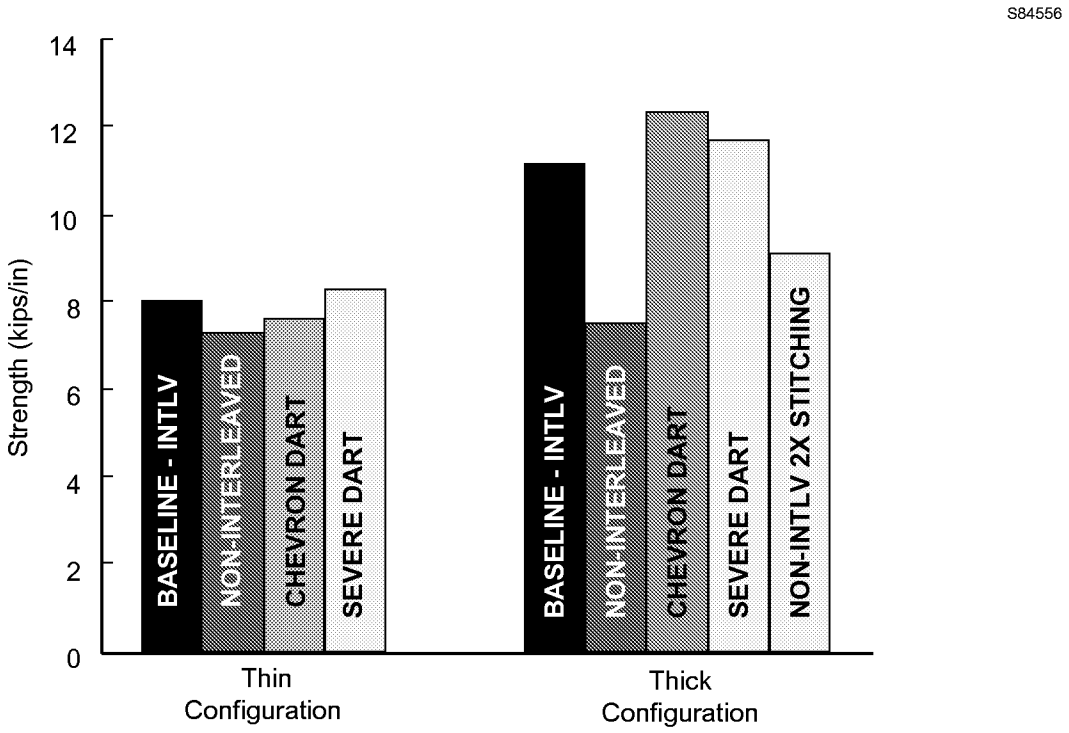

Figure 25. Comparison of the spar cap shear strength of different test configurations.

of the stitched composite. Further, both the 1- and 2-stack drop-off specimens failed when the stress in the reduced section reached 60 ksi which suggests that a 2-stack drop-off is not significantly different than a 1-stack drop-off.

4.1 Durability and Damage Tolerance (D&DT) Studies

As part of the AST Composite Wing's S/RFI structural demonstration approach, a review of aircraft certification guidelines was performed to identify significant design issues for these materials. The AST program uses the Federal Aviation Regulation Part 25 document as its principal certification guideline. A discrete source damage (DSD) event is described in Section 25.571 of this document as one facet of a damage-tolerant design that must be considered for certification. A DSD event is an incident that is immediately apparent to an aircraft's flight crew or ground personnel at the time of its occurrence, and the damaged structure must withstand at least 70% of its design limit load. This type of damage is often caused by projectiles emanating from disintegrating engine components with variations in projectile mass, velocity, and impact location. These variables create a complex problem for engineers designing structures that are DSD tolerant. To reduce this design complexity, DSD evaluations are typically simplified by evaluating the residual strength of multi-stringer test panels containing a two-bay crack or slot across a principal stiffening element. Certification guidelines also state that any future application of composite materials in primary structures will be required to demonstrate a level of damage tolerance after the occurrence of such an event. Therefore, the successful development and verification of a DSD analysis methodology for stitched composites would reduce future certification costs of any advanced composite structures fabricated with these materials.

Test Panel and Material Description. Eight panel configurations were used in the Durability and Damage Tolerance (D&DT) evaluations of S/RFI structures. The DSD test matrix (Table 6) shows the test specimens were evenly divided between tension and compression test articles. Both compression and tension test panels were constructed from orthotropic stacks of warp-knit fabric having a carbon fiber orientation of $[45/-45/0_2/90/0_2/-45/45]$. As noted in Table 6, the only difference between the materials used for either the tension or compression specimens was the type of fibers used to construct the fabric. The compression specimens contained only the standard modulus HTA 5131 fibers from Tenax, while the tension specimens contained intermediate modulus IMS 5131 fibers from Tenax in the zero-degree direction and HTA 5131 fibers in the other three orientations.

Four panel geometries were evaluated for each type of warp-knit fabric used to fabricate the test specimens. Blade height and skin thickness were the two variables selected for evaluation. All the panels were fabricated with three warp-knit stiffeners, and the height measurement was made from the base of the blade-stiffener to the blade tip, as shown at location A in Figure 26. Blade heights of 1.8 inches and 2.3 inches were used in this study. Two skin thickness combinations, as indicated at location B in Figure 26, were also used to construct the panels described in Table 6. These geometry variations allowed this study to compare how a panel's stiffening ratio affected its DSD damage tolerance behavior. A panel's stiffening ratio is defined as stiffener cross-sectional area divided by the section's total cross-sectional area because the same material is used for both the skin and stringers. Each panel's stiffening ratio is shown in the last column of Table 6. Blade thickness was held constant for each panel at eight stacks. This dimension is indicated at location C in Figure 26. Figure 26 also shows the width of each panel at location D.

Table 6. Test Matrix for DSD Evaluations

Panel Loading Direction	Panel Fiber Type	D&DT Test No.	Nominal Blade Height (in)	No. of Skin Stacks	Nominal Stiffening Ratio
Compression	HTA 5131	1	2.3	6	0.364
		2	2.3	4	0.462
		3	1.8	6	0.328
		4	1.8	4	0.423
Tension	HTA and IMS 5131	5	2.3	6	0.364
		6	2.3	4	0.462
		7	1.8	6	0.328
		8	1.8	4	0.423

S84222

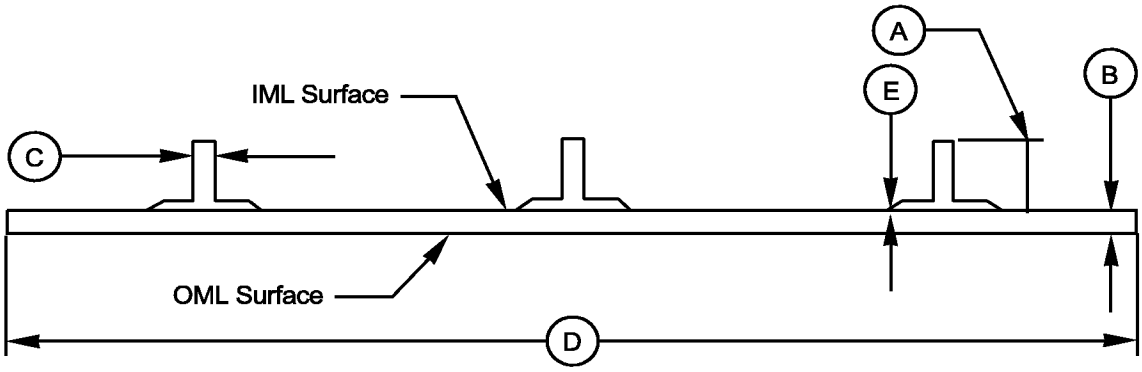

Figure 26. Cross-section of typical three-stringer DSD test article.

All the test specimens were derived from individual stitched dry fiber preforms fabricated to a consistent set of manufacturing specifications developed by the AST Composite Wing program. These preforms were all stitched at 40 penetrations per square inch, with a 0.2 inch row spacing. A 1600-denier Kevlar 29 penetration thread and a 400-denier Kevlar 29 bobbin thread were used to stitch these preforms together. Hexcel's 3501-6RC epoxy resin system was used to infuse the preforms. All the panels were successfully processed without any abnormalities. Ultrasonic inspections were conducted after preform infusion as a final check on panel quality. No fabrication abnormalities were identified in any panel by these C-scan inspections.

DSD Geometry. An initial demonstration of discrete source damage tolerance of S/RFI materials applicable to primary wing structures used machined slots (saw cuts) to simulate DSD sites. Also, prior discussions with Federal Aviation Administration and B-2 bomber durability and damage tolerance personnel strongly suggested the use of a two-bay slot to demonstrate DSD residual strength of composite structures. This geometry provides a low-cost alternative to ballistic tests, and it produces a repeatable

damage site at a precise location that offers consistent test comparisons between data sets. All the slots were positioned in the center of each specimen, both in the vertical and horizontal directions.

The machined slot geometries used for the compression and tension test specimens are shown in Figure 27. Routing templates were created for each slot pattern to aid in consistently locating and machining these slots into each three-stringer test article. Both slots were 7.0-inches long with a 0.094-inch tip radii. However, the compression slot was modified into a diamond configuration to reduce the possibility of the upper and lower surfaces coming into contact during testing. Straight slots were used in the initial DSD evaluation of S/RFI structures, and post-failure analysis of the compression specimen raised concerns the slot had closed under load during the test and loaded the machined surfaces. Minimizing the potential for the machined surfaces to contact each other during a test was considered an experimental refinement over the prior DSD compression test approach.

Loading Frame. A servo-hydraulically actuated Baldwin loading frame was used to perform all eight DSD panel tests for this program. This machine was rated for loads up to 600 kips, and its hydraulic system was calibrated to 500 kips. All the tests were performed in position control at a displacement rate of 0.05 inch per minute. A stand-alone digital data acquisition system was used to collect machine load and displacement information and to record signals from instrumentation mounted on each panel.

Compression Test Articles. The three-stringer compression panels were 24-inches wide and 39.5-inches long. Both the top and bottom loading surfaces of these panels were ground flat and parallel to within 0.005 inch of each other. These ends were then potted into welded steel frames using an epoxy resin system. Global panel buckling was minimized in the compression test articles through the use of knife-edge supports on the unloaded edges. A compression test article and the antibuckling hardware are shown in Figure 28. Also mounted to the load frame support columns, but not visible in Figure 28, were two deflectometers. The deflectometers were used to measure any out-of-plane deflections during the compression tests.

S84225.1

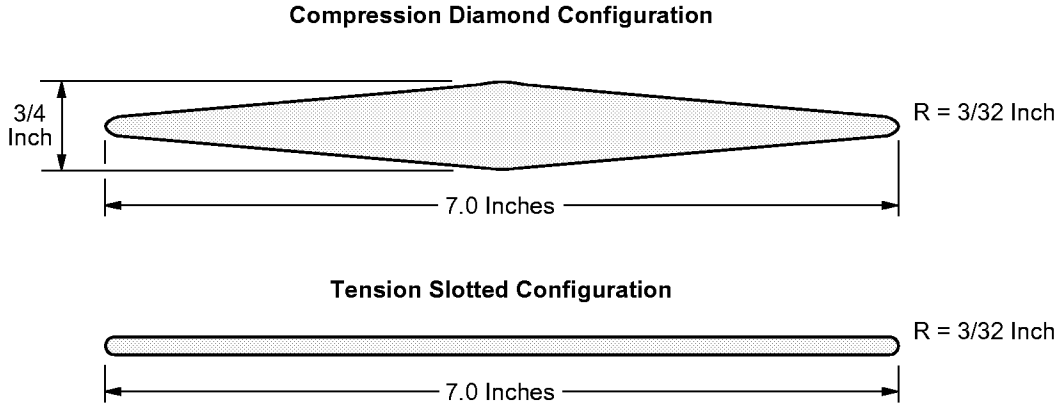

Figure 27. Compression and tension slot geometries used to simulate DSD.

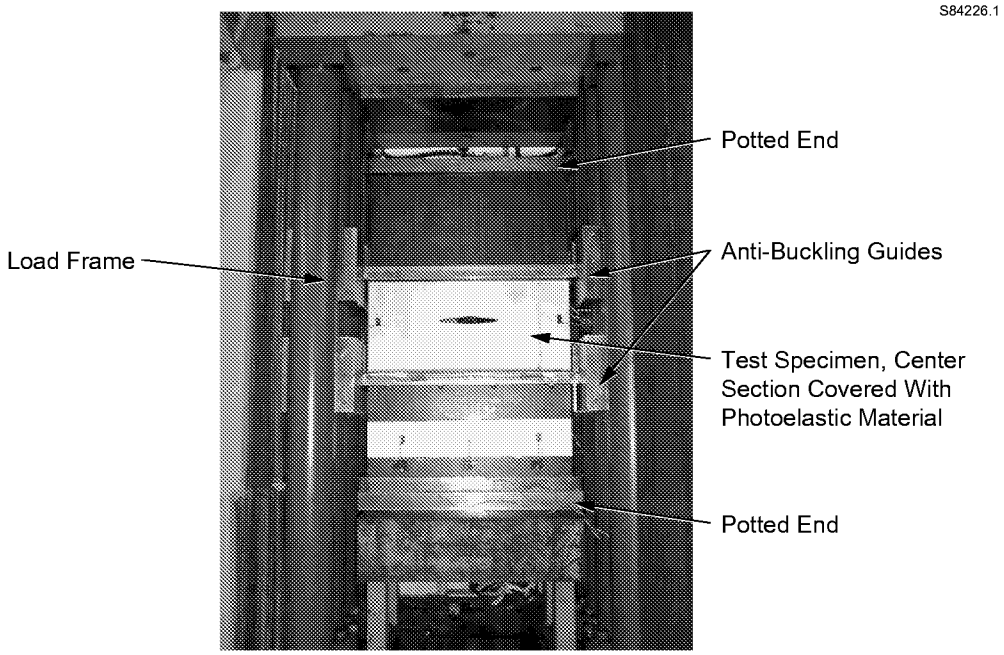

Figure 28. A compression test article and antibuckling guides.

Tension Test Articles. The three-stringer tension panels were 24-inches wide and 49-inches long, not including the length of the loading tabs. Figure 29 shows a fully assembled tension specimen positioned in the loading frame. The large 4-inch diameter pin-loaded tabs were designed using GENOA's FEA capabilities to achieve a strain distribution of no more than 0.005-inch across the tab-to-specimen interface region at 600 kips. Each tab required a 6.5-inch interface region to allow for three rows of fasteners. This requirement provided for a tension specimen gage length of 36 inches. The tension tab design also included angle plate attachments to each stringer of the test article to introduce loads into the stiffeners. This stringer loading feature was developed out of lessons learned from the initial DSD study of S/RFI structures. The test approach used in the initial study did not directly load each stringer. This design limitation allowed a premature tab failure to occur in the tension specimen.

Test Instrumentation. Strain gages were the principal instrumentation installed on all the DSD test articles. As many as 42 gages were attached to a panel to monitor the strain distributions during testing. Axial strain gages were placed at locations away from the slots to record far-field strains. These strain gages were mounted either individually or in back-to-back pairs so loading irregularities could be monitored in a panel. Other gage installation sites included locations near the expected damage propagation path. Rosette gages were placed near the slot radii and other axial strain gages were positioned outward from the slot along its centerline. Finally, several back-to-back axial gages were positioned just slightly above and below the expected damage propagation path.

Crack propagation gages were also mounted on the inner mold line (IML) of selected compression and tension test articles. The objective of these gages was to monitor how damage grew outward from the slot on the three-stringer panels, if stable damage growth indeed developed during a test.

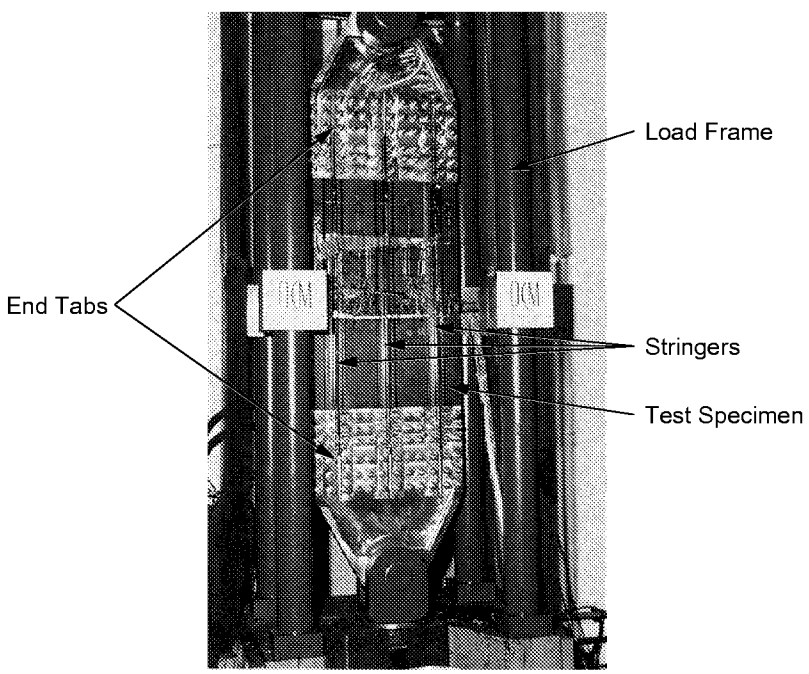

Figure 29. A tension test article positioned in the loading frame.

A photoelastic film was mounted on the outer mold line (OML) surface of each three-stringer panel. This film was 0.125-inch thick with a 0.15 strain optical coefficient. Photoelastic fringe patterns were observed using a NASA-Langley supplied polariscope. Such data provided information on the strain fields that developed under the film in each panel. The strain fields around the slot radii were monitored using this technique, and the loads introduced into the test sections of each panel were also recorded. Photoelastic data were recorded by still photography through the polariscope.

Two video cameras were used to record how damage developed in each specimen's test section. One camera recorded damage propagation on the OML surface of a test article, and the second camera observed damage growth on the IML surface. With audible load call outs at each 10 kip load increment, these video recordings proved an invaluable aid in assessing when damage propagation occurred in the test specimens.

Compression DSD Failure Behavior. Damage development in the compression specimens progressed in a stable manner from the slot radii toward the outer stringer flanges. The development of this type of failure mode from a flaw site is consistent with behavior observed in compression-dominated post-impact fatigue tests performed on S/RFI materials. The stringer-flange regions of the test articles are indicated at location E in Figure 26. Once the compression damage reached the flanges of the test articles, the damage progress was halted until at least an additional 5 kips was applied to the panel. The additional load required to cause ultimate panel failure through the outer stringers indicates the stitched stringers can inhibit damage growth. The minimum load value of 5 kips required to cause catastrophic failure was observed in the test article having the highest stiffener ratio (0.462). Therefore, this stiffener ratio appears to be near a design limit that can halt damage propagation in S/RFI structures due to a DSD event.

A close-up view of one edge of a failed compression test article is shown in Figure 30. This picture is a typical view of the failures observed in the compression test articles. The compression failures displayed classic transverse shear surfaces typically observed in stitched composites. Another feature of the failure mode of these compression test articles included no observed stringer pull-off.

Tension DSD Failure Behavior. Generally, the three-stringer tension specimen failures are characterized by initiation of damage at the radii of the slots. Increasing the applied load on each panel caused the tension failure damage to rapidly propagate transversely to the loading direction until it reached the inner flanges of the outer stringer region of each specimen. Once this tension damage reached the outer stringer flanges, the damage then propagated parallel to the flanges in the loading direction. This vertically oriented translaminar shear failure mode was observed in all four tension test articles, and the stable propagation of this shear failure mode continued until the damage neared the loading tabs and caused catastrophic panel failure. A post-test view of a tension panel is shown in Figure 31.

Because of the highly orthotropic material properties of the S/RFI panels, failure modes could be directly related to material directionality. Once tension failures propagated from the slot radii to the inner flanges of the outer stringers, the load on the skin in the bays adjacent to the outer stringers diminished significantly. The strain gage data shown in Figure 32 are graphical representations of this behavior. The strain gages are located as shown in the inserted diagram of the panel. The large strain variation can be observed between the flange-mounted gage (#32 IML) and skin gage (#34 IML) that are separated by less than 0.5-inch. Development of translaminar damage in the tension test articles necessitated the development of shear coupon test data to refine the material database, and this led to the creation of the unified S/RFI database. The development of this strain pattern also indicates the tension panels were not long enough to allow loads in the outer stringers to be transferred into the adjacent skin bay and central stringer through shear-lag. It is suggested that this finite length issue be evaluated in future DSD evaluations on S/RFI test specimens.

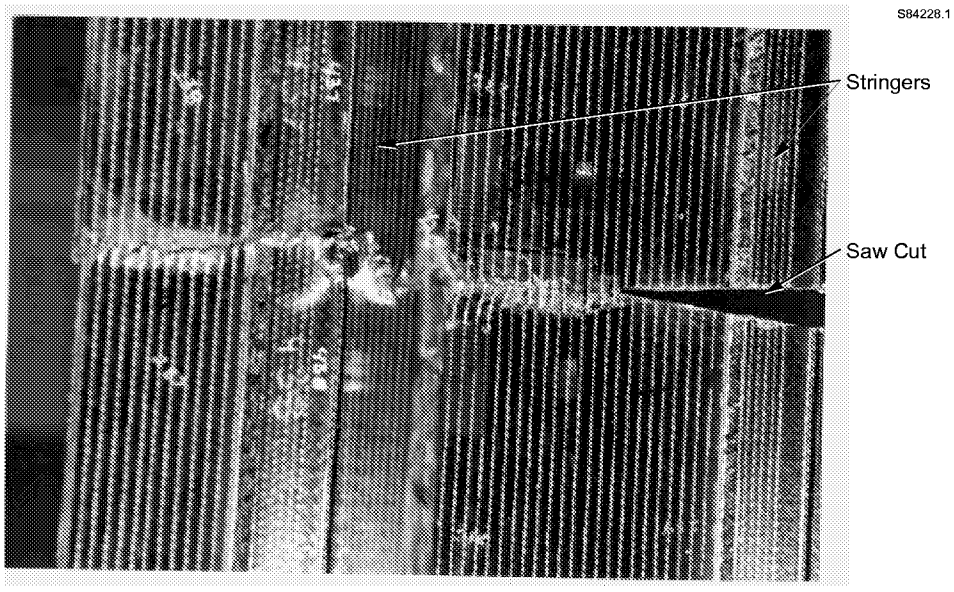

Figure 30. Close-up view of compression test article failure zone.

S84229

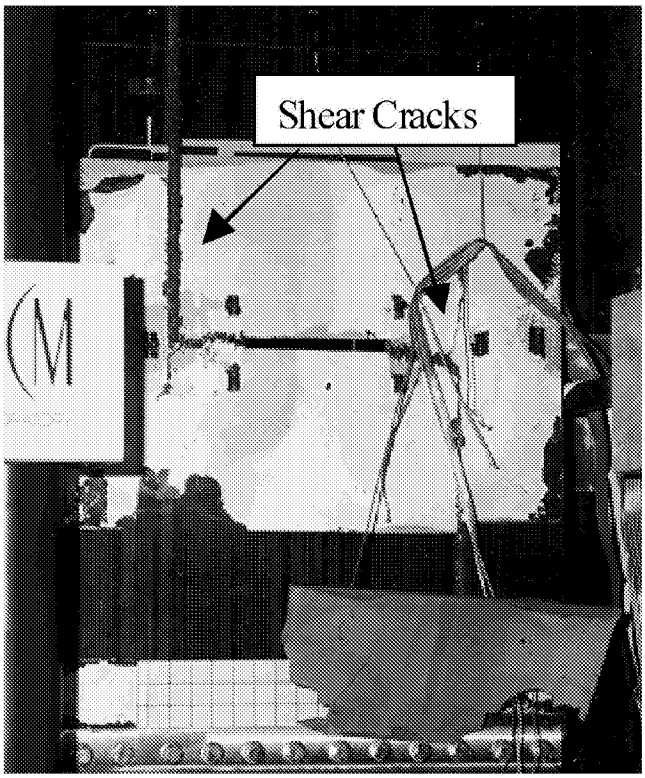

Figure 31. Tension test article trans-laminar shear damage zones.

S84230.1

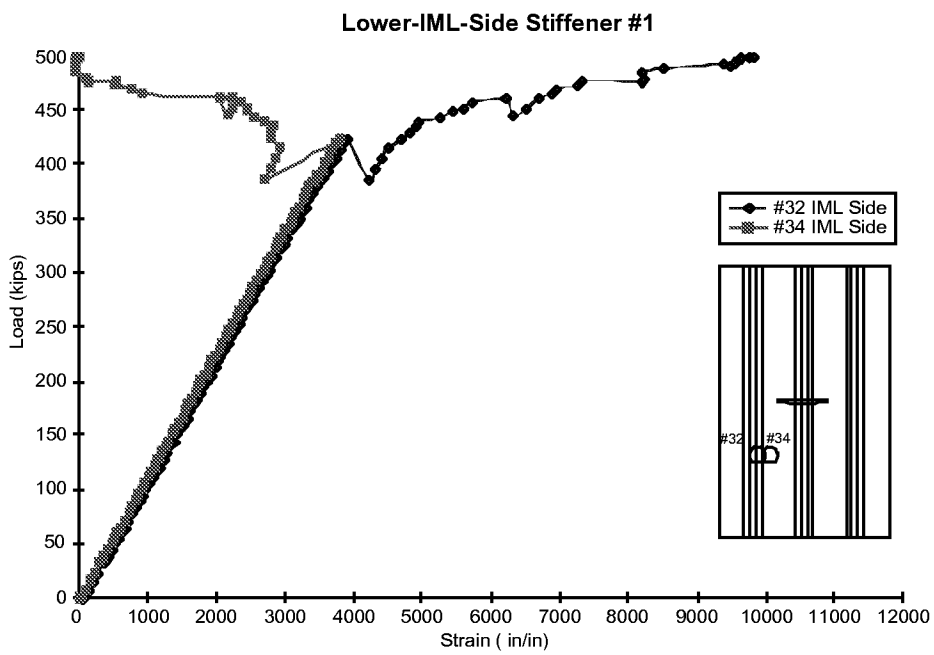

Figure 32. Plot of tension strains indicating development of a shear failure zone.

DSD Residual Strengths. Results of the residual strength tests and analytical predictions for the three-stringer S/RFI panels containing DSD sites are shown in Table 7. Each test panel's geometry is identified in the table's first column, and then the table is broken into the major column headings of compression and tension predicted and experimental results. For loading conditions, the first column provides the GENOA analytical predictions that were submitted prior to each test.

The unified S/RFI database was developed after the DSD compression and tension testing had been completed and was based on coupon-level compression, tension, and shear test data. The goal of establishing the unified S/RFI material database was to provide the most up-to-date constitutive material properties for input to the GENOA database. The use of a single S/RFI material database was considered important to the DSD analysis methodology because the use of independent compression and tension material databases would inhibit an accurate assessment of GENOA's ability to simulate damage propagation in S/RFI structural panels. Moreover, this methodology ensured that the GENOA code was not used to determine constituent material properties, but rather that properties were derived independently from experimental test data.

The increased differences between the pre- and post-test calculated results from the experimental ones are an outcome of the use of the single material database. These increased differences imply that either the finite element model or the micromechanical model within GENOA needs further refinement to reduce these differences.

The next column presents the experimental load at which failure was considered to occur in each test article. The catastrophic failure behavior of the compression test articles allowed the ultimate load a panel carried to be used as its failure load. However, the more complex behavior of the tension panels required closer reviews of strain gage and video data to determine when each panel reached its defined ultimate failure load. As previously discussed, tension panels were considered to have failed when translaminar damage started to propagate along the inner flanges of the outer stringers.

The compression and tension loading fixtures functioned as anticipated, and all the test specimens were loaded uniformly. Figure 33 is an example of strain gage data obtained from back-to-back and side-to-side installations on a typical tension specimen. The IML gage locations are identified in the insert diagram as the solid symbols, while the open symbols represent data from the OML skin gages. These far-field strain gages show that out-of-plane bending and in-plane deformations were minimized by the tension load introduction fixtures until failure in the test articles was imminent. Photoelastic results also provide a qualitative indication of uniform specimen loading. The formation of symmetric fringe patterns relative to the severed middle stringer of a compression test article can be seen in Figure 34.

Table 7. Summary of GENOA Predictions with Experimental Results

	Compression Strength, kips			Tension Strength, kips		
Panel Geometry	**Pre-Test Analysis**	**Post-Test Re-analysis**	**Experimental Value**	**Pre-Test Analysis**	**Post-Test Re-analysis**	**Experimental Value**
6-Stack Skin 2.3 Inch Blades	291	314	294.0	421	422	427
6-Stack Skin 1.8 Inch Blades	270	292	272.5	364	336	382
4-Stack Skin 2.3 Inch Blades	238	247	226.6	294	341	309
4-Stack Skin 1.8 Inch Blades	199	230	206.8	294	278	298

S84231.1

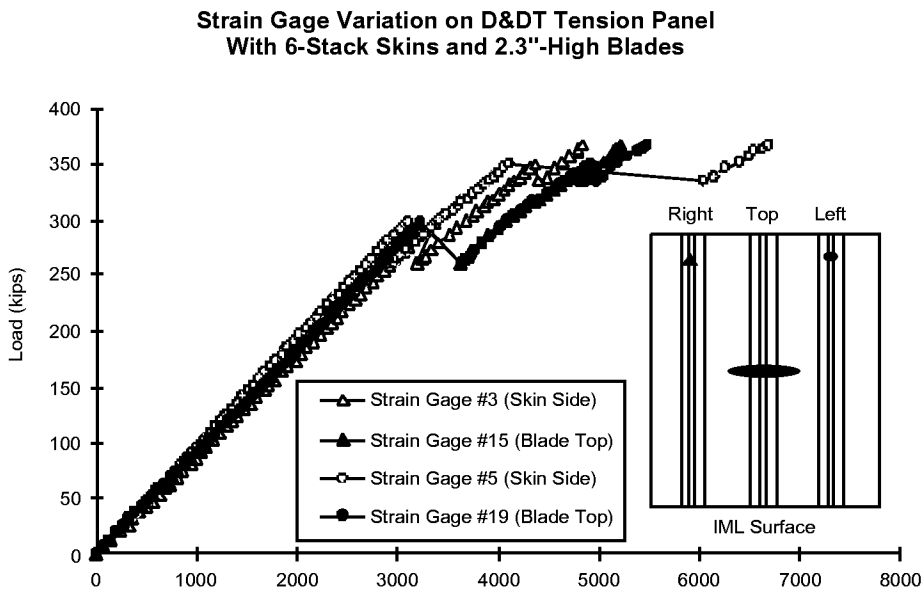

Figure 33. Far-field strain results for a tension test article.

S84232

Figure 34. Photoelastic fringe pattern from a compression test article under load.

Deflectometer data from the compression specimens also showed minimal global buckling occurred in these test articles, and these results suggest the antibuckling guides functioned properly for the compression tests. Post-test inspections of the compression specimens determined the diamond slot surfaces did not come in contact with each other during the tests. Therefore, the residual strength values observed for each test article can be considered to be free of loading irregularities that would cause premature failures or atypical damage propagation behaviors.

The computer predictions provided in Table 7 indicate the analysis methodology shows promise for predicting the residual strength of S/RFI structural panels containing DSD sites. The pretest predictions for the compression panels were within 5% of the experimental failure loads and, using the unified material database, the analytical methodology still predicted failure loads within 11% of the experimentally observed values. Analytical predictions of tension residual strengths were also reasonably close to the experimental values. The pre-test tension predictions were conservatively below the test results by no more than 5%, and the post-test analyses were within 12% of panel failure loads using the unified material database.

Conclusions

The primary focus of this study was the evaluation of discrete source damage tolerance of S/RFI structures applicable to commercial primary wing designs. Four three-stringer panel configurations were tested under both tension and compression loads. After discrete source damage was introduced into each panel using a machined slot, their residual strength was determined. These experimental results were then compared to analytical results obtained through the use of a discrete source damage analysis methodology.

Experimental results provided positive evidence of the discrete source damage tolerance that stitched structures can offer to advanced aircraft designs. Damage always initiated at the slot radii and then was halted at the stringers for both the compression and tension test articles. The compression specimens initiated stable damage growth away from the slot radii toward the stringers, and then these panels displayed no further damage propagation until they failed catastrophically across the stringers at a higher load. However, tension damage propagation was characterized by rapid initiation of damage from the radii to the stringers. Once the damage was stopped at the stringers, increasing loads caused the development of stable translaminar shear damage propagation along each stringer.

A discrete source damage analysis methodology was compared to the experimental results. Initially, residual strength predictions were made prior to each test using this DSD analysis methodology, and these predictions demonstrated the analysis process was capable of reasonable accuracy when calculating the residual strength of the S/RFI panels containing discrete source damage. Post-test refinements to this methodology used a unified material database for S/RFI composite materials to recalculate the residual strengths of each test article. These post-test analytical results showed the methodology was able to predict failures within 12% of the experimental values.

These analytic results were obtained using a relatively coarse GENOA FEA mesh and a minimally demonstrated material database. Refinements to both these elements of the DSD analysis methodology could improve its failure prediction capabilities. Issues concerning the computational intensity of this analysis methodology should also be mitigated in the future as faster computer processors become more available. Such an analysis process, if completely developed, should reduce the cost and time required to certify the damage tolerance of S/RFI primary wing structures subjected to DSD events. While additional refinements and verifications will be required to gain added confidence in this discrete source damage analysis methodology, this study demonstrated the potential of the approach to adequately model residual strengths of S/RFI structures.

5. Manufacturing Studies—Process Development

5.1 S/RFI

Introduction

In order to determine the most critical parameters in the S/RFI process, Boeing performed a QFD (Quality Function Deployment) assessment. In this analysis, key quality and processing parameters were placed in a matrix and ranked as to their correlation—strong, moderate, or weak. Additionally, the importance of the quality requirements to the customer were also ranked in a similar manner—very strong, strong, moderate, weak, or very weak. The quality vs. processing matrix was then multiplied by the customer importance matrix to rank the most critical processing parameters. A summary of these rankings is shown in Table 8.

The QFD process permitted a quantifiable technical evaluation of all critical parameters identified. Furthermore, the parameters that were most critical to the customer could similarly be identified. The QFD matrix, as shown in Table 8, allowed the technical rankings to be combined with the items of most importance to the customer such that these could be ranked in a meaningful way. In this manner the areas of most importance could be identified to permit the planning of a process development program that would yield the greatest benefit to improving the S/RFI process.

This study addresses several critical parameters affecting preform quality in the S/RFI process. Techniques to measure the thickness of carbon fabrics accurately were developed and the effects of stitching speed, thread tension, and presser foot pressure were quantified. Controlled thickness measurements led to improved material quality control. Improved control of stitching parameters resulted in more consistent stitched preform quality. Furthermore, the improvement in the understanding of these items led to the creation of a visual guide in the form of a stitching standard that provides stitch machine operators with a guide to stitch preforms properly. Such a visual standard is provided for each machine to furnish a visual aid at all times to the stitching operator to aid in identifying suitable stitch formation.

In addition to these developments, the effects of needle wear on knot formations were examined to further aid stitch machine operators in identifying worn needles so that timely replacement could be made before any damage to the preforms occurs. The visual stitch standard helps the operator in identifying needle wear as well. Lastly, 3-D woven fillets were selected from a variety of fillets to improve the quality of T-blade stiffeners. These 3-D fillets significantly reduced the handling and cost compared to the previously used fillets. All these developments led to significant improvements in the quality of preforms used in the Composite Wing Program.

5.2 RFI Temperature Cycle Development

The objective of the temperature cycle investigation was to examine the 3501-6 reduced catalyst (RC) epoxy resin system (Hexcel, Magna, UT) using rheology testing and part fabrication to determine the temperature ramp rates that would satisfy RFI processing requirements. Specifically, the minimum allowable temperature-rise rate for 3501-6 RC resin was to be determined and temperature cycle guidelines to reduce risk in the RFI processing of semi-span wing cover panels.

Table 8. S/RFI QFD Matrix

WHAT vs. HOW Legend

Effect

Effect	Symbol	Value
Strong	●	5
Moderate	○	3
Weak	□	1

#		Customer Importance	1	2 Fillet Formation	3 Stitch Form./Preform Comp	4 Bobbin Thread Tension	5 Needle Thread Tension	6 Pressure Foot Force	7 Needle Wear	8 Stitch Speed	9	10 Perform Tooling	11	12	13 Temperature Cycle	14 1st Heat Ramp	15 1st Hold	16 1st Part Delta	17 1st Overshoot
				PREFORM FABRICATION							PREFORM TOOLING				RFI PROCESSING				
1	Resin-Starved Areas	●		□												●	●	○	○
2	Stringer, Spar Cap, Rib Clip Location	●										○							
3	Fiber Damage (wrinkle, kinks, buckles)	○		●					□			●							
4	Void Content	○		○		□	□	□	□	□		□				□	□	□	□
5	Loft	□																	
6	Skin Thickness	□		○		●	●	●	●	□		□				●	○	●	●
7	Stringer, Spar Cap, Rib Clip Thickness	□		□		□	□	□	□	□		□							
8	Resin-Rich Areas	◆		●		●	●	●	●	○		●				●	●	●	●
9	Surface Finish	■		●		○	○	○	○	□						□	□	□	□
	Importance Rating			105		55	55	55	62	27		94				93	83	75	75
	Importance Rank			4		16	16	16	12	20		5				6	8	10	10
			1	2	3	4	5	6	7	8	9	10	11	12	13	14	15	16	17

#		18 2nd Heat Ramp	19 2nd Hold	20 2nd Part Delta	21 2nd Overshoot	22 Pressure Cycle	23 Initial Pressure	24 Initial Vacuum	25 Final Pressure	26 Resin Allocation	27 Initial Resin Content	28 Filming/Degassing Method	29 Initial Resin Distribution	30 Resin Bleed	31 Bleed Cloth Amount	32 Bleed Cloth Distribution	33	34 RFI TOOLING	
		RFI PROCESSING																	
1	Resin-Starved Areas						●	□			●		●		□	□		●	1
2	Stringer, Spar Cap, Rib Clip Location		□															●	2
3	Fiber Damage (wrinkle, kinks, buckles)												□					●	3
4	Void Content						●	●	●		□	●	□		□	□		●	4
5	Loft			□														●	5
6	Skin Thickness						●	□	●		●		●		●	●		●	6
7	Stringer, Spar Cap, Rib Clip Thickness	○	○	○	○				○				○					●	7
8	Resin-Rich Areas						●	□	□		●	□	●		●	●		●	8
9	Surface Finish						●	●	●		□	●	○		□	○		●	9
	Importance Rating	15	24	20	15		125	57	83		93	43	117		57	59		255	
	Importance Rank	23	21	22	23		2	14	8		6	19	3		14	13		1	
		18	19	20	21	22	23	24	25	26	27	28	29	30	31	32	33	34	

Processing Parameters = Hows

Quality Requirements = Whats

Customer Importance: ●-Very Strong (9); ○-Strong (7); □-Moderate (5); ◆-Weak (3); ■-Very Weak (1)

Importance Rating: $\sum_{i=1}^{9} (\text{Customer Importance})_i \, (\text{Effect})_i$

The baseline requirement, outlined in DMS 2439 - "B" Stage Bulk Resin for the Resin Film Infusion (RFI) Process, states that "the resin shall have a minimum viscosity of 10 poise or less and a maximum viscosity of 30 poise for 120 minutes during the RFI processing cycle. Previous work in monitoring resin flow through preforms using dielectric sensors has shown, however, that only a 90-minute process window is required for this resin system. Because the same resin and preform types were used in the present study as were used in generating these previous results, the 90-minute limit was used.

The temperature cycle investigation was divided into two studies. The first study, the Resin Viscosity Study, evaluated the effect of thermal history, due to resin degassing and filming, and RFI processing temperature-rise rate on the viscosity characteristics of 3501-6 RC resin using rheology testing. The viscosity data from this study were used to establish a degassing procedure and minimum allowable temperature-rise rate for successful RFI processing. The second phase of the temperature cycle investigation verified the minimum allowable temperature-rise rate during the RFI manufacturing process. Temperature cycle requirements for successful semi-span wing cover panel processing were established. Both rheological tests as well as part manufacturing tests were used in the second phase.

Preliminary resin rheology/temperature-rise rate studies of the 3501-6 RC epoxy resin system show that this resin system when heated at 2°F/min satisfies resin viscosity requirements as given in DMS 2439. However, due to the addition of a resin-degassing requirement to the RFI process to improve surface quality, further study was needed.

Although higher temperature-rise rates may be desired to reduce autoclave processing time, faster temperature-rise rates, while lowering the minimum viscosity, may unacceptably decrease the processing window. This can be seen in the RDS dynamic ramp viscosity profiles of 3501-6 RC resin degassed and filmed at 180°F for 60 minutes and tested at temperature-rise rates of 1.0, 2.0, and 3.0°F/min. These test results show that the minimum viscosity decreases from 6.12 to 5.68 to 4.01 poise while the processing window decreases from 135 to 115 to 105 minutes. All of these values still satisfy RFI processing minimum viscosity and process window requirements, however.

Because resin flows faster at lower viscosities resulting in reduced processing times, maximum temperature-rise rates are desired for RFI processing. This maximum temperature-rise rate is limited, though, based on a required processing window greater than or equal to 90 minutes. Based on the 3501-6 RC resin viscosity profiles, the maximum allowable temperature-rise rate for RFI processing cannot yet be determined because the fastest temperature-rise rate tested to date, 4.0°F/min., with a process window of 100 minutes, still satisfies the RFI process window requirement. Until additional rheology tests are performed at greater temperature-rise rates, 4.0°F/min. should be used as the upper temperature-rise rate bound for RFI processing. Also, the slowest temperature-rise rate that satisfies RFI processing resin viscosity and processing window requirements for 3501-6 RC was found to be 0.5°F/min.

Resin rheological studies provided a good basis for establishing RFI temperature cycle processing parameters. These studies were useful in establishing guidelines for processing the semi-span cover panels.

5.3 Effects of Processing Pressure

The objectives of this study were to determine how processing pressure and resin bleed interact in the RFI process. In order to determine the interactive relationships between pressure and resin bleed, preform compaction and resin-bleed RFI processing characteristics were simultaneously evaluated. The pressure cycle and resin bleed studies were established to determine the preform compaction characteristics and whether processing/compaction pressure alone could be used as the controlling process parameter instead of the amount of bleeder cloth allocated to control resin bleed and final resin content.

Earlier work in this program identified the need for a higher-flow resin. In that study, it was determined that the original epoxy resin used—Hexcel 3501-6—did not have a sufficiently large process window or a low enough viscosity to infuse thick stiffened structures such as the wing cover panels made for this phase of the program. As a consequence of this, a series of experiments was conducted, at the end of which a reduced-catalyst version of 3501-6 epoxy resin was selected to provide the needed processing parameters without sacrificing mechanical performance. All work described below was done with this reduced-catalyst resin.

The pressure cycle/resin bleed investigation was completed in two phases. In the first phase of the investigation dry preforms were evaluated. These results were then utilized during the second phase using saturated preforms to determine pressure cycle and resin bleed parameters for high-quality RFI processing. Results from this study were used to establish pressure and resin bleed requirements for the fabrication of semi-span wing upper and lower cover panels.

The compaction characteristics of dry preforms vary with the number of stacks of warp knit carbon fabric, whether the preform is heat-set or not, the level of heat-set pressure, and whether the panel is flat or stiffened. Results have shown that thicker dry preforms compact to higher fiber volume fractions than thinner preforms at the same compaction pressure. This is believed to occur because fibers nest more easily in thick than in thin preforms. The difference in preform compactability, however, decreases with increasing compaction pressure. Heat-setting a preform, regardless of thickness, increases its compactability and higher heat-set pressures have higher compactibilities than lower pressures. After heat-setting a preform, the preform does not return to its original uncompacted thickness. When the preform is compacted again, the fibers are believed to nest better and thus the preform requires less pressure to achieve the same fiber volume fraction. The differences in fiber volume fraction of heat-set and non-heat-set panels, compacted at the same pressure, decrease with increasing pressure.

Regardless of panel thickness, saturated preforms achieve similar fiber volume fractions—within 0.3 percentage points—for any given compaction pressure. This means that if pressure alone were allowed to control part thickness and final resin content by using excess bleed cloth, an RFI processing pressure of 40 psi would be required to fabricate a variable thickness part within the part thickness tolerance requirements of 0.055 ± 0.015" per stack.

However, pressure alone cannot be used to control final resin content because fabricating a panel in this manner leads to poor part quality in the form of dry fibers and visible surface porosity—the former listed as one of the most critical parameters in Table 6. Additionally, such panels have void contents greater than 2.5%, which is above the RFI processing criterion of less than 2%, which can adversely affect compression properties. These manufacturing defects do not occur when final resin content or resin bleed is controlled through the allocation of bleeder cloth. For this reason, bleeder cloth allocation using a fixed pressure is the recommended method for controlling final resin content and resin bleed during RFI processing.

To be able to control resin content through bleeder cloth allocation, the processing pressure needs to be high enough to force the desired amount of resin through the preform and into the bleeder material prior to resin gel, and low enough to prevent over-compaction. Resin gel prior to complete infiltration leads to resin-rich and resin-starved areas and out-of-tolerance skin thicknesses. Resin-rich OML surfaces can also occur when a preform is over-compacted by excessive autoclave pressure.

Compaction pressure studies indicate that performs will relax as much as 4 percentage points of fiber volume fraction after pressure is removed. During RFI processing, this generally occurs after the bleeder packs are completely saturated. For the consistent, robust RFI fabrication of high-quality parts, the

pressure applied during RFI processing should be between 80 and 120 psi and resin bleed and final resin content should be controlled by the bleeder cloth allocation method.

A minimum of 80 psi is required to ensure consistent RFI processing of integrally stiffened panels. Processing at this pressure minimizes the difference in fiber volume fraction for variable thickness panels and ensures proper fiber wet-out and resin bleed for part heat-up rates greater than 1°F/min. For the resin viscosity profile at this temperature-rise rate, the resin flow rate of 3501-6 RC at a processing pressure of 80 psi allows sufficient time for resin infiltration and bleed prior to resin gel. Higher pressures should be used for temperature-rise rates between 0.5 and 1°F/min. At these rates, resin viscosity is higher and greater pressure is required to force the resin through the preform and into the bleeder packs. Pressures up to 120 psi can be used to decrease infiltration times thereby ensuring the wet-out of thick integrally stiffened panels. However, the higher the pressure, the more the preform is compacted and the greater the risk of resin-rich OML surfaces unless resin allocation is properly adjusted.

5.4 Resin Allocation

Because full and uniform infiltration of the preform has been identified as being among the most critical factors for success in producing high-quality parts in the S/RFI process (shown schematically in Figure 35) a set of experiments was designed to characterize the resin and its flow behavior for use in the RFI process. These experiments included rheometry to measure the process window and useful outlife of the resin as well as subscale part manufacture to quantify different means of resin allocation and resin flow. Another goal was to improve the thickness uniformity of cured S/RFI parts. Proper allocation and bleed of the resin play a major role.

S84129

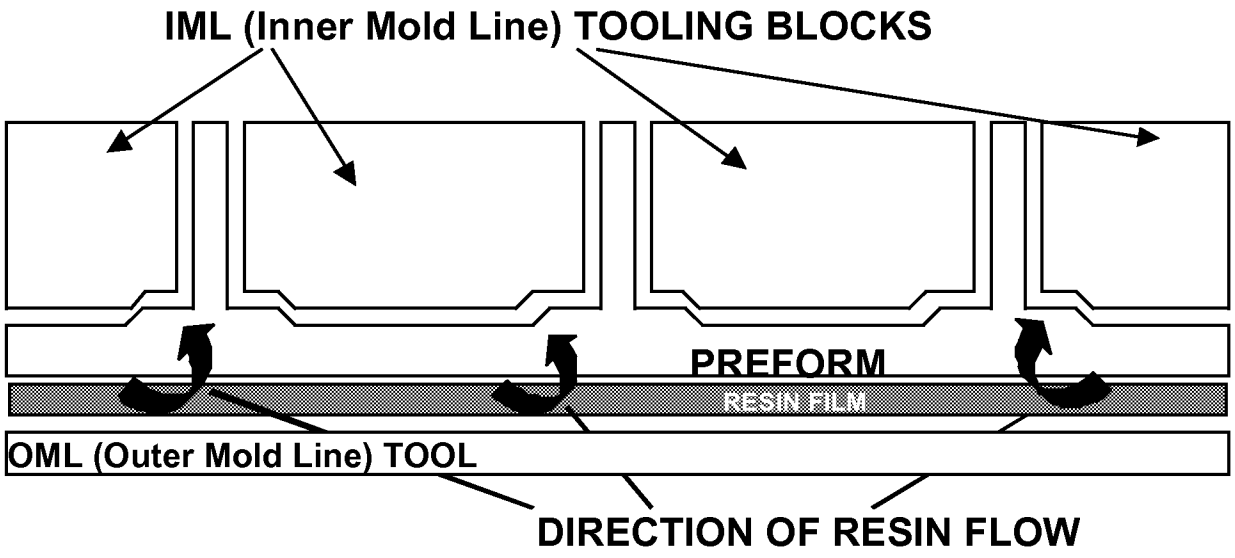

Figure 35. Schematic of RFI process showing OML and IML tooling, preform, resin, and direction of resin flow through preform.

Materials and Test Methods

The fabric used for the skin stacks was Saertex orthotropic (44% 0° plies, 44% ±45° plies, and 12% 90° plies) warp-knit carbon fabric. The preforms were stitched at 40 penetrations per square inch. The epoxy resin used to infuse each preform was 3501-6 RC (Reduced Catalyst) manufactured by Hexcel. The resin is degassed prior to use in the RFI process to reduce the potential for void formation in the processed part. Bleeder packs used to absorb excess resin after it had infiltrated the preform and passed through vent holes in the IML tooling blocks were made from fiberglass cloth. Typically, these bleeder packs were located above stringer blades and intercostal rib clips. A fluorescent dye powder from Ciba Specialty Chemicals was used as tracer material to track resin flow by placing plugs of it into resin tiles prior to RFI processing.

The RFI cure cycle used for all the experiments was 2°F/min ramp to 250°F followed by a hold at this temperature for 60 minutes, a second ramp at 2°F/min to 350°F followed by a hold for 120 minutes at this temperature before cool-down. Full vacuum plus 85 psi pressure were applied until the end of the 250°F hold, at which time the vacuum was vented and the pressure increased to 100 psi. The pressure was removed at the end of the processing cycle.

Resin viscosity characterizations to determine process windows and useful outlife were performed using a Rheometrics RDS rheometer by simulating the cure cycle described above.

Resin Outlife Study

In order to reduce risk in the manufacture of large stitched wing cover panels, the useful lifetime or outlife at room temperature of the 3501-6 RC resin was examined. Because it is known that epoxy resin systems such as 3501-6 RC will advance at room temperature, a test program to establish processing constraints to characterize the resin outlife for use in the RFI process was conducted. The study included various preheat conditions encompassing the range of practical temperatures that had been previously used for degassing the resin and preparing the resin tiles. The purpose of these tests was to establish the useful outlife of this resin system by considering several of the heat conditions that represent the degassing and tiling process.

Summary of Processing Studies

In the process development work presented above, it was determined that the 3501-6 RC resin has sufficient outlife to accommodate production process flows of composite wing structures for large transport aircraft.

A series of scale-up panels made to simulate sections of the semi-span lower cover panel provided useful information as to resin flow and resin allocation. These experiments also demonstrated that simplified flat geometries may be used to simulate more complicated stiffened and curved structures in developing proper processing parameters.

Resin allocation experiments showed that, because of the limited in-plane flow, significant customization is required in resin allocation. Many regions must thus be overallocated to prevent regions from being incompletely infused.

5.5 VARTM Process Studies

The VARTM (vacuum assisted resin transfer molding) process was studied in this contract to further extend the possibilities of reducing up front tooling and capital costs associated with conventional autoclave processed composite systems.

The VARTM process is a composite fabrication process by which a dry fiber preform is vacuum-bagged against a single-sided tool and is infused with resin that is drawn in a controlled manner into the evacuated preform. Vacuum pressure alone is used to compact the preform and at least an initial cure occurs in the vacuum bag (full cure may occur in the bag or using a freestanding post-cure depending on the resin formulation). As with any liquid-molding process, control of the resin flow front is necessary to assure that the preform is completely and uniformly infused with resin.

A one-sided (typically outer moldline) tool is used to support the preform during infusion and cure with the preform accurately located on the tool, then bagged with either a reusable or nylon bag. A resin distribution medium is used to assist the flow of the resin over the preform surface. The medium helps to control and direct the resin flow. The bag contains both resin feed ports and vacuum ports for resin input and extraction. Vacuum feed hoses are submerged in a resin reservoir while vacuum is applied through the vacuum ports to draw resin into the preform as shown in Figure 36.

Initial development and evaluation studies were done to adapt the Vacuum Assisted Resin Transfer Molding (VARTM) process for commercial wing applications. This work included processing and mechanical property evaluations of candidate VARTM resins, design and fabrication of low-cost VARTM substructural elements, and design development of a low cost unitized wing box made using the VARTM process.

VARTM-PB (Tooling/Process Development) Background

Due to the size and complexity of structural components such as airplane wings, the formation of these structures using composite materials in a single-step molding process historically has not been possible. Until recently, processes capable of holding critical dimensional features within narrow tolerance ranges for large complex composite structures did not exist. Typically a complex part is broken down into multiple pieces of simple design that are subsequently assembled into a larger complex structure. The cost to manufacture structures in this manner is significantly higher than molding a single part. The application of Vacuum Assisted Resin Transfer Molding (VARTM) has also grown over the past ten years to include the fabrication of large composite structures for the marine industry as well as secondary structure for military aircraft (engine inlet ducts). Recently, advances have been made under the Composite Wing Program in the development of a new process called VARTM-PB (VARTM with pressure bleed). VARTM-PB combines traditional VARTM with an autoclave cure to achieve the high fiber volume fractions required of aircraft primary composite structure, a requirement VARTM by itself has failed to meet.

Currently there are only two liquid-molding methods that have proven applicable to the fabrication of high performance large composite structures such as aircraft wings: RFI and VARTM. RFI involves the use of a resin film placed directly in contact with the dry fiber preform and mold tool. The tool/part assembly is vacuum bagged and, under temperature and pressure inside an autoclave, the film of resin infuses through the thickness of the preform. This process requires the displacement of the mold tool and, in some cases, the fiber preform itself. As a result of this displacement, tool sealing has proven difficult when large thick films of resin are employed. This results in a certain degree of risk associated with complete impregnation of the preform. VARTM, on the other hand, offers the potential for a more robust process for impregnation of the dry fiber preform. In VARTM a liquid resin is infused into the preform by pulling a vacuum on the mold tool. The resin is introduced to the preform with inlet tubes and a manifold system located on the outer surface of the preform. In this process, the mold tool requires only slight movement to compensate for bulk reduction in the preform as force is applied through vacuum. Tool sealing is extremely simple compared to current RFI methods. However since VARTM only uses

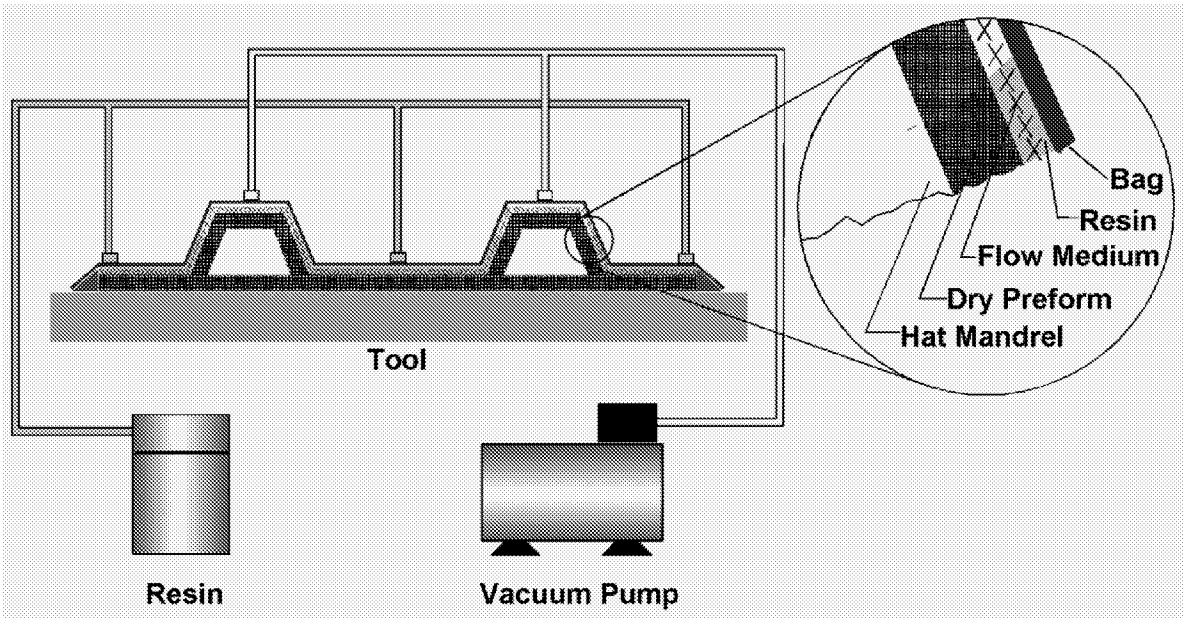

Figure 36. Schematic of a typical VARTM process.

vacuum pressure (out of the autoclave process) to infuse the preform, resulting fiber volume factions are too low (54% or less) for the performance levels typically required on aircraft heavy gauge primary structures. Fiber preforms with thick cross sections typical of transport aircraft primary structure require significant pressures during processing to remove bulk and raise fiber volume fractions to acceptable levels (57% - 60%).

VARTM offers a robust process for resin infusion of thick dry fiber preforms. However, because traditional VARTM uses vacuum pressure only, it cannot produce high fiber volume fractions on thick preforms unless debulking of the preform is performed prior to VARTM processing. By contrast, VARTM-PB is a robust resin infusion process capable of producing large fiber-reinforced composite structures with high (57%+) fiber volume fractions. In addition, when used with the new mold tool system developed by Boeing, VARTM-PB is capable of holding critical dimensional features within narrow tolerance ranges for large complex composite structures (Figure 37).

5.6 VARTM Unitized Structure Development

In order to assess the benefits of unitized structure to reduce the costs of aircraft part manufacture, a manufacturing study was initiated using the vacuum assisted resin transfer molding (VARTM) process. This study describes various candidate manufacturing approaches that might be used for a generic unitized wing box structure using stitched preform technology combined with the VARTM process. A summary of the material and configuration selection process and a discussion of the tooling and processing methods necessary to produce a unitized wing box are presented.

Trade studies were performed to identify innovative concepts for composite wing structure with the goal of achieving additional significant cost savings through the use of low cost manufacturing methods and/or unitized structure designs. These concepts were rated against the 'baseline' S/RFI composite wing configuration developed in the NASA AST Composite Wing Program. This baseline wing is already a highly unitized design with integral stringers, spar caps, and rib-attach clips on the cover panels. It

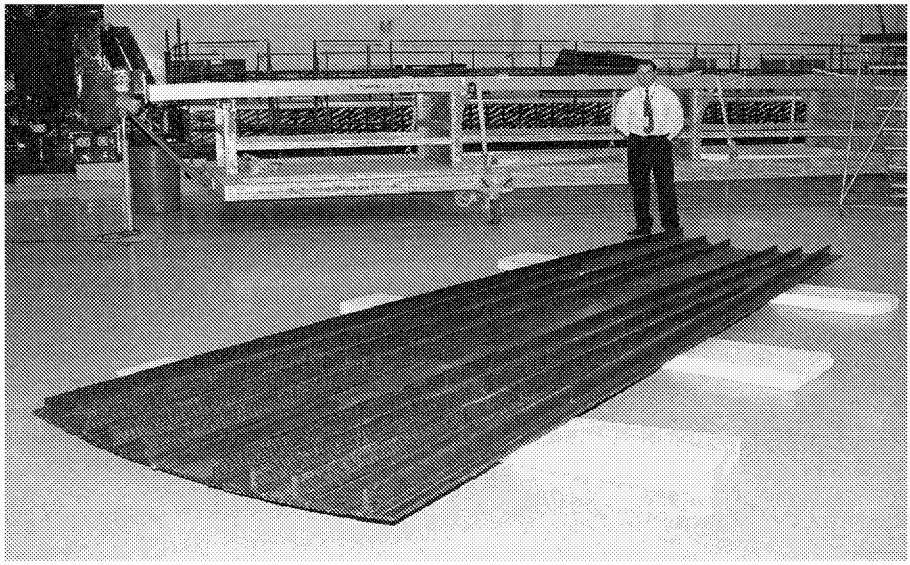

Figure 37. Wing Cover Panel part processed using the VARTM –PB process

represents a substantial part count reduction compared to a conventional metal wing, and approximately an 86% reduction in fasteners compared to a metal wing. The goal of this trade study was to identify additional cost savings beyond those already achieved in the 'baseline' configuration.

Unitized structure concepts were developed by an Integrated Product Development (IPD) team and evaluated using a standardized scoring system. The team consisted of representatives from major disciplines representing Design, Strength, Materials and Processes, Tooling, Manufacturing, and Quality. Eight evaluation criteria were established for rating the cost, performance and risk of each concept, and weighting factors were assigned to each team members' ratings to emphasize cost more than performance and risk since cost reduction was the primary objective of these design studies.

Following initial evaluations of 28 different concepts, the top five were identified and moved into a more detailed evaluation phase. In this phase, an entire wing box was conceptually laid out using these concepts. Individual joint configurations were identified as well as manufacturing plans for all parts. This exercise identified potential tooling, strength and assembly problem areas. Projected part count and cost savings relative to the baseline wing were also identified during this phase. At the end of these detailed evaluations, the best overall concept was chosen to carry forward for a manufacturing demonstration (Figure 38). However, due to funding restrictions, the manufacturing demonstration article was not fabricated.

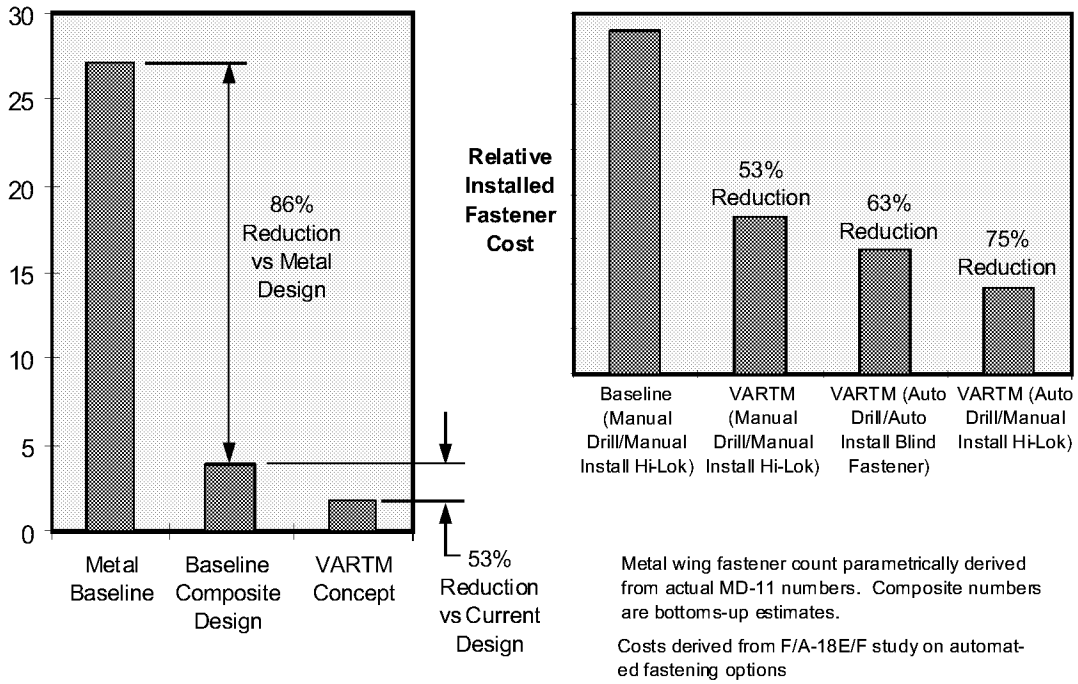

Figure 38. Cost savings from reduced fastener count and automation.

6. Semi-Span Fabrication

6.1 Cover Panels Tooling and Component Fabrication

Advanced Stitching Machine (ASM) Development

Boeing has been developing a manufacturing process for stitched, carbon fiber, resin film infused preforms for application to transport aircraft primary wing structures since 1978. Since 1989 under NASA contract, Boeing has conducted research in this composite technology with a primary focus on basic material forms, resin film infusion and scale up to various element and subcomponent panels. That research culminated in the design, manufacture and test of a 8 ft. by 12 ft. wing stub box test article.

To support this initial effort two stitching machines were purchased by NASA. One multi-needle quilting machine and one computer controlled single needle machine were designed and manufactured by Pathe Technologies Inc. in Irvington, NJ under the direction of Boeing. The multi-needle machine was utilized for the assembly of the basic skin stack material as well as heavy density stitching of wing skins for element and subcomponent panels. The single needle sewing machine was designed with computer controlled, X-Y motion, and consisted of a gantry type configuration containing one single needle stitching head capable of sewing up to 1.00 in. in thickness. The primary purpose of this machine was to create detailed stitch patterns and to attach the prefabricated stringer and intercostal clip details to the previously stitched wing skins.

In 1992, phase "B" of the Advanced Composites Technology (ACT) program, the task of procuring an advanced sewing machine capable of stitching 3-dimensional lofted wing cover panels for transport aircraft began. This effort included the development of a machine specification as well as the solicitation for proposals from potential suppliers. Based upon lessons learned from operating existing machines at Pathe, it was determined that the experience of the machine tool industry would need to be brought together with the sewing technology developed by Pathe. Ingersoll Milling Machine Co. and Pathe Technologies Inc. were selected as the contractors to work with Boeing and NASA in the design, fabrication and development of the ASM. The primary objective of this project was to deliver a machine capable of stitching complex contour wing cover panels for a 42-ft. semi-span wing [Reference 4].

The requirements driving the application of stitching in transport aircraft composite wing skins is damage tolerance and cost reductions. Boeing has proven through mechanical property testing that the cost to manufacture is significantly reduced while the retained strength of damaged composite structure is significantly increased with through the thickness stitching of the structure. In an effort to meet these requirements and to keep manufacturing costs down, Boeing has incorporated the use of stitched carbon fiber preforms in its wing cover panel design.

The ability of the stitched structure to retain a given level of strength is directly related to the stitch density, stitch formation, and the tensile strength of the thread itself. These three factors determine the effect stitching has on preventing the propagation of delamination for a given amount of impact energy inflicted on the structure. Current design stress levels for the semi-span wing dictate a stitching density of 40 penetrations per square inch using a Kevlar 29, 1600d thread. The formation of the stitch must be such that the penetrating thread passes completely through the thickness of the material with the lock between itself and bobbin thread lying on the lower surface of the part.

In addition to providing damage tolerance to the structure, the application of stitching also provides a cost effective manufacturing approach to the fabrication of the cover panel. Through stitching the process of assembling the skin stacks together and the attaching of stringer and intercostal clip details to the skin is automated. In order to optimize the cost effectiveness of stitched preforms, manufacturing worked

closely with design to address certain manufacturing issues. For example, to simplify the requirements of the sewing equipment, a stitching reference plane was created for each panel to define the vertical axis of the stitch thread relative to the lofted geometry of the cover. The standing column of thread was placed in the structure normal to the stitching reference plane as opposed to being normal to the lofted surface. This allowed the use of 3 axis machinery which is significantly less complicated to design and operate than 5 axis machinery, which would be required to place the thread normal to the loft surface at any given location. In addition the stringer planes were located parallel to one another and normal to the stitching reference plane. This allowed access for inserting the inner row of stringer flange stitches that attach the stringer to the skin.

In addition to the stitching requirements, the overall physical size and geometry of the semi-span wing cover panel also played an important role in determining the design of the ASM. The cover panel has a span of 42 ft. and an 8-ft. wide cord at the root. The depth of the wing across the cord is 18 in. with a 4° dihedral break along the span. The combination of these two specific features, along with a significant amount of twist in the span-wise direction, creates a lofted surface with a complex double curvature.

Upon evaluating wing cover panel design requirements, a series of studies were identified to help further define the equipment needed for the fabrication of a full-scale transport aircraft wing cover panel preform. The first was a thick stitching study where sample panels representing the maximum thicknesses of the wing cover panel were sewn. The objective of this experiment was to develop needle technology for the stitching of thick cross sections of carbon fiber fabric and to evaluate the ability of the current stitching head to sew through these thicknesses. The result was the selection of two existing needle designs from two separate manufactures that proved to be successful at all the cross sectional thicknesses of the cover panel.

The second study related to the formability of the warp knit fabric and the required support of that fabric during the stitching process. This study focused on the ability of knitted material to conform to the complex curvature of the lower wing skin surface in the sewn and unsewn conditions. It was hoped that the preform could be stitched together in the flat condition and then formed to the loft surface of the wing as opposed to having to stitch the material while being held in the lofted shape. This would simplify the design of the equipment required to stitch the preform and thus reduce the overall cost of the sewing machine and fabrication cost of the preform. Results showed that not only would the stitched preform not conform to the lofted surface of the wing, but the individual stacks of full width fabric themselves would not conform to the double curvature. In order to achieve conformability to the complex surface, the skin stacks would require a span-wise splice and support to achieve the shape of the loft surface while sewn together.

The ASM provided Boeing and NASA with a foundation upon which the required tools and processes were developed for the stitching of 3-dimensional carbon fiber preforms for full size transport aircraft wing cover panels, Figures 39 and 40 [Reference 5].

S84167

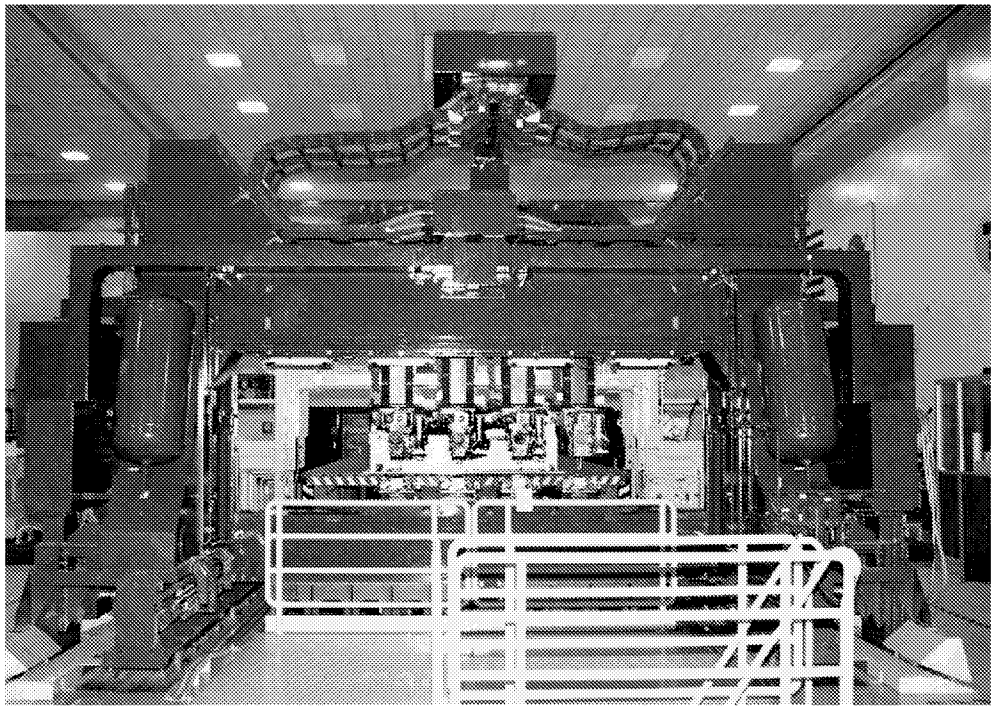

Figure 39. Advanced stitching machine gantry with 4 stitching heads and bobbins assemblies.

S84168

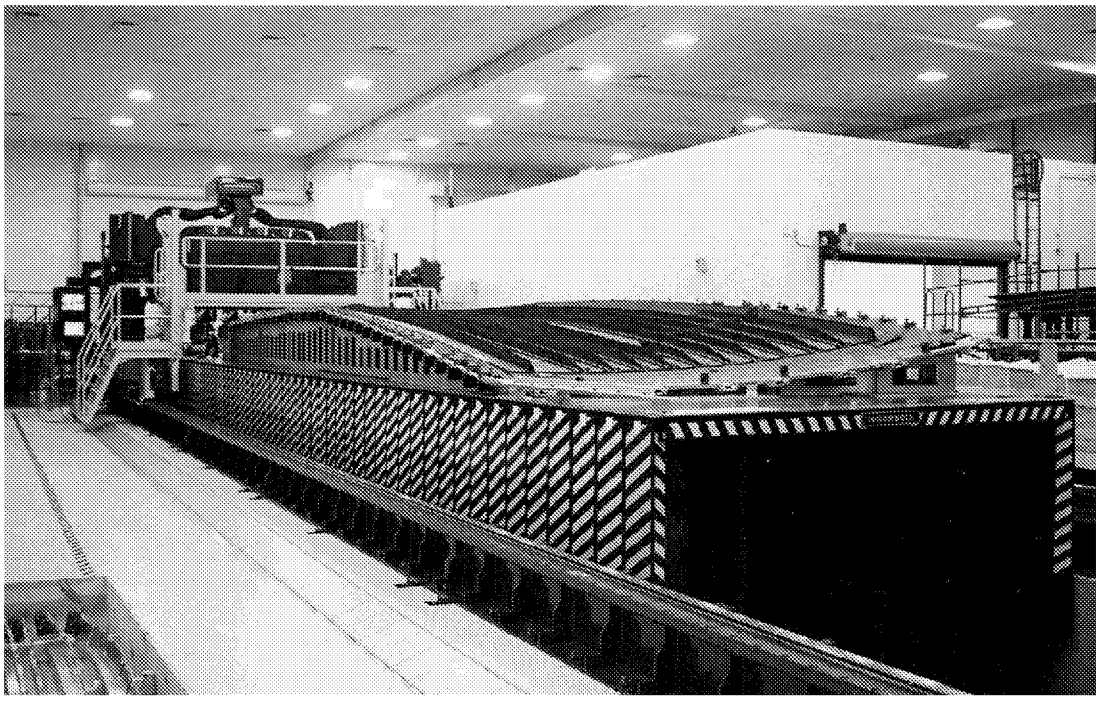

Figure 40. Semi-Span wing cover panel with complex contoured loft structure on advanced stitching machine.

The first generation stitching machines developed by Boeing proved invaluable in maturing the stitching process for assembling near net shaped fiber preforms. A considerable amount of knowledge was gained in needle design, sewing thread construction as well as perform construction and handling. However, these machines were limited in material thickness, part size and geometric configurations that could be stitched. For all practical purposes only panels with a flat outer mold line surface could be accurately stitched on these machines. With the scale up to the semi-span wing, the issue of complex contoured loft surfaces as well as an overall part physical size of 42-ft. by 8-ft. had to be addressed with a new Advanced Stitching Machine. Advances in stitching head technology were also required to increase stitching output to simulate production manufacturing rate requirements for commercial aircraft. A higher quality fabric than that used previously was necessary for improved structural performance and preform handling. For the resin film infusion process, a new tooling approach was required to meet the tight dimensional tolerances demanded by wing box assembly and compound curvature of the lower cover panel. A more robust resin system with refinements to the previous method of resin allocation and resin bleed was needed to address the thickness variations of the skin and overall part geometry.

Manufacture of the semi-span wing cover panels has validated all the engineering solutions to these technical challenges. This report describes fabrication of the semi-span wing lower cover panel with information being presented on material, tooling, equipment, preform stitching, and resin film infusion processing of the stitched preform.

Design Data and Preform Materials

The semi-span wing cover panel is a one piece integrally stiffened carbon fiber/epoxy primary structural component that is approximately 42-ft. long by 8-ft. wide and has a complex contoured loft surface with roughly 24-in. of depth from root to tip (Figure 41). The variable thickness skin ranges from 5 to 11 stacks but has localized buildups at the root and main landing gear stations. A maximum of 17 stacks or 0.940-in. cured thickness is represented in this part. Along the leading and trailing edges of the panel are the front and rear spar caps. The spar caps are interleaved with the base skin stacks for efficient shear load transfer from spars to skin. The vertical blade of the spar cap is 0.440-in. thick and 3.40-in. tall. Ten (10) stringers ranging from 0.470-in. to 0.800-in. thick and up to 3.40-in. tall are located on top of the wing skin inner mold line surface. In between the stringers orientated in a cordwise direction are 16 rows of intercostal clips, which define rib planes for wing assembly. Intercostal clips range from 0.220 in. thick for lightly loaded ribs to 0.440-in. thick for fuel pressure and main landing gear bulkheads. Height of intercostal clips coincides with the height of interfacing stringer blades. All stringer and intercostal clip details are stitched to the wing skin.

The wing cover panel skin, spar cap and intercostal clip details are all constructed of multi-axial wrap/knit carbon fiber fabric. This material consists of 7 layers of carbon fiber knitted together with a 72 denier polyester thread using warp/knitting machinery from the textile industry.

Preform Assembly

Assembly of the wing cover panel preform began with the lay up of the wing skin on the tooling bed of the ASM. Located on top of the ASM bed were 50 loft support modules. The series of modules were pinned and bolted to the lift tables to create the outer loft surface of the lower cover panel. Positioned around the perimeter of the loft modules was the aluminum-stitching frame. The frame was supported off of each module by steel angles, which contained large tapered pins for indexing the stitching frame to the loft modules. The precut wing skin stacks were positioned by hand inside the stitching frame on the loft surface of the modules, utilizing a ceiling mounted laser projection system (LPS). Technicians precisely located each piece of material by lining up the edges of the fabric with the laser projection outline. Once

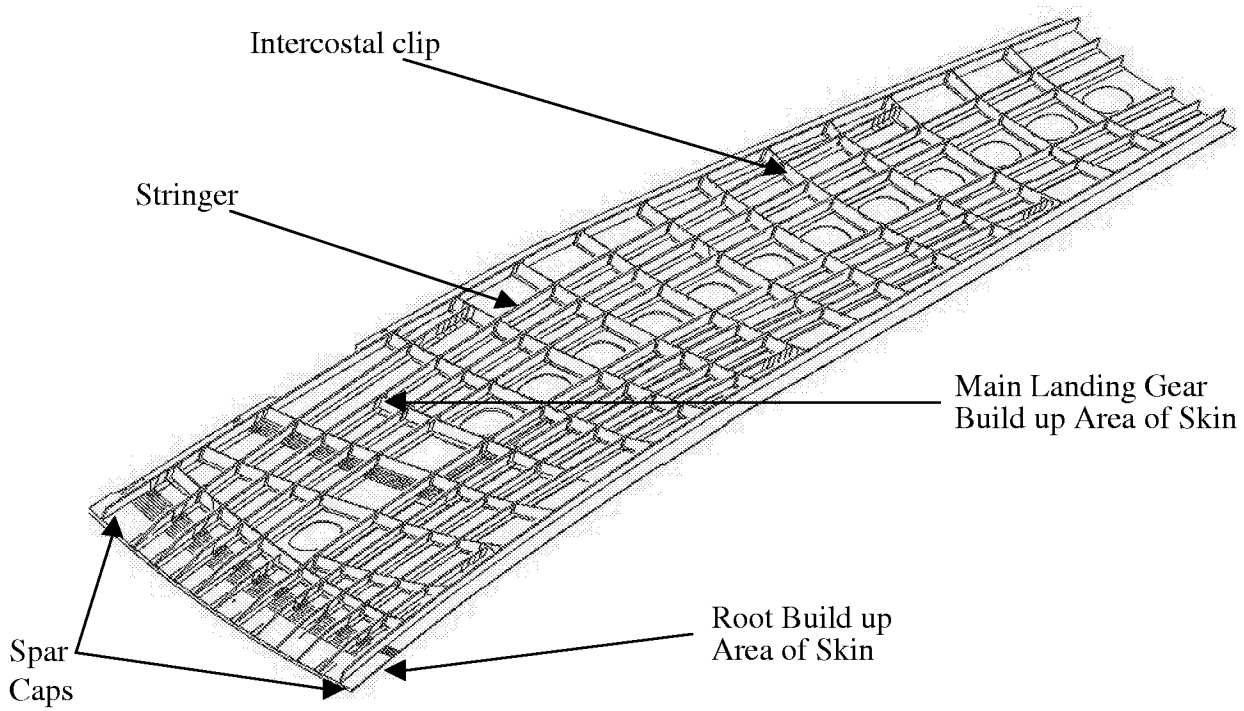

Figure 41. Semi-Span wing cover panel design.

the base (plies of material covering entire loft surface) lay-up was complete, the front and rear spar caps were positioned and secured in place using jig tooling (Figure 42). The remaining skin stacks were then placed on top of the base skin stacks between the front and rear spar cap details. The leading and trailing edges of the skin stacks were butt spliced with the inner spar cap flange stacks in a stepped sequence to create an interleaved spar cap flange and skin. Lay-up of the wing skin was completed with the placement of build up stacks at the root end of the panel.

A total of 25 NC programs were executed in stitching the wing skin/spar cap assembly. Stitching consists of parallel rows spaced at 0.200-in. apart with a stitch pitch of 8 stitches per inch. Those areas of the skin that fell under a stringer flange were left unstitched for subsequent attachment stitching of the stringers to the wing skin. This process eliminated double stitching of the skin. The leading and trailing edges of the panel were stitched last to complete the assembly of the skin stacks and spar cap details (Figure 43).

Stringer details were first located over the skin assembly by hand. Outline templates projected from the LPS were used to define critical stringer positions and establish proper location of the stringer in the spanwise direction. A jig was used to hold the root end of each stringer detail during attachment stitching of the stringer flange to the wing skin to prevent movement of the stringer longitudinally. A locating device was mounted to the stitching head to locate the stringer details during the stitching process (Figure 44). Once both flanges of the stringer had received a single row of stitching, the tooling devices were removed and the remaining stitch rows were inserted into the stringer flanges.

S83876

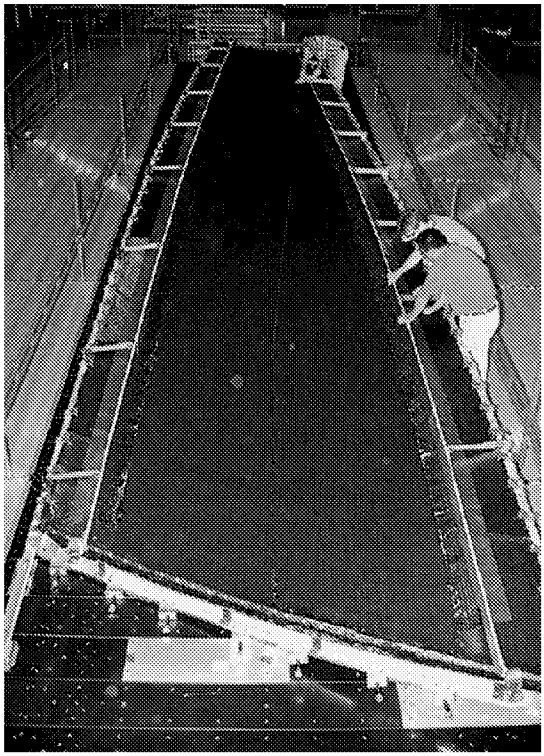

Figure 42. Base skin lay-up with spar caps.

S83877

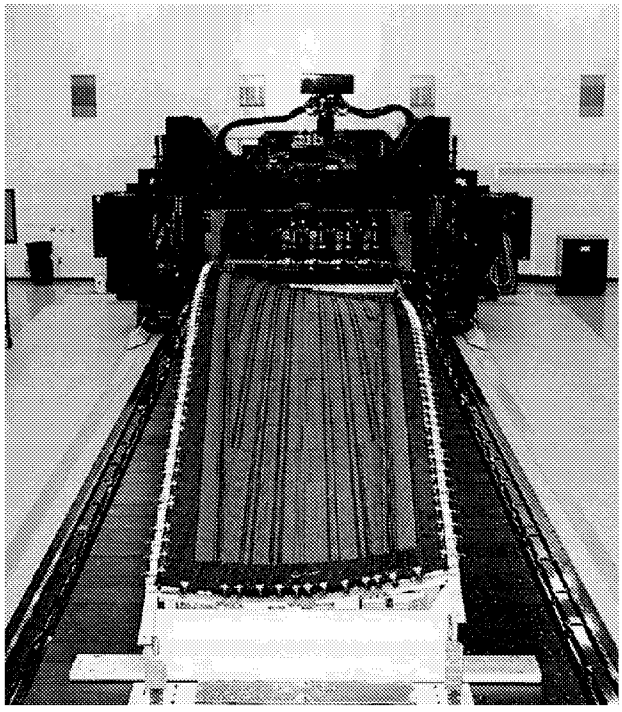

Figure 43. Stitched skin with integral spar caps.

S83878

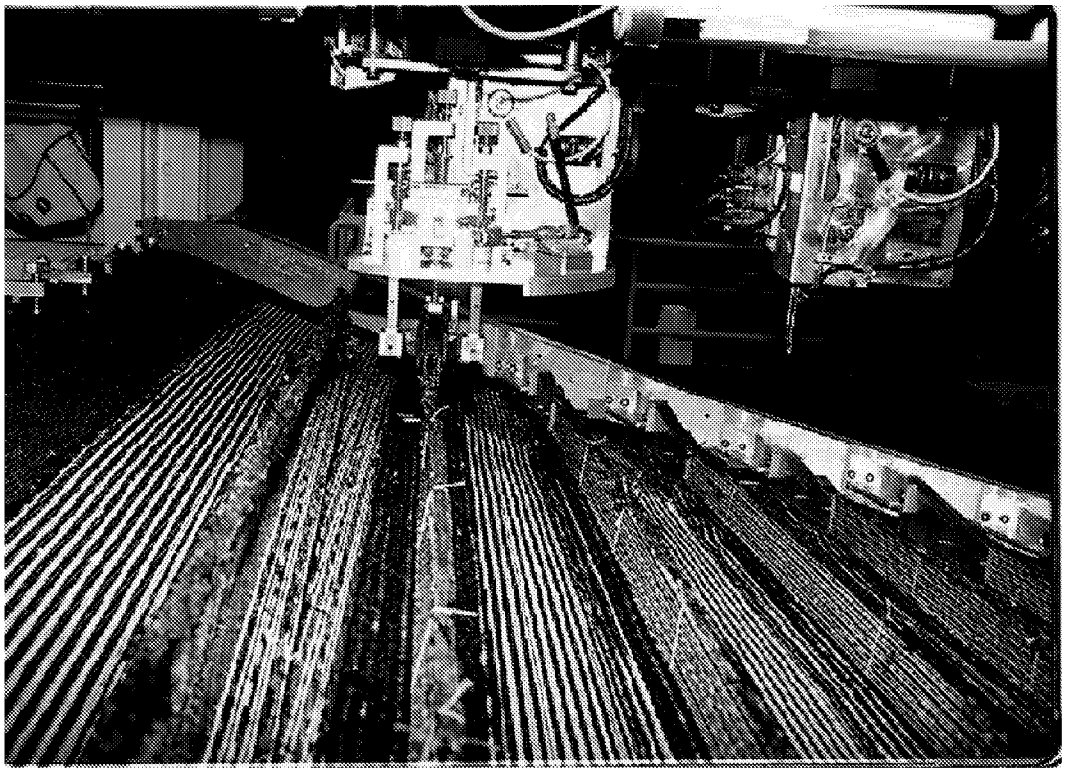

Figure 44. Stitching of stringer to skin.

The intercostal clip details were placed onto the preform assembly at each rib station. Aluminum locator jig tooling was used to position the intercostal clips in their respective rib planes. The inboard flange of each clip received a single stitch row to hold location. The locator jig was then removed and the remaining stitch rows were inserted into the inboard and outboard flanges of the clip (Figure 45). Once complete (Figure 46), the preform was transferred from the stitching machine to the cure tool. The completed preform then sits on top of the resin tiled OML tool. IML tooling blocks are then added on top of the preform and coordinated to the OML tool by a series of metal bars that define the shear web plane. Once locked in place, bleeder packs and sealing material are used along with a reusable rubber vacuum bag to seal the cover panel completely. The preform and tooling are then wheeled into the autoclave for curing.

Post Cure Analysis of Lower Cover Panel

Upon completion of the cure cycle, a detailed post cure analysis was conducted on the cured cover panel (Figure 47). The predicted vs. actual results are given in Table 9. The results show that a cured resin content of 31.4% by weight was achieved. Resin bleed analysis showed that the actual resin bleed was within 2.25% of predicted value. Theodolite inspection of the cover panel revealed that the mold tooling was extremely successful at establishing the critical design engineering datums for wing box assembly. Rib, spar plane, and loft definition was held to within 0.020-in.

S83879

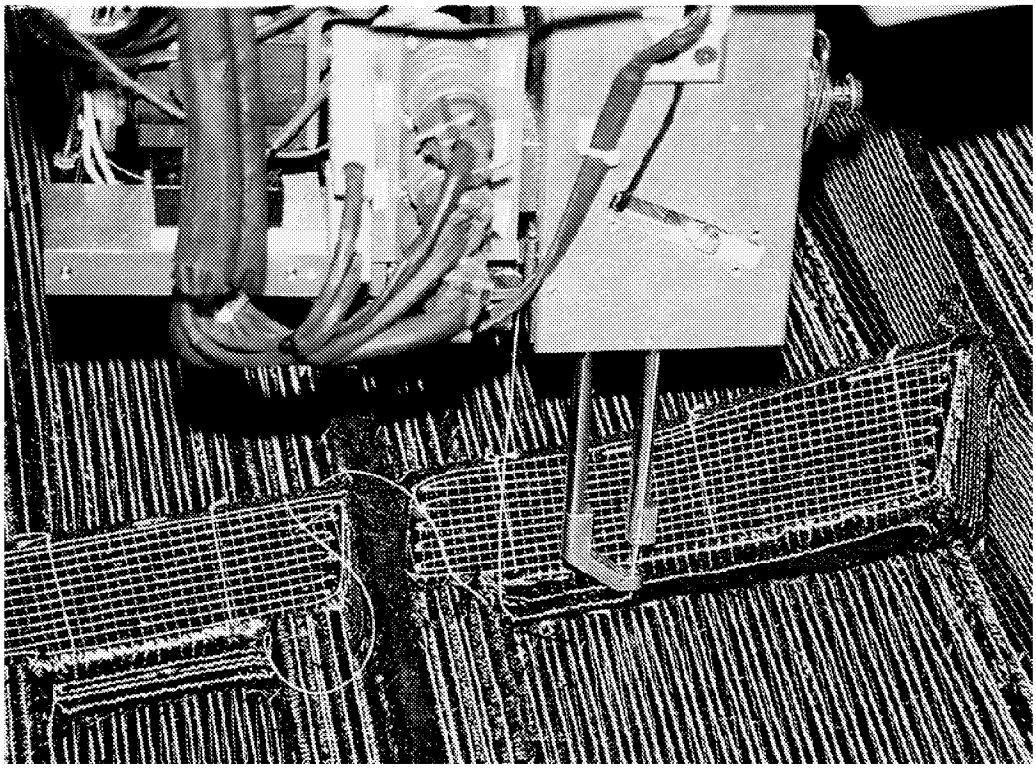

Figure 45. Stitching of rib clip to skin.

S83880

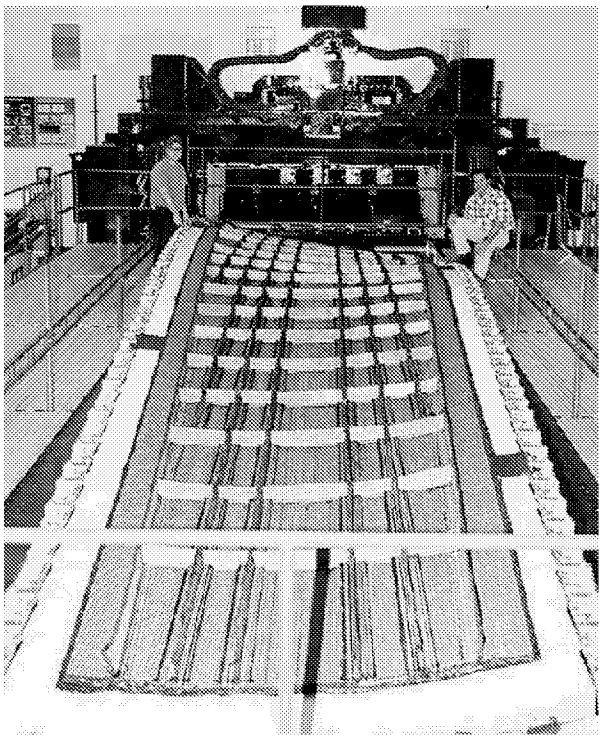

Figure 46. Stitched wing cover panel preform.

S83888

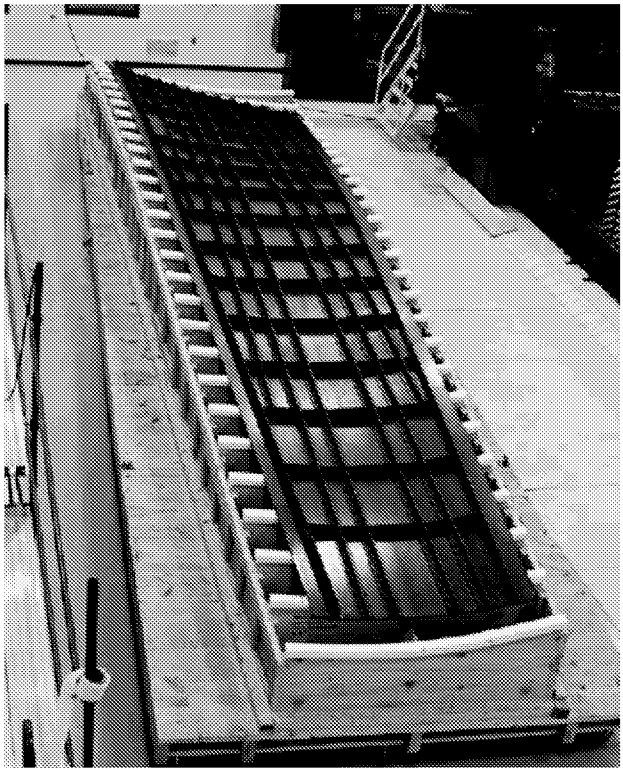

Figure 47. Stitched resin film infused Semi-Span wing cover panel.

Table 9. RFI Processing Results of Lower Cover Panel

	Predicted	Actual
Stitched Perform Wt.	1042-lb.	1064-lb.
Cured Part Wt.	1531-lb.	1548-lb.
Resin Bleed	43-lb.	44-lb.
Cured Resin Content	32.0%	31.4%
Fiber Volume	59% skin 57% stringer blade	59% skin 57% stringer blade
Rib Plane Definition	Tooled for ±0.015-in.	-0.010/+0.020-in.
Spar Plane Definition	Tooled for ±0.015-in.	-0.020/+0.015-in.

Boeing and NASA have demonstrated the ability to manufacture transport aircraft size composite primary wing structures with the fabrication of semi-span wing cover panels. The results indicate that large complex structures can be processed to tight engineering tolerances using the S/RFI process. Large integrally stiffened carbon fiber performs with complex contoured loft surfaces can be fabricated using full width multi-axial fabrics and stitching technology derived from the textile industry. Subsequent impregnation of these enormous performs with epoxy resin was demonstrated with the film infusion process.

Wing Box Assembly

Traditional metallic wings are assembled in a picture frame fashion. Spar web assemblies and the main landing gear (MLG) fitting are located in the assembly jig first followed by machined bulkheads and remaining ribs. Rib installation completes the framing process of the wing box. The wing skins are then located to the substructure for fastener hole processing and final installation. The AST Composite Wing assembly process differs significantly from metallic wing assembly. The cover panels, for example, combine traditional wing skins, stringers, intercostal clips, and rib locating features into one co-cured detail, see Figure 48. This greatly reduces the number of required parts and fasteners. Approximately 80 details make up the 42-ft. AST Composite Wing Box, excluding load introduction structure/hardware. Final assembly of the composite wing begins with the cover panels. Both cover panels are located to the contour boards, rear spar plane, and MLG bulkhead plane on the assembly fixture. The ribs are then located to the cover panel intercostal clips. The last details to be installed are the forward and aft spar webs.

Assembly Process

A key objective in defining the assembly process was to provide as much access to the work area as possible, particularly when processing thousands of rib web-to-intercostal fastener holes. The resulting assembly sequences for the semi-span wing box is as follows: The upper and lower cover panels are positioned to the contour boards and indexed to three locating features of the assembly fixture, two at the rear spar plane and one at the rib 6 plane, Figure 49.

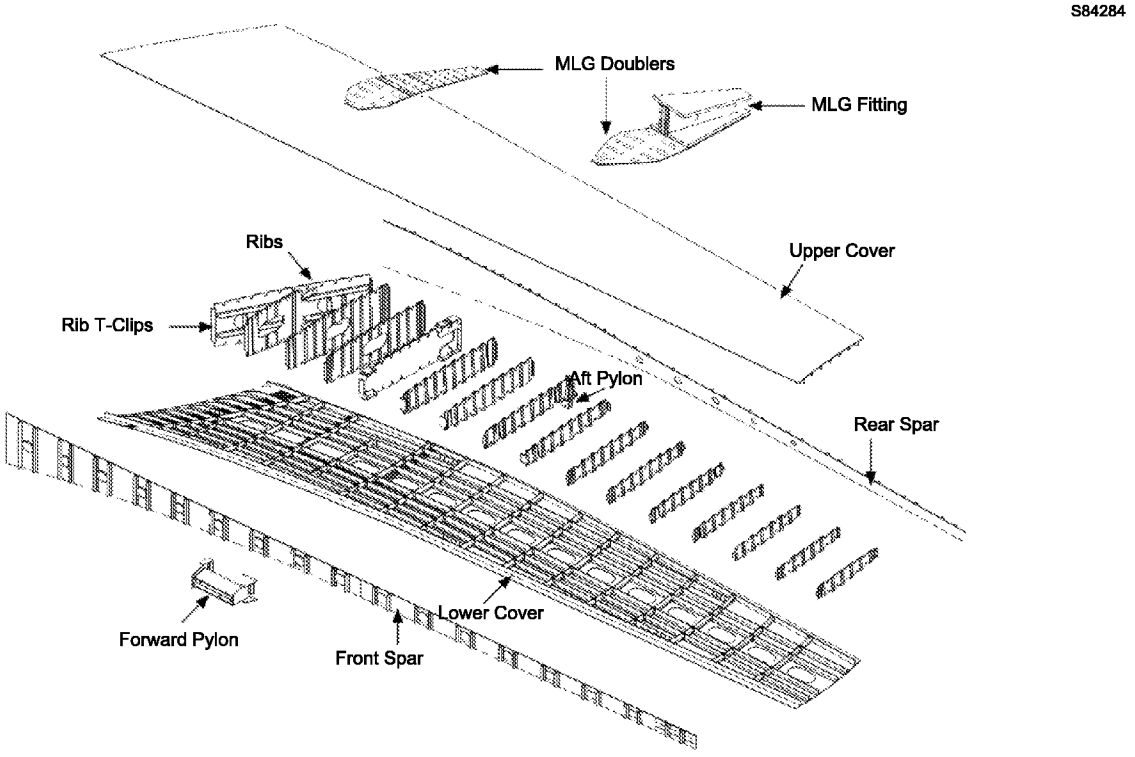

Figure 48. Semi-Span structural arrangement.

S84285

Figure 49. Cover panel locating features.

Rib webs are located on the cover panel intercostals insuring adequate fastener edge distance. Temporary attachments are used to secure the ribs to the upper and lower covers. The lower cover temporary attachments are then removed and the jig is opened with the ribs attached to the upper cover. The rib web to upper cover panel attachment holes are then processed to full size in this opened condition. After the jig is closed, the ribs are again temporarily attached to the lower cover. The upper cover temporary attachments are then removed and the jig is opened. Fastener holes in the lower cover are then processed to full size and the permanent fasteners installed, Figure 50.

When the jig is again closed, permanent fasteners are used to attach the upper cover to the ribs. After the ribs are permanently installed, all rib web to spar web t-clips are installed, Figure 51. The root splice transition structure fittings are located, drilled, and installed next, Figures 52 and 53. The outboard and inboard rear spar web sections are then located and installed, Figure 54. After the MLG fitting has been craned into position on the assembly fixture, the skin doublers are placed into position and used to attach the MLG fitting to the upper and lower covers of the wing box. The MLG-to-spar web attach angles are then installed, Figure 55. Final close-out of the outboard wing box occurs with installation of the outboard and then inboard front spar web sections. The remaining load introduction structures are then installed including the root splice spar extensions, side-of-body bulkhead (Figure 56), rib 6 front spar fitting, forward and aft pylon mounts, rib 13 saddle (Figure 57), and rib 18 close-out structure.

S84286

Figure 50. Lower cover panel fastener hole processing.

S84287

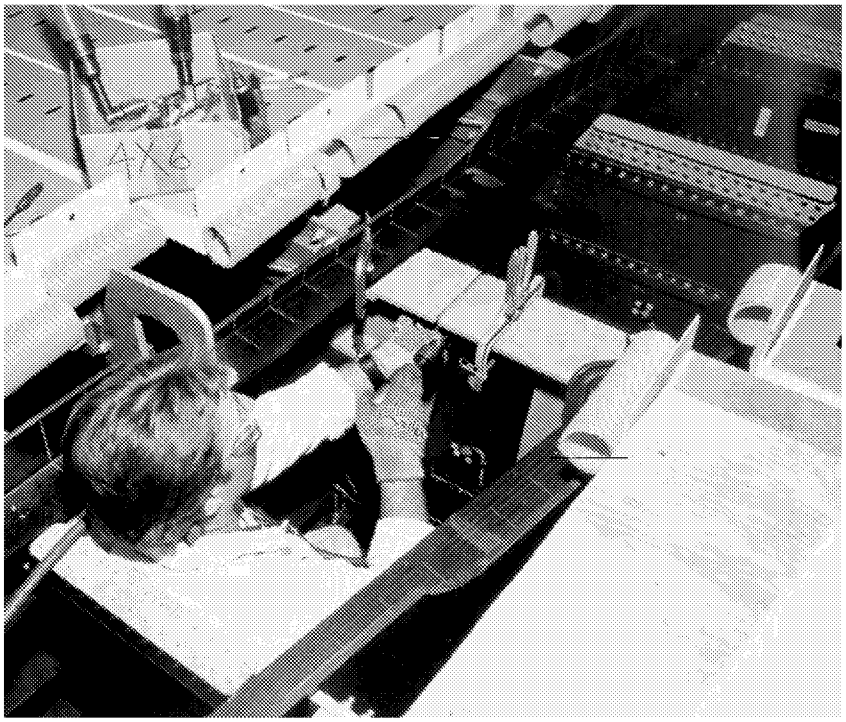

Figure 51. Rib web to spar web clip installation.

S84288

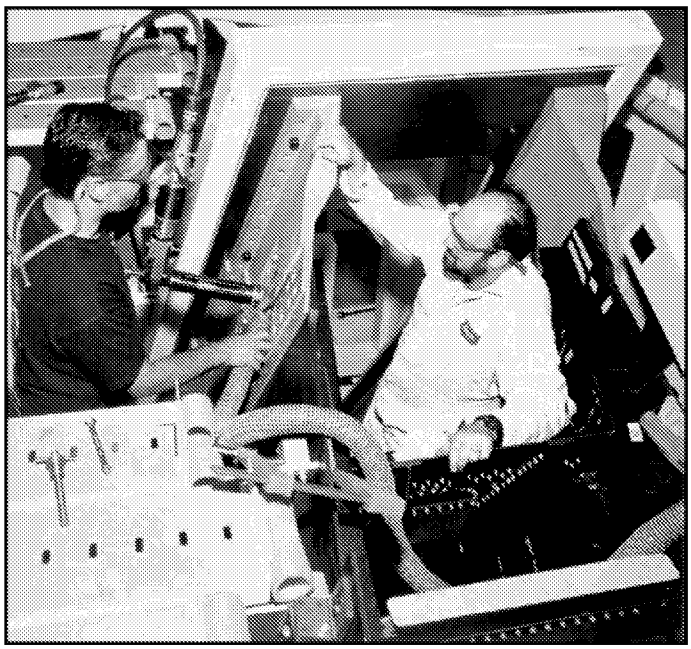

Figure 52. Upper cover Transition Splice Fitting (TSF) installation.

S84289

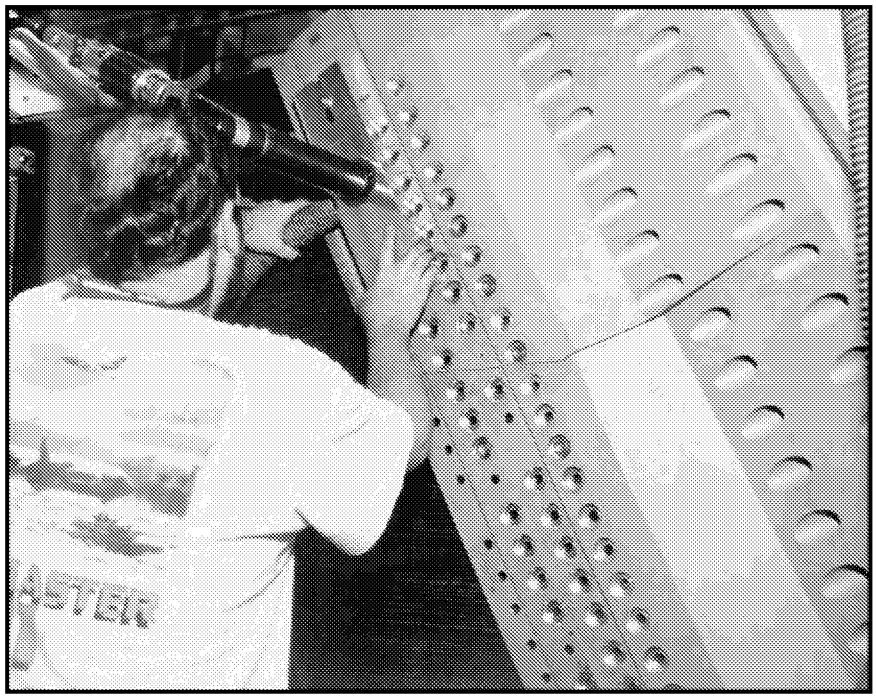

Figure 53. Lower cover Transition Splice Fitting (TSF) installation.

S84290

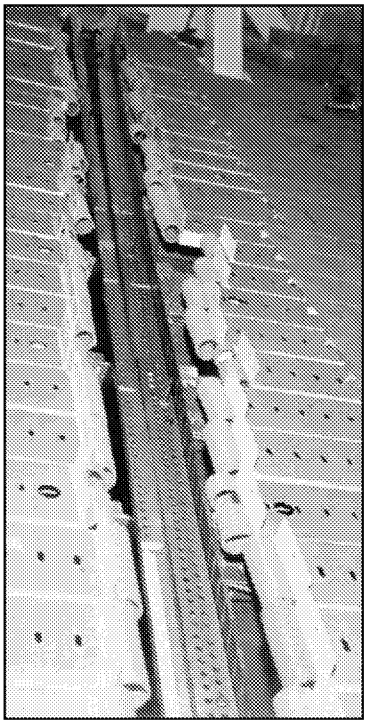

Figure 54. Rear spar installation.

S84291

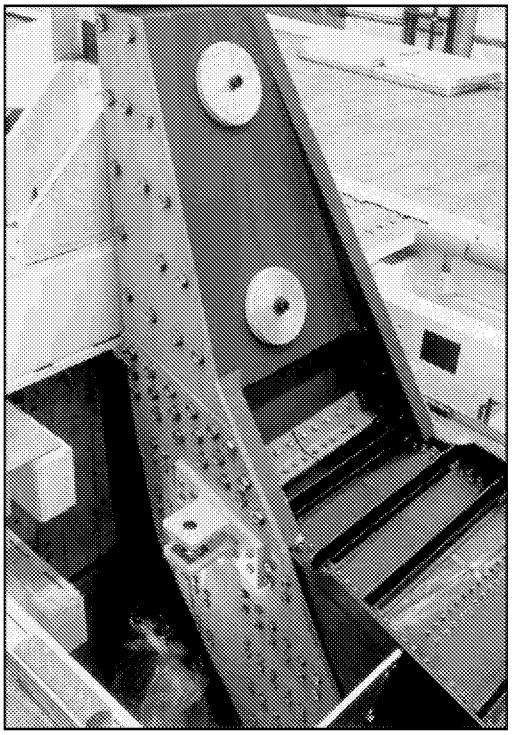

Figure 55. Main landing gear fitting installation.

S84292

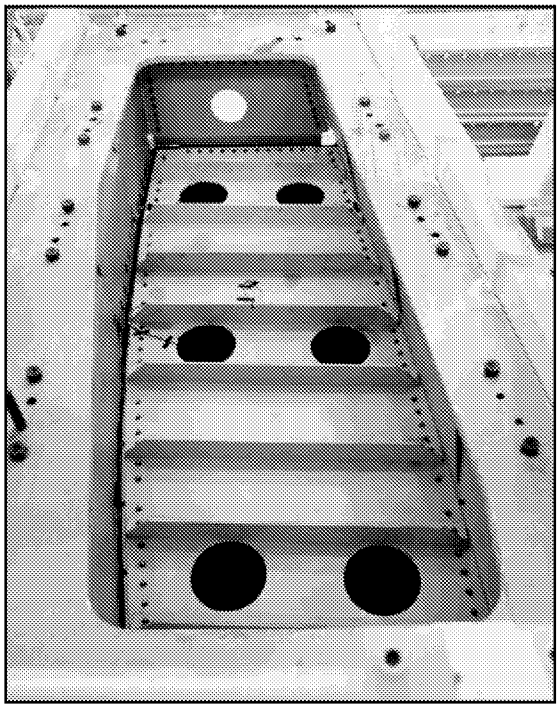

Figure 56. Side-of-body bulkhead.

S84293

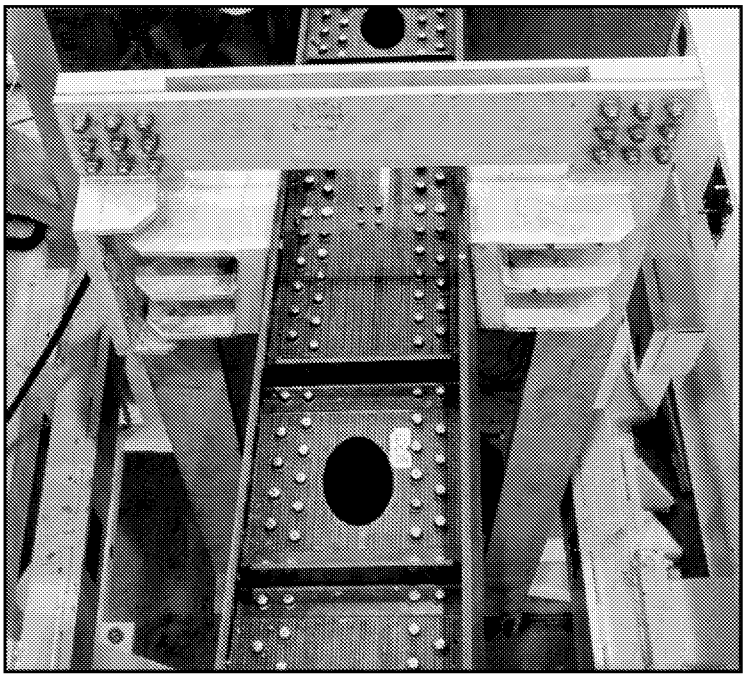

Figure 57. Rib 13 saddle installation.

Cost Studies and Analyses

The primary objective of the cost study activity was to validate the cost effectiveness of the stitched/resin film infusion (S/RFI) manufacturing process. This was to be achieved by collecting labor data throughout the fabrication of ten semi-span lower cover panels. Additionally, the data collection and analysis from fabrication and assembly of the S/RFI semi-span wing box test article has been incorporated into this section. The semi-span wing box consists of an upper and lower cover panel and the substructure (primarily the spars and ribs). This data is the basis for cost projections and comparisons to the program cost goal of 20% below the cost of a comparable present day aluminum wing box structure. An aluminum wing box cost baseline and the S/RFI cost goal were developed from a large parametric cost model drawing upon over 300 cost estimating relationships.

The S/RFI wing box cost analysis incorporates actual labor data collected during the manufacture of eight lower cover panels along with projections for the manufacture of wing box substructure and projections for assembly of the components into a wing box structure (based on historical industry data and cost estimating relationships). Results of this analysis are summarized in Table 10.

The actual labor data collected during the "one-time" manufacture of the substructure and assembly of the semi-span wing box test article is not sufficient to predict with any certainty the real world production implications. Additionally, the observation of the assembly of the transition structure fittings and other development tasks for test purposes rather than the actual assembly of the landing gear and pylon fittings and the absence of other production operations such as sealing and shimming for fuel pressure integrity is questionable in terms of a direct comparison. It does, however, provide a gage or starting point for realizing the potential impact of S/RFI technology to the manufacture of military and commercial aircraft components. The labor data and weight have been analyzed and adjusted by a "sizing" factor to develop MD-XX configuration labor and weight projections. Performance ratings, and personal, fatigue, and delay allowances have been applied to develop the projected "actual production" labor hours. Although substructure labor is higher than anticipated, assembly labor is significantly lower than projected by parametric and historical extrapolations. This is in part due to the considerations discussed earlier in this section.

A final look at the S/RFI wing box cost analysis incorporates actual material cost which is based on the "development" quantities and pricing used during this contract which is approximately double the expected cost of higher quantities of material in a production environment. The potential impact to the structural wing box cost, based on the single data point for substructure and assembly and actual material costs, is shown in Table 10. The demonstrated learning curve for cover panel manufacturing is also incorporated into this analysis.

In this analysis, the increased cost of manufacturing S/RFI cover panels compared to aluminum panels is a direct result of the actual "development" quantity material cost being at least double the expected cost of higher production quantities of material. The substructure comparison is based on one data point which was extrapolated from financial records rather than observed and documented. Additional data and analysis are necessary to further substantiate the findings.

The assembly comparison is also based on the analysis of the one time assembly of the wing box. The significant improvement in labor hours compared to assembly of an aluminum wing box is due primarily to the S/RFI integrated structure concept which eliminates many traditional assembly tasks. Also, the parametric (weight-based) projections of the aluminum wing assembly, as well as the S/RFI assembly projections, are being compared to actual labor hours accounting for the significant reduction in hours.

Table 10. Wing Box Cost Analysis Summary including Cover Panel "Actuals"

MDXX Cost Parameters (CY96 M$)	Aluminum Wing Box Cost	S/RFI Wing Box Goal Cost	S/RFI Cost	Program Performance Goal vs. Actual	Program Performance Actual
Structural Wing Box (Cum. Avg., 300 Ships)	$3.181	$2.544	$2.557	-20.0%	-19.6%
Structural Wing Cover (Cum. Avg., 300 Ships)	$1.516	$1.147	$1.160	-24.3%	-23.5%
Wing Substructure (Cum. Avg., 300 Ships)	$0.461	$0.429	$0.429	-6.9%	-6.9%
Wing Assembly (Cum. Avg., 300 Ships)	$1.204	$0.968	$0.968	-19.6%	-19.6%

Overall, the resulting program performance to the goal of manufacturing a S/RFI structural wing box at 20% below the cost of a comparable present day aluminum wing box.

7. Semi-Span Test Description

7.1 Overview

This section includes the design, analysis, and manufacturing planning for fabrication and installation of the structural loading hardware needed to introduce test loads into the semi-span wing box structure. The NASA-requested modifications to the transition structure that ties the structure to the test wall to react the test loads were also provided. This task also identified, checked, refurbished, and shipped the required Boeing load jacks, end fittings, and pins needed to introduce the loads through the test hardware into the box.

The load introduction hardware developed under this task included attachment fittings at the front and rear spar at the main landing gear bulkhead, the Rib 13 "picture frame," and Rib 18 closeout bulkhead (Figure 58). Load jacks are also attached at the pylon mounts. Front and rear spar web shear connections were requested after the critical design review to reduce the risk of a connection failure.

7.2 Structural Loading Hardware

The objective of semi-span wing box is to demonstrate that a carbon epoxy wing box using the S/RFI process for the spar webs and skin covers can be fabricated to aircraft quality standards. Along with building the box, it must also be demonstrated that this wing box and its detail features are capable of meeting structural design requirements. This is done by subjecting the wing box to loads that are representative of flight and ground loads. Therefore, only representative loads, shears, moments, and torques that influence the design of the wing are introduced by load jacks in a minimal number of locations to closely approximate the loads this wing box would experience if it were being tested to FAR 25 requirements. The load introduction hardware transfers the load from the jacks and applies it to the wing test box.

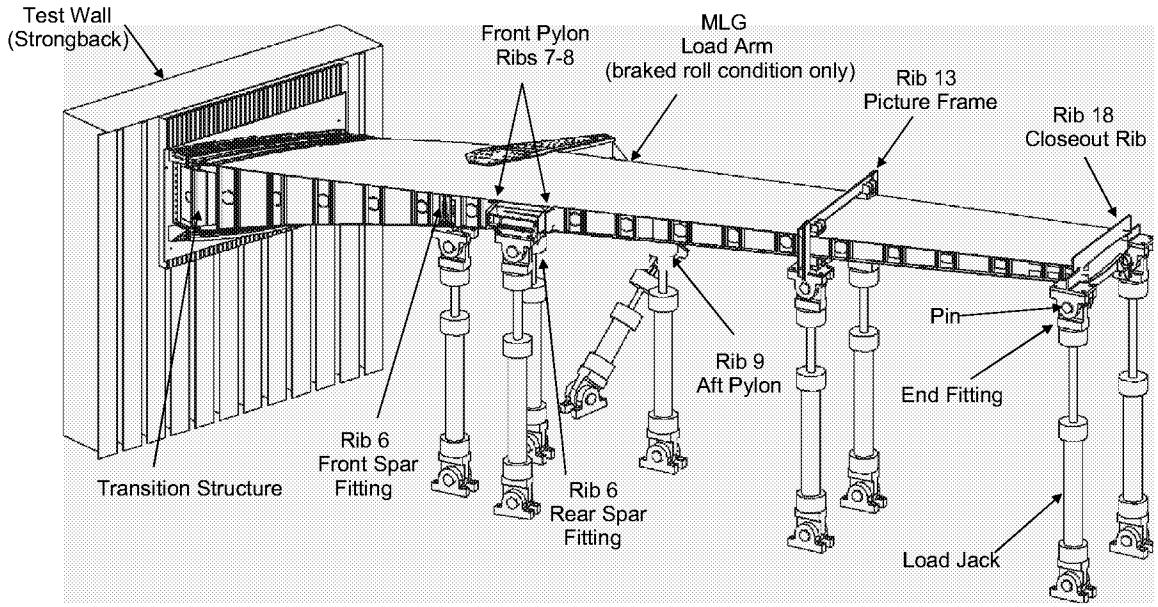

Figure 58. Test hardware setup.

The loads at Positions 1 and 2 are applied to the box through Rib 18. The rib is a 3/4-inch-thick aluminum plate (7075-T651) mechanically attached to the upper and lower covers by machined aluminum fittings acting as shear clips attached to the OML of each skin. It is also mechanically attached through the front and rear spar webs (double shear) by internal and external aluminum angle fittings. The critical load conditions for this hardware, the 2.5-upbending and -1.0-downbending, are introduced into the plate by angles pinned to monoball fittings, which allow rotation of the jack connection. Because of the introduction of large concentrated loads at the end of the box, the internal loads in the outboard rib bay of the box are not representative of those experienced in typical wing box structure.

The loads at Positions 3 and 4 are introduced into the semi-span box by using a picture frame fixture to apply loads through pads into the upper and lower covers of the box at the intersection of Rib 13 with the front and rear spars. This low-cost arrangement is thought to minimize the influence of attaching structure on the behavior of the box, thus limiting the area of nonrepresentative internal loads. The welded and mechanically assembled frame that wraps around the box consists of an upper and lower beam mechanically attached to vertical braces at each spar. Two pads are welded onto each beam and bonded to the upper and lower skins at the spars. The lower beam also has pads welded on to attach clevis-type actuator fittings where loads are introduced by the jacks.

Load Points 5and 6 take advantage of the existing fittings designed to represent the engine pylon attachment. Attachment Points 7b and 8 are at the MLG bulkhead and rear and front spar intersections, respectively. Because of the internal fittings at the MLG bulkhead, which are needed to handle the high shear loads from the simulated braked roll test condition, a machined fitting forward of the front spar web and a welded fitting at the rear spar are used to introduce the loads into the box. The welded fitting, made from ASTM A36 steel, is fastened through the lower MLG doubler and connects to a monoball fitting attached to a load jack. The front spar fitting is machined from 7075-T651 plate. An adapter fitting, bolted through the skin to the spar and to an internal bulkhead fitting, matches the lower cover contour and is used to attach the angles used to secure a monoball fitting with a pin. Like all previously mentioned load points, the critical loading conditions used to design the attaching hardware are the 2.5-upbending and -1.0-downbending load cases.

Load Point 7a hardware is designed for the braked-roll load case. The design of the attachment hardware was based upon a design used for an internally funded Boeing MLG joint test. A large steel arm made from ASTM A36 steel is used to introduce loads from the actuator into a representative MLG fitting attached to the wing box by two 6-inch-diameter bolts.

The purpose of the transition structure is to react the loads introduced into the box by the load jacks. The structure connects the root portion of the box with a stationary wall. The region of the box connecting to the transition structure is not representative of a wing design. Modifications were made after the Critical Design Review to add the front and rear spar web extensions. These are made from 7075-T651 aluminum plate and are 3/8-inch-thick. The web extensions are tied to the wall and transition structure using aluminum angle shear ties.

The appropriate Boeing load actuators (jacks) with end fittings and pins where located using criteria for load capacity, stroke length, and rotational movement because of wing box bending.

7.3 Cover Panel Repair Design

Prior to ultimate loading, several discrete source damage sites were chosen to apply two, 7-inch saw-cuts. According to the Semi-Span test plan , two major bolt-on repairs were attached to the upper and lower cover panels of the Semi-Span. The repair splices the region which was damaged by the saw-cuts, which cut through a stringer and the two adjacent skin bays. The repair must carry enough load from the cut

stringer and skin so that the stress concentration produced by the cut-out material is reduced to satisfactory levels. The lower cover repair is located between ribs 8 and 9 and between the access hole and the front spar. The upper cover repair is located between ribs 10 and 11 near the rear spar. Prior to repair, the 7-inch saw-cut damage was removed via cutting a elliptical shaped hole around the damage in the two cover panel sites. A view of the basic layout for both the upper and lower design is shown in Figure 59.

This repair splices a stringer and the two skin bays on either side. The upper skin splice plate is 0.25 inch thick. The lower skin splice plate is 0.16 inch thick. The upper stringer splice plate is 0.25 inch thick. The lower stringer splice plate is 0.19 inch thick. All bolts through the skin are 5/16 countersunk. In the upper cover, there are two columns of 5/16 bolts through the stringer blade. In the lower cover, there is one column of 3/8 bolts through the stringer blade. The splice plate material was made from aluminum 7075-T6 plate.

7.4 Strain Gages

Strain gages are located throughout all the components of the Semi-Span. A total of 461 gages were applied to the Semi-Span test box. 222 of these gages are external and 239 internal. The purpose of these gages is to provide a comparison between actual strains verses predicted strains and to validate the general load distributions and the level of stress concentrations. The general load distributions and the level of stress concentrations at structural discontinuities are determined by relating the strain data near the cut-out to the far field laminate strains. Also, at locations where failure could occur, gages are placed with the intent of possibly indicating load redistribution or imminent failure. The cover gage locations and labels are shown in Figure 60 and Figure 61. Sets of gages were placed chordwise across several sections of the cover panels so the strain distribution across the panels could be checked. Rosettes are placed on all the cover skins, rib webs and spar webs to check the shear strain in these members. Gages are placed on the root splice plates to check the bending and axial loads in this joint. Gages are placed on the main landing gear splice plates to check the axial loads in this joint. Back-to-back gage sets were placed on top of stringers and the skin it is attached to check the axial and bending loads in the stiffened sections. Gages were placed next to the impact damage sites and the saw-cuts to provide a possible indication of imminent failure. Gages were placed near structural discontinuities which caused stress concentrations such as access holes, stringer runouts, the root joints, the main landing gear joints or repairs.

Strain gage predictions for the Semi-Span were made throughout the wing box. The strain gage predictions were determined from finite element analyses which model the regions where the gages are positioned on the test article. The global model as shown in Figure 62 was used for the gages away from structural discontinuities. However, special local models such as the one for the upper cover runout shown in Figure 63 were made for gages near these features where strain would be affected by the gradient produced by these structural discontinuities. These local models can account for the effect of these discontinuities on the strain. Also, nonlinear analysis were performed near access doors that had low margins of safety. Linear strain gage predictions were made for all gages except those near the root which is the only location where significant nonlinearites were expected.

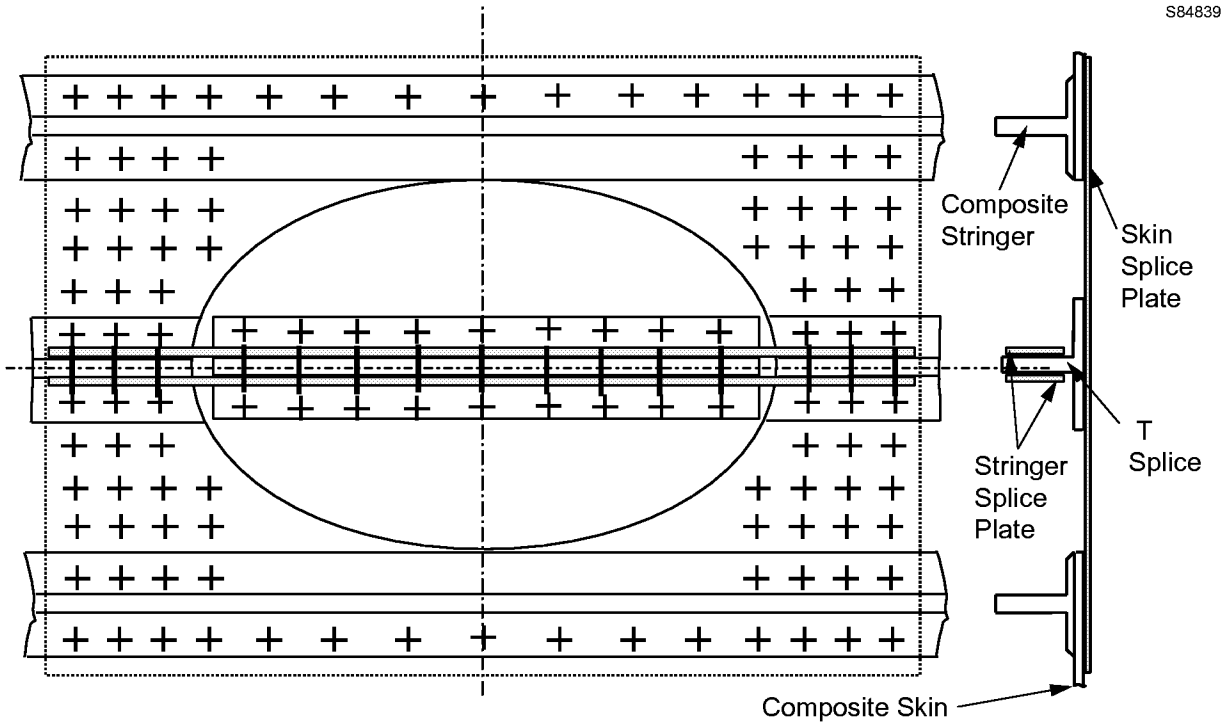

Figure 59. Trimetric view of Semi-Span repair.

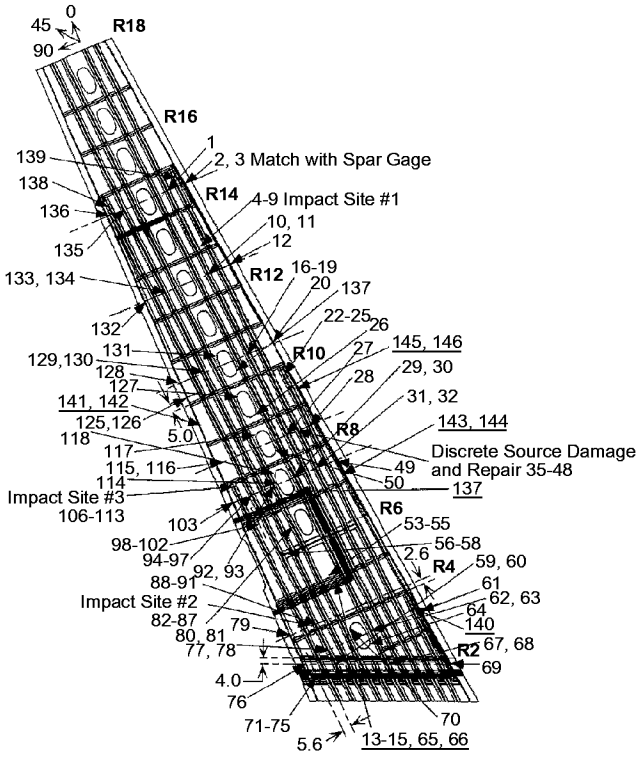

Figure 60. Plan view of lower cover gage locations and labels.

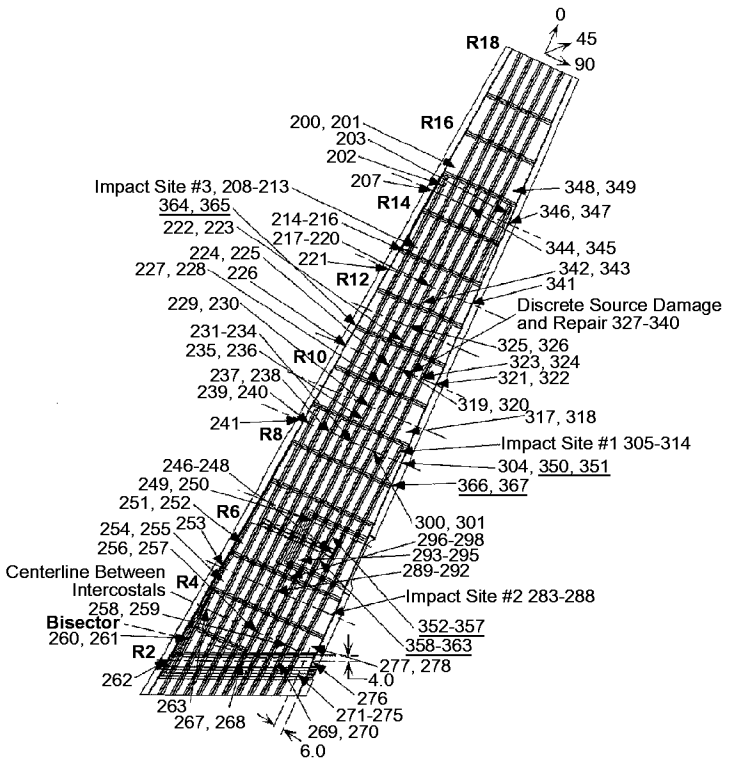

Figure 61. Plan view of upper cover gage locations and labels.

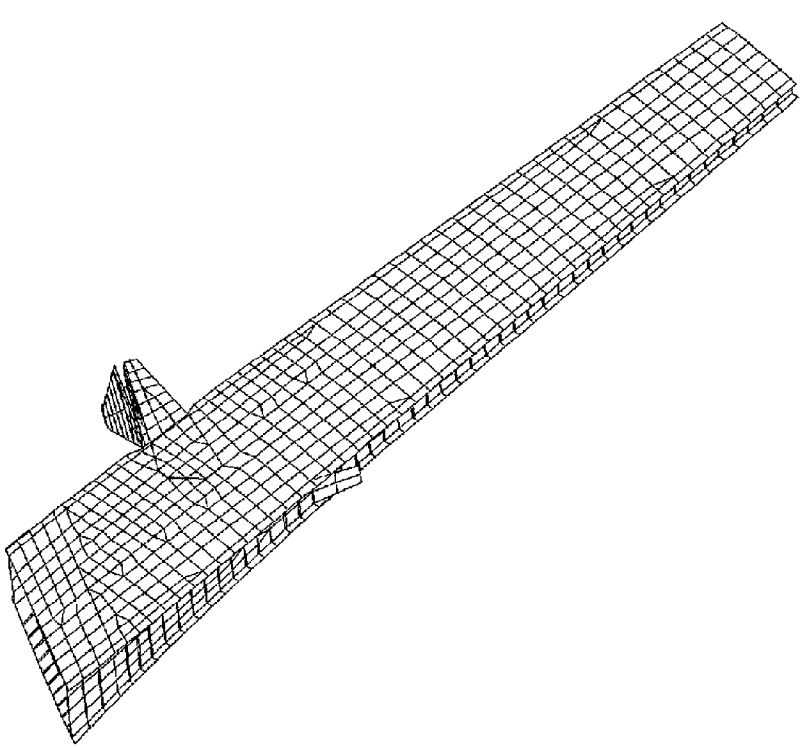

Figure 62. Trimetric view of global model.

S84843

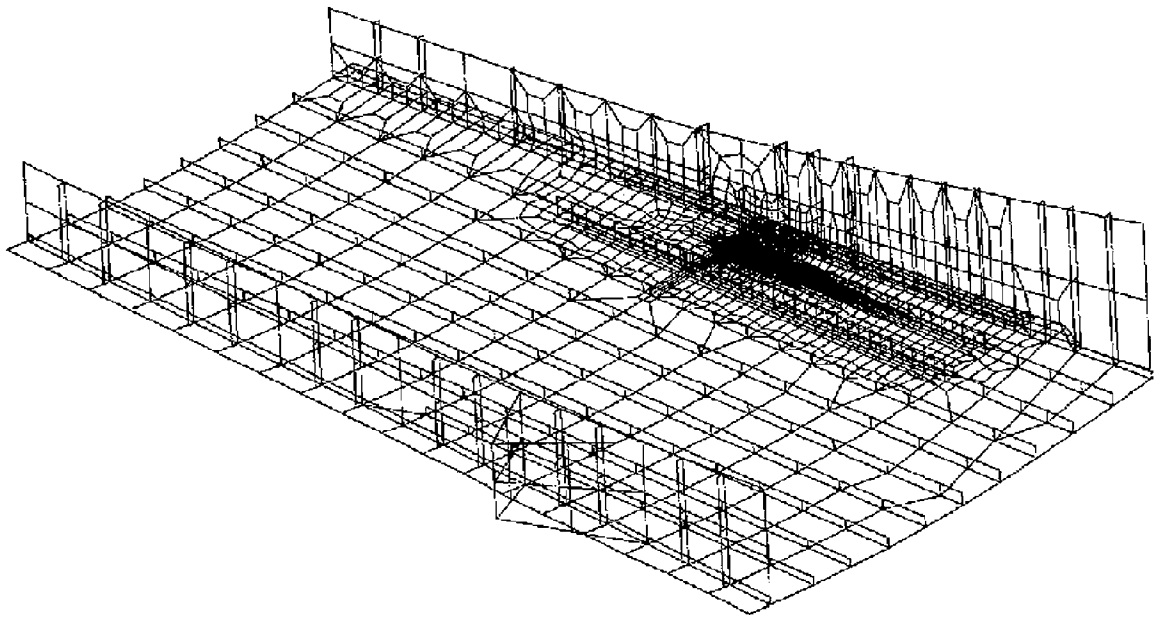

Figure 63. Trimetric view of detail stringer runout FEM.

NASA successfully completed a series of semi-span tests: Brake-Roll at design limit load (DLL), -1.0-g down bending at DLL, 2.5-g up bending at DLL, and discrete-source-damage in the upper and lower cover panels at 70% of 2.5-g up-bending DLL. Testing concluded with the 2.5-g wing up-bending test-to-failure June 1, 2000. Final failure occurred in the lower cover panel of the wing box at 97% of the 2.5-g design ultimate load (DUL) (Figure 64). Failure initiated from lower cover access hole between Ribs 8 and 9 based on strain gage data. The access hole strain gage readings dropped off at 91.4% DUL. This failure initiation location coincides with the lowest margin of safety location. The failure propagated from the access hole and through the lower cover into both spars. The cover panels had discrete source damage repairs (one per cover panel) and selected impact damage sties (including one stringer runout site per cover panel). Prior to the semi-span ultimate test, NASA had conducted a pre-test analysis on wing tip condition displacement during structural loading and prior to reaching failure. The results are shown (Figure 65). The exact failure sequence is difficult to determine. NASA is performing the post test analysis that may provide a more comprehensive understanding of the failure events.

Figure 64. Semi-Span lower cover panel failure.

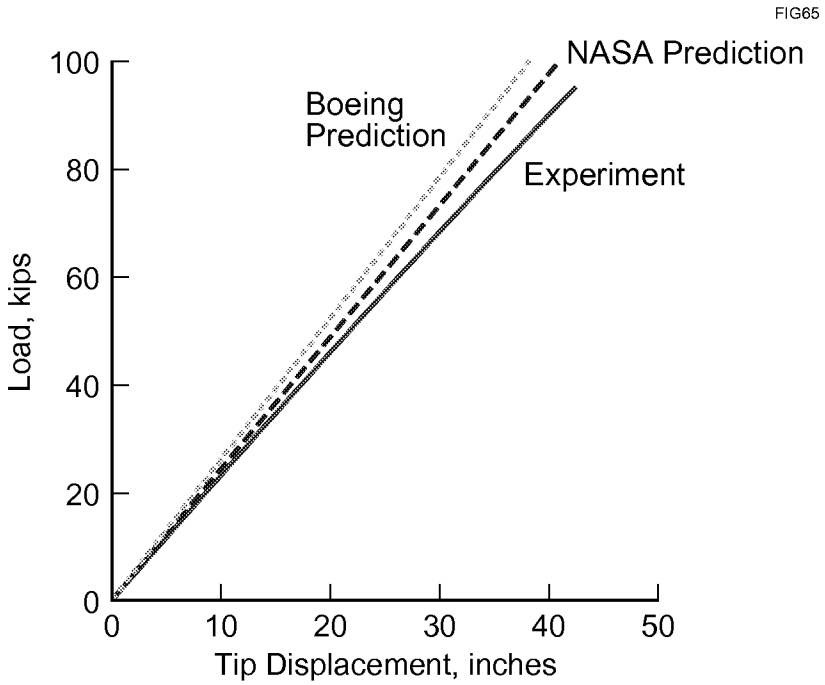

Figure 65. NASA Pre-test analysis on Wing Tip condition displacement.

8. Concluding Remarks

The work summarized in this report describes the development or maturation of technologies related to S/RFI processing to reduce the risk and improve the quality of parts processed in this manner. The Durability and damage tolerance studies and the process modeling work demonstrated that the use of sophisticated computer models can, with reasonable accuracy, predict the behavior of S/RFI parts. Specifically, the software code GENOA was shown to give reasonable estimates of damage progression and residual structural strength for the structural components tested. Although these tools need further refinement, they clearly demonstrate that large cost reductions in design and processing analyses may be achieved through the use of these computational tools by reducing the necessity for large structural tests or process trials.

Through the design and manufacture of a semi-span wing test article, the goals of this program of 25% weight reduction and 20% cost reduction over metallic structure were realized.

Through the design and test verification process, credibility has been given to the utilization of heavily loaded composite structures for primary wing structure of commercial aircraft. Furthermore, the stitched/resin film infusion (S/RFI) concept of manufacture has evolved to offer a unique and effective solution for the production of large, heavily loaded wing primary aircraft structure. The manufacturing and processing characteristics and risk of scale-up using the S/RFI process have been largely mitigated through the successful manufacture of eight (8) lower cover panels. The quality of each panel saw marked improvement as process refinements were implemented. Also, during the same time, process improvements, work flow changes, and new concepts for tooling and manufacturing were implemented to bring marked and fundamental improvement to the cost data curve development. The evolution of this process during the manufacture of the eight lower cover panels resulted in cost projections of 19.6% below the cost of an aluminum wing box essentially achieving the 20% cost reduction goal.

Materials and process studies demonstrated how a systematic approach could be successfully used to reduce the risk of processing large, integrated composite structures. This systematic approach focused on the basic parameters in S/RFI technology: stitching preforms, preform quality, and resin infusion. Stitching studies concentrated on improving stitching quality by determining the factors that would ensure proper thickness and knot formation while simultaneously maintaining or enhancing stitching speed. By creating a visual guide as well as a set of stitching parameters for each machine, stitching machine operators were given tools with which they could maintain preform quality, detect problems, and resolve them efficiently. Processing guidelines for resin handling (temperature and pressure) were developed to ensure that cured parts would meet the desired thickness, and hence resin-content levels. Moreover, these parameters served to reduce the risk of producing out-of-specification parts. The resin allocation study showed a systematic process for reducing the risk associated with scaling-up the resin film infusion of stitched preforms. The result of this study was the requirement for a highly customized resin allocation in order to provide both within-specification part thicknesses as well as thickness uniformity.

The VARTM process studies demonstrated that significant work is still required before this technology reaches the maturity level of RFI or RTM for producing aerospace-quality composite parts. However, it was demonstrated using the VARTM-PB process that many of the lessons learned in S/RFI development may be directly applied to VARTM. Furthermore, VARTM-PB showed the benefits of autoclave pressure to overcome the low fiber volumes associated with vacuum-only processes for thick structures.

The efforts described in this report summarize materials and process developments for reducing the costs and risks associated with the manufacture and design of structural components using the S/RFI process. Adoption of the methods described herein has been successfully demonstrated to improve part quality during the manufacture of cover panels under the AST Composite Wing Program.

9. References

1. Arthur V. Hawley, : *Development of Stitched/RTM Primary Structures for Transport Aircraft.* (NASA CR 191441, July 1993)

2. Arthur V. Hawley, *Detail Design Development of a Transport Aircraft Composite Wing.* (NASA CP 3326, Vol. 1, Part 1, pp. 131-154, June 1996)

3. Markus, A.M.; Rohwer, K.M.; Thrash, P.J.; Sutton, J.O. and Madan, R.C.: *Fabrication Processes, Analysis Methods, and Test Results for Stitched Composite Structures.* (NASA CR 191599, March 1994)

4. Patrick J. Thrash and Jeffery L. Miller, *Design of a Stitching Machine for Transport Aircraft Composite Wings.* (NASA CP 3326, Vol 1, Part 1, pp. 191-208, June 1996)

5. Jeffery L. Miller, and Patrick J. Thrash,: *Fabrication, Assembly, and Checkout of an Advanced Stitching Machine.* (Published in the Proceedings of the 11th DoD/NASA/FAA Conference on Fibrous Composites in Structural Design. WL-TR-97-3009, Vol II, pp. XIII 55-73, October, 1996)

REPORT DOCUMENTATION PAGE

Form Approved
OMB No. 0704-0188

1. AGENCY USE ONLY *(Leave blank)*	2. REPORT DATE	3. REPORT TYPE AND DATES COVERED
	March 2001	Contractor Report

4. TITLE AND SUBTITLE
AST Composite Wing Program - Executive Summary

5. FUNDING NUMBERS
522-83-11
NAS1-20546

6. AUTHOR(S)
Michael Karal

7. PERFORMING ORGANIZATION NAME(S) AND ADDRESS(ES)
The Boeing Company
2401 E. Wardlow Road
Long Beach, CA 90807

8. PERFORMING ORGANIZATION REPORT NUMBER
CRAD-9503-TR-7323

9. SPONSORING/MONITORING AGENCY NAME(S) AND ADDRESS(ES)
National Aeronautics and Space Administration
Langley Research Center
Hampton, VA 23681-2199

10. SPONSORING/MONITORING AGENCY REPORT NUMBER
NASA/CR-2001-210650

11. SUPPLEMENTARY NOTES
Langley Technical Monitor: Dawn C. Jegley

12a. DISTRIBUTION/AVAILABILITY STATEMENT
Unclassified–Unlimited
Subject Category 24 Distribution: Nonstandard
Availability: NASA CASI (301) 621-0390

12b. DISTRIBUTION CODE

13. ABSTRACT *(Maximum 200 words)*

The Boeing Company demonstrated the application of stitched/resin infused (S/RFI) composite materials on commercial transport aircraft primary wing structures under the Advanced Subsonic technology (AST) Composite Wing contract, NAS1-20546. This report describes a weight trade study utilizing a wing torque box design applicable to a 220-passenger commercial aircraft and was used to verify the weight savings a S/RFI structure would offer compared to an identical aluminum wing box design. This trade study was performed in the AST Composite Wing program, and the overall weight savings are reported. Previous program work involved the design of a S/RFI-baseline wing box structural test component and its associated testing hardware. This detail structural design effort which is known as the "semi-span" in this report, was completed under a previous NASA contract (NAS1-18862). The full-scale wing design was based on a configuration for a MD-90-40X airplane, and the objective of this structural test component was to demonstrate the maturity of the S/RFI technology through the evaluation of a full-scale wing box/fuselage section structural test. However, scope reductions of the AST Composite Wing Program prevented the fabrication and evaluation of this wing box structure. Results obtained from the weight trade study, the full-scale test component design effort, fabrication, design development testing, and full-scale testing of the semi-span wing box are reported.

14. SUBJECT TERMS	15. NUMBER OF PAGES
Composite Wing, Stitched Composites, Resin Film Infusion, Braiding	98
	16. PRICE CODE: A05

17. SECURITY CLASSIFICATION OF REPORT	18. SECURITY CLASSIFICATION OF THIS PAGE	19. SECURITY CLASSIFICATION OF ABSTRACT	20. LIMITATION OF ABSTRACT
Unclassified	Unclassified	Unclassified	UL